PAUL SCHERRER INSTITUT

PSI

# Mechanistic Sorption Model for Clay Minerals; 2SPNE SC/CE

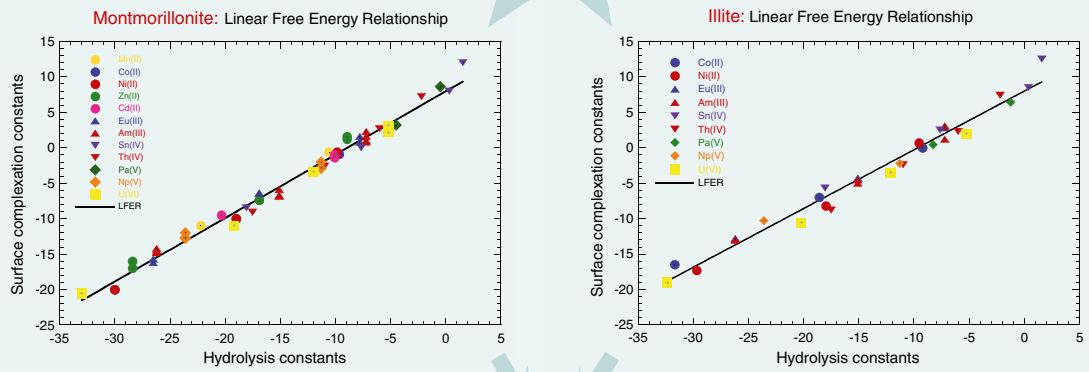


## Influence of Speciation/Sorption Competition

## Thermodynamic Sorption Data Bases

Progress Report 2008

# Laboratory for Waste Management

Nuclear Energy and Safety Research Department

**Cover**

Montmorillite and illite are the major clay minerals in bentonite and argillaceous rocks respectively, which are responsible for sorption. The 2 site protolysis non electrostatic surface complexation and cation exchange (2SPNE SC/CE) model has been used to describe quantitatively sorption measurements in these two systems. A linear free energy relationship (LFER) between surface complexation constants and the corresponding hydrolysis constants has been established in both cases. LFERs allow surface complexation constants to be estimated for metals, particularly those for which no sorption data exist, and enable their uptake properties to be predicted. In order to use the sorption model and LFER data to calculate metal uptake in natural systems, the influence of aqueous speciation and competitive sorption needs to be quantified. The ultimate aim is to develop sorption data bases which are based on thermodynamic concepts.

PAUL SCHERRER INSTITUT

PSI

# Progress Report 2008

---

# Laboratory for Waste Management

Nuclear Energy and Safety Research Department

## Preface

The Laboratory for Waste Management has two tasks: (i) to carry out an R&D programme strengthening the scientific basis for nuclear waste management, and (ii) to operate – together with the SLS team – a micro-XAS beamline.

In its first task, the Laboratory serves an important national role by supporting the Swiss Federal Government and Nagra in their tasks to safely dispose of radioactive wastes from medical, industrial and research applications as well as from nuclear power plants. The activities are in fundamental repository chemistry, chemistry and physics of radionuclides at geological interfaces and radionuclide transport and retardation in geological media and man-made repository barriers. The work performed is a balanced combination of experimental activities in dedicated laboratories for handling radioactive elements, field experiments and theoretical modelling. The work is directed towards repository projects and the results find their application in comprehensive performance assessments carried out by Nagra.

This report summarises the activities and results achieved in the reporting period. It is organised as an overview followed by individual reports on the six waste management sub-programmes and a section on the micro-XAS beamline.

We gratefully acknowledge the help of the Institute's management and of Nagra in our work.

.

# Table of Contents

**1 OVERVIEW ..... 7**

1.1 Introduction ..... 7
1.2 General ..... 7
1.3 Performance Assessment (PA) ..... 10
1.4 Foundations of repository chemistry ..... 10
1.5 Repository near field ..... 11
1.5.1 Clay systems ..... 11
1.5.2 Cement ..... 12
1.6 Repository far field ..... 13

**2 GEOCHEMICAL MODELLING ..... 17**

2.1 Overview ..... 17
2.2 Thermodynamic databases and software ..... 17
2.2.1 PSI/Nagra Chemical Thermodynamic Data Base 12/07 ..... 17
2.2.2 OECD/NEA TDB iron review ..... 18
2.2.3 GEM-Selektor program package v.2-PSI ..... 19
2.2.4 Sensitivity analysis in the Uncertainty Space ..... 20
2.3 Solid Solutions ..... 20
2.3.1 Thermodynamics of hydrotalcites ..... 20
2.3.2 Radium interaction with clays and minor minerals (JAEA-LES) ..... 21
2.3.3 Revision of the C-S-H solid solution model ..... 21
2.4 Glass corrosion, spectroscopy ..... 22
2.5 Other Activities: Teaching at university level ..... 24
2.6 References ..... 24

**3 TRANSPORT MECHANISMS ..... 25**

3.1 Overview ..... 25
3.2 Data acquisition from experiments on the laboratory and field scales ..... 25
3.2.1 Modelling of field experiments in Mont Terri ..... 25
3.2.2 Reactive transport modelling of laboratory Cs diffusion experiments ..... 26
3.2.3 Design of the experimental setup for laboratory diffusion experiments ..... 27
3.3 Predictive modelling of in-situ repository evolution ..... 28
3.3.1 Reactive transport modelling of porosity evolution in a L/ILW repository near field ..... 28
3.3.2 Reactive transport modelling of Ra retardation in bentonite ..... 29
3.4 Understanding of radionuclide transport mechanisms ..... 29
3.4.1 Reactive transport modelling of Ni competitive sorption in bentonite ..... 29
3.4.2 Molecular modelling of crystalline cement phases ..... 31
3.5 "Know-how" transfer, connection with universities and benchmarking of coupled codes ..... 33
3.5.1 Fluid-rock interaction modelling ..... 33
3.5.2 Benchmarking of coupled codes ..... 33
3.6 References ..... 34

**4 CLAY SYSTEMS ..... 35**

4.1 Summary ..... 35
4.2 Performance assessment ..... 35
4.3 Sorption studies on illite and Linear Free Energy Relationships ..... 36
4.4 6th EC Framework Projects ..... 38
4.4.1 FUNMIG IP ..... 38
4.4.2 INCA ..... 39
4.4.3 Np(V) investigations on clay: Macroscopic and microscopic analysis ..... 40
4.5 References ..... 41

**5 CEMENT SYSTEMS ..... 43**

5.1 Overview ..... 43
5.2 Uptake of dose-determining radionuclides ..... 44
5.3 Redox chemistry in cementitious systems ..... 44
5.3.1 Neptunium(V) sorption studies ..... 44
5.3.2 Fe speciation in cement ..... 45
5.4 Uptake of lanthanides and actinides by cementitious materials ..... 46
5.4.1 Nd(III) and Eu(III) uptake processes ..... 46
5.4.2 Spectroscopic investigations of U(VI) uptake processes ..... 48
5.5 CI project ..... 49
5.6 References ..... 50

**6 COLLOID CHEMISTRY ..... 51**

6.1 Introduction ..... 51
6.2 Activities in the CFM project ..... 51
6.3 Other colloid activities ..... 53
6.4 Future work ..... 54
6.5 References ..... 54

**7 DIFFUSION PROCESSES ..... 55**

7.1 General ..... 55
7.2 Diffusion in Opalinus Clay ..... 55
7.3 Transport phenomena in compacted clay systems (TRAPHICCS) ..... 57
7.4 Dynamics of water in compacted clay systems ..... 58
7.5 DINAPOR ..... 59
7.6 Micro-heterogeneous systems ..... 59
7.7 References ..... 59

**8 THE MICRO-XAS BEAMLINE PROJECT: SPECTROMICROSCOPY GOES MICROSPECTROSCOPY ..... 61**

8.1 General ..... 61
8.2 Two-dimensional micro-X-ray-diffraction ..... 61
8.3 Micro-X-ray-absorption-spectroscopy ..... 62
8.4 Outlook ..... 64
8.5 References ..... 64

**9 PUBLICATIONS ..... 67**

9.1 Peer reviewed journals and reports ..... 67
9.2 Conference proceedings ..... 69
9.3 Conferences/Workshops/Presentations ..... 69
9.4 Invited talks ..... 71
9.5 Other presentations ..... 71
9.6 Internal reports ..... 73
9.7 Internal presentations ..... 73
9.8 Others/Teachings ..... 73
9.9 PhD and Diploma Theses ..... 71

# 1 OVERVIEW

*Mike Bradbury*

## 1.1 Introduction

The progress made in the Laboratory for Waste Management (LES) over the period from 1 January, 2008 to 31 December, 2008 is summarised in the first part of the report. LES is organised into two projects; the Waste Management Programme and the Micro-XAS Beamline Project. The activities carried out in the former are described in Chapters 2 to 7 according to each group and are either predominantly "experimental" or predominantly "modelling" in their nature. However, there are strong interactions between groups and between experimentalists and modellers. The status of the Micro-XAS Beamline Project is given in Chapter 8. The aim of this project is to gain insights into reactions occurring at the molecular level at solid surfaces. X-ray absorption spectroscopy studies have become an integral tool in LES.

## 1.2 General

The existing nuclear power plants at Mühleberg (355 MW), Canton Bern and Beznau I and II (together 730 MW), Canton Aargau, will have to be replaced after 2020. In addition, important electricity supply contracts with France will be reaching the end of their term in the same time period. Switzerland is undergoing what might be termed a nuclear renaissance with the Swiss electric utilities currently planning to build three new nuclear power plants with a total output of 4,800 megawatts. In June 2008 Atel submitted an application for a new plant, Gösgen II. Axpo and BKW have established a joint company to develop plans for two new nuclear power plants replacing the existing plants at Mühleberg and Beznau (I and II). In all cases commissioning is envisaged after 2020 and the plans will be subject to a referendum, probably in 2012 or 2013.

The "Sachplan Geologische Tiefenlagerung" (Sectoral Plan) is a planning instrument in which the government has laid down site selection criteria for the deep geological disposal of low and intermediate level waste (SMA), and high level waste, spent fuel and long-lived intermediate level waste (HAA) in Switzerland. The long-term safety and the environment are the two priority considerations. The process of site selection is intended to ensure that the public are continually and transparently informed and that there is close co-operation at the Canton, local authority and neighbouring country levels. In March 2006 the Department of Energy presented the first draft of the conceptual part (Part 1) of the Sectoral Plan for Site Selection. After a considerable consultation and revision process, this part of the Sectoral Plan was approved by the Federal Council on the 2nd of April 2008.

In Part 2 of the Sectoral Plan, 3 implementation steps are foreseen. Step 1 is the identification of 6 potential regions for an SMA waste repository and 3 potential regions for a HAA repository. (Regions suitable for combination repositories may be included.) In October 2008 Nagra submitted a report to the government identifying such potential regions ("Vorschlag geologischer Standortgebiete für SMA und das HAA-Lager. Darlegung der Anforderung des Vorgehens und der Ergebnisse") At the same time the "Entsorgungsprogramm Bericht" (Disposal Programme) was also submitted. Issues such as radionuclide inventories and their allocation to the different repository types, the required deep geological repositories and their layouts, repository realisation plans, costs and timescales, financial modalities etc. are described and discussed.

The 3 regions for HAA and the 6 regions for SMA proposed by Nagra as being potentially suitable for constructing the appropriate repository type were announced in Bern through the Department of Energy on the 6th of November 2008. These regions are:

HAA: Zürcher Weinland, Opalinus Clay (OPA), Nördlich Lägeren (OPA), Bözberg (OPA).

SMA: Südranden Schaffhausen (OPA), Zürcher Weinland (Brauner Dogger, OPA), Nördlich Lägeren (Brauner Dogger, OPA), Bözberg (OPA), Jura-Südfuss (Effinger Schichten, OPA), Wellenberg (Mergel).

The construction of a new gallery (Gallery 08) was started at the Mont Terri Rock Laboratory, Canton Jura, in October 2007. On the 25th of August 2008, Gallery 08 was linked with the rest of the rock laboratory (the "cutting through" event). The new gallery will contain four experimental niches and completion is planned by December 08.

As mentioned in the LES Annual Report for 2007, the Entsorgungsprogramm contains a section on the longer term R & D requirements. In connection with this, and the need for LES to document its future plans, a research strategy paper divided into time periods of 3, 6 and 10 years was developed. This

strategy document, "LES Research Strategy: 2007 - 2017", was published on the 7th of April 2008 and subsequently widely distributed.

The micro-XAS beamline has now completed its second full year of operation serving a broad community of users. During this time the most prominent core competences which have evolved are (spectro)microscopy, ultrafast X-ray science involving diffraction and spectroscopy, in-situ micro-diffraction and, last but not least, radioactive microprobe analysis. During the past year efforts have been focused on micro-X-ray-diffraction and micro-X-ray-absorption-spectroscopy. Micro-XAS is considered to be the center-pieces of any hard-X-ray microprobe. A rapid development of micro-XRD has taken place due to the very high level of interest in the user community. In addition to the original static, 'point' measurements, a two-dimensional raster scanning scheme has been implemented which allows two-dimensional images of crystallographic information to be collected.

As the region under investigation and the X-ray beam diameter approach ~1µm (or below) micro-spectroscopy becomes a real challenge. The necessity of varying the wavelength of the beam in spectroscopy requires movable optical components. Considering that the optical arrangements have to be changed using lever arms several meters in length, a requirement of 'zero' beam motion for a micron sized object with a 1µm$^2$ beam demands that the magnitude of the beam-to-sample fluctuations and drifts be as small as a few nanometers. This is technically extremely demanding. Two examples of the application of this technique are given in Chapter 8. The first is a micro-EXAFS investigation of an 80 nm thick grid of Ni squares (line thickness 1µm, side length 10 µm). The second concerns a corrosion study on primary circuit components of nuclear power plants. An irradiated zirconium alloy tube segment with a ~10 µm thick oxide layer was cut from the original Zr/Nb cladding. A novel sample preparation technique using a focused ion beam allowed detailed investigations on the oxide layer to be performed using microscopic, spectromicroscopic (elemental distribution maps, oxidation state maps) and micro-EXAFS and micro-XANES methods.

Significant improvements are planned for both two-dimensional micro-X-ray-diffraction and micro-X-ray-absorption-spectroscopy. In the context of microspectroscopy, an improved signal normalization scheme as well as the full implementation of the 32 element solid state detector will be of the highest priority in 2009. The latter is essential for the planned future investigations on surface speciation at low loadings (50-100ppm) of radio-elements, particularly actinides, on clay minerals and argillaceous rocks.

The two 6th EU Framework Programmes in which LES was participating; IP FUNMIG and the ACTINET Network of Excellence (micro-XAS beamline in the pooled facilities) officially finished at the end of 2008.

In the 7th EU Framework Programme LES is a work package leader in WP4, Redox Reactions of Radionuclides, in RECOSY, "Redox Phenomena Controlling Systems" (start date 1 April 2008, duration 4 years). LES is also in the core group of ACTINET I3 in which the micro-XAS beamline is part of the pooled facilities. The proposed start date is in early 2009 and the duration of the project is 3 years. The commissioning of the 32 element detector is vital for an effective participation in this programme.

Bilateral co-operations with external institutions and scientists have continued and are summarized in Table 1.1.

***Table 1.1:*** *National and international co-operations*

| **Co-operations** |
|---|
| **Nagra**<br>Major financial contribution<br>Various technical working groups |
| **Multinational**<br>6th FP (NoE ACTINET-6, IP FUNMIG),<br>7th FP (RECOSY),<br>OECD/NEA TDB III (Fe),<br>Mont Terri Project (DR, CI experiments)<br>Grimsel Test Site (Colloid Formation Migration) |
| **Universities**<br>Bern, Switzerland (mineralogy, petrography)<br>UC London, UK (molecular modelling)<br>Mainz, Germany (cement, montmorillonite)<br>Strasbourg, France (glass)<br>Tübingen, Germany (geosphere transport) |
| **Research Centres**<br>CEA*, France (near and far field)<br>EAWAG, Switzerland (cement)<br>EMPA*, Switzerland (cement)<br>INE, KIT*, Germany (near and far field; TRLFS)<br>JAEA, Japan (Ra in bentonite/argillaceous rocks)<br>IFR, FZD*, Germany (XAS, TRLFS)<br>SCK/CEN, Belgium (clays)<br>VTT, Finland (pH in compacted bentonite)<br>*formal co-operation agreements |

The joint project between JAEA (Japan) and LES set up to investigate the partitioning of Ra(II) between aqueous solutions, bentonite and clay rocks, in the presence/absence of minor minerals (barite, calcite and witherite) is scheduled to be completed at the end of March 2009. The possibility of continuing this co-operation is being investigated.

Again in 2008 LES could welcome a guest scientist from Japan, Dr. Akira Kitamura (Research Scientist at JAEA). He began a 1-year sabbatical in March 2008 in the XAS sub-programme.

A further guest scientist, Dr. Javier Gaona, from Amphos XXI Consulting, Spain, began a 2-year stay in the Cement Systems Group in September 2008. During his stay in LES Dr. Gaona will be involved in the redox work on cement, particularly the uptake of Np(IV/V) and the accompanying EXAFS and XANES investigations.

During 2008 two of the three Euratom Training Fellowships: Inter European Fellowships (Marie-Curie Euratom Fellowship) ended. One of the fellows, Dr. Maria Marques, has taken up the vacant position in the Clay Sorption Mechanisms Group within LES. The other, Dr. Jens Mibus, has secured a position at Nagra. The third Inter European Fellowship project, MISUC "Microscale investigations of the speciation and mobility of U(VI) in cementitious materials", carried out by Dr. Nathalie Macé, is scheduled to continue until 31 August, 2009.

The post doc position for the project "Crystallographic analysis of micro-diffraction images from heterogeneous, polycrystalline samples: A novel approach to determine the mineral composition in the cement matrix and at cement/Opalinus Clay interfaces" which is fully financed by PSI/FoKo has been filled by Dr. Dmitry Popov, who took up the position in May 2008. In connection with ACTINET pooled facility activities, the vacant post doc position will be re-advertised in 2009. A further post doc position for which the candidate has been identified, and 50% of the finance is provided by CEA, has been approved by PSI/FoKo with a probable starting date of March 2009. Finally, LES won the internal department competition for the NES financed post doc position, which will become available in April 2009. The titles of these two post doc activities are "Assessing heterogeneities on the microscopic scale and implementation of such structures in a 3D transport model for compacted argillaceous materials" and "Two dimensional investigations of reactive transport processes at heterogeneous interfaces", respectively.

Four PhD studies were being carried out in LES during 2008. One of them, "Mechanisms of Nd(III) and Eu(III) uptake by cementitious materials" was completed and successfully defended in November 2008. A second one is ongoing, with a projected finishing date of December 2009; "Thermodynamic stability and radionuclide binding mechanisms in hydrotalcite-like solid solutions". Two new PhD studies began in the autumn of 2008: "Uptake of iodide species by selected mineral phases relevant to radioactive waste repository environments: a combined radiochemical and spectroscopic study" and "Simulation of geochemical processes in enhanced geothermal systems". The former PhD work is partly funded through the Virtual Institute of Advanced Solid-Aqueous Radiogeochemistry (INE, KIT) and the latter through the Competence Centre for Environment and Sustainability.

An additional PhD position for which finance has already been approved (Swiss National Science Foundation) with the title "Quantitative analysis of micro-heterogeneous systems: A joint employment of complementary micro beam techniques: determination of narrow diffusion profiles: micro-XAS and laser ablation" will be advertised at the end of 2008/ begining 2009.

The intention is to make proposals for at least two further PhD positions in 2009, one in the Clay Sorption Mechanisms Group and the other in the Transport Mechanisms Group.

Towards the end of 2007 a search was launched to fill an assistant professor position, tenure track, in Repository Geochemistry in the Department of Earth Sciences at the ETHZ. The aim was to create a joint position between PSI and the ETHZ to strengthen the collaborative research work and to establish joint research and education programmes. After an intensive evaluation process, and interviews of 3 short listed candidates, the action was terminated in March 2008 since none of the candidates met the somewhat stringent conditions set for the position.

Finally, as can be seen from the LES Organigram in Table 1.2 on page 15, Andreas Jakob has stepped down as group leader of Transport Mechanisms Group and has been replaced by Sergey Churakov. Also, the former Sorption Mechanisms Group has been split into two groups, the Clay Sorption Mechanisms Group (group leader Bart Baeyens) and the Cement Systems Group (group leader Erich Wieland).

On February 26 and 27, 2008, the Waste Management Program Committee (PCM) met for their annual meeting. The work performed within LES and the

future plans were discussed as usual (AN-44-08-07). The valuable help and input from the members of the committee, both at the meeting, and throughout the year is appreciated by the whole Lab.

Professor Thomas Fanghänel, a long serving and highly valued member of the PCM expressed the wish to step down from the committee due to increased work commitments. We would like to thank Thomas for his constructive criticisms, positive and active contributions in the meetings and his support for LES over the years. His presence at the PCM will be missed by the Lab. As a replacement, we are pleased to welcome Professor Horst Geckeis (INE, KIT) to the PCM who we know well from our long-term co-operation with INE and we look forward to working with him over the coming years.

### 1.3 Performance Assessment (PA)

With the announcement of proposed regions for SMA and HAA radioactive waste repositories, the first step of Part 2 of the Sectoral Plan has been completed. Thus step 2 of Part 2 has now begun i.e. the selection of at least 2 sites for each repository type within the potential regions.

LES has contributed to the regional selection process by providing a generic study on the influences of mineralogy and water chemistry on sorption, and a series of generic sorption databases (SDBs) for provisional performance assessment (PA) studies used in the selection of regions. These sorption databases covered the major rock type catagories; argillaceous rocks (five SDBs), granite (five SDBs) and calcareous rocks (one SDB), and the range of water chemistries expected in Switzerland (pHs and ionic strengths), as well as considering reducing and oxidising conditions. With the aim of selecting 2 sites for each repository type over the next 2-3 years the proportion of time spent in LES directly for PA activities will certainly increase. Indeed, the information, databases and modelling results required by Nagra are already factored into the work programme for 2009.

The key issues for PA such as the justification of high sorption values, the transfer of sorption data and models derived from dispersed systems to intact rock and compacted systems, Ra solubility (solid solution formation), $^{14}C$ in small organic molecules produced through anaerobic steel corrosion etc., remain, and will be pursued in the future. However, because of the efforts required in the PA activities, the rate of progress will undoubtedly decrease. This will be true to a greater or lesser extent of all of the research activities currently underway. The momentum will be to some extent maintained through the work carried out by post docs and within PhD projects and through the researchers within LES who are not directly involved in PA activities.

The longer term goal for the realisation of SMA and HAA radioactive waste repositories is an application for general licences, which will be applied for in 2014/2016. It is clear that over the next 10 years or so LES will be intensively involved in the processes leading up to this and what follows.

### 1.4 Foundations of repository chemistry

In preparation for the PA studies required in Phase 2 of Part 2 of the Sectoral Plan, and six years after the publication of the Nagra/PSI Chemical Thermodynamic Data Base 01/01, an update on this database has begun. This update should be finished in the Spring of 2009 since the thermodynamic data needs to be fixed so that water chemistries, solubilities and sorption databases can be calculated/developed within a consistent framework. Within this context, the work being performed in the framework of the OECD/NEA TDB iron review project is still continuing. The amount of time and effort required for this activity was severely underestimated. A very detailed investigation of Fe(II)-carbonate complexes has recently been completed. Here again, what appeared to be a relatively simple task turned out to be considerably more complex than anticipated.

The development of the GEMS-PSI code is continuing but with the main load of this work now being performed through external co-operations and collaborations. The stage has now been reached where the future of GEMS lies more and more in its application. This process is already well underway. The performance of the numerical kernel of the GEMS-PSI code for coupling with fluid mass transport (FMT) is now comparable with that of PHREEQC. GEMS is being applied in a PhD study aimed at understanding the thermodynamics of hydrotalcite– pyroaurite solid solution systems, in the joint JAEA – LES project on radium interaction with clays and minor minerals, and in the reactive transport modelling of Ra retardation in bentonite. Also, within the scope of GEMS-PSI code application, the solid solution model of C-S-H phases has been revised using recent structural and spectroscopic information.

The dissolution rate measurements associated with long-term glass corrosion experiments in LES are still on going, but the focus has shifted to the evaluation of the X-ray spectroscopic data collected in 2007. Micro-XANES results have shown that cerium exists predominantly in the reduced form within the alteration products (clay phases), whereas in the

unaltered core regions of the glass the oxidized form predominates. These results have implications for the fate of Pu in the real glass.

## 1.5 Repository near field

### 1.5.1 Clay systems

Several problems associated with diffusion measurements in compacted swelling clay minerals are being investigated in the TRAPHICCS programme. Measured diffusion profiles in compacted montmorillonite have often shown (apparent) fast and slow diffusion rates which have been interpreted in terms of dual porosity models. Investigations have shown that the more likely explanation is "edge effects" in which the compacted material near the confining filter plates has a different density to the "bulk" material. Once this is taken into account, in Cl diffusion profiles for example, there is no need for a fast and slow diffusion process to explain the results; a single diffusion coefficient is sufficient.

Diffusion experiments in compacted clay samples require confining filters of sintered stainless steel. Investigations have shown that for very thin compacted clay samples, such as required when studying the diffusion of strongly sorbing tracers, radionuclide transport may be dominated by the confining filters. "Flushed filter systems" are being developed to overcome this problem by rapidly saturating the filter plates with tracer. Unlike conventional experimental setups, a "flushed filter" on the high concentration side of the diffusion cell maintains a constant source concentration in contact with the sample, thus imposing a steep tracer gradient through the clay sample right from the start of the experiment. If the source concentration reservoir is sufficiently large, and the flushing efficient, then sorption effects on cell components could be overcome by this technique. 3D-calculations using COMSOL-Multiphysics were carried out in order to investigate the filter's transport properties, to optimise the filter's geometry and to justify the use of 1-D models in the analysis of diffusion experiments. The calculations also provided a good visualisation of what was happening in the "flushed filter". First diffusion experiments are underway using this novel arrangement.

Through-diffusion experiments with HTO, $^{22}Na^{+}$, $^{36}Cl^{-}$ and $^{85}Sr^{2+}$ in Na-montmorillonite at dry bulk densities of 1300 and 1600 kg $m^{-3}$ indicated that the measured effective diffusion coefficients depend on the external salt concentration. Increasing fluxes of cations with decreasing external salt concentrations were observed in accord with previous experiments on samples with dry bulk densities of 1900 kg $m^{-3}$. The conclusion is that the fluxes are driven by the gradients built up by the sorbed cations which are assumed to be mobile in the interlayer pore space.

The influence of carbonate complexation on the uptake characteristics of U(VI) and Eu(III)/Am(III)/ Cm(III) on montmorillonite (INCA, Marie-Curie Euratom Fellowship) has been studied in wet chemistry experiments, modelling, and by various spectroscopic methods; EXAFS, TRLFS. The information yielded in this work was essential for an understanding of factors important for the modelling of the real bentonite/porewater system. The level of understanding is now such that measured sorption isotherms for Ni(II), Eu(III) and U(VI) in bentonite/porewater systems have successfully reproduced in blind modelling exercises using the 2 site protolysis non electrostatic surface complexation and cation exchange sorption model (2SPNE SC/CE).

Reactive transport models are becoming increasingly important tools needed to properly understand and model the transport, sorption and mineral alteration processes occuring in the complex compact mineral assemblages in the near- and far fields. One problem, as always, is the input data required for such models.

Mineralogical transformations at interfaces between cement and clay rocks where strong geochemical gradients are present, are of prime importance for the safety of radioactive waste repositories because mineralogical transformations may lead to the formation of thin layers of precipitated material, so called "skins", which may influence the transport of radionuclides through the system of engineered and geological barriers. Within the framework of an MSc thesis the evolution of the cement-bentonite interface was described based on a simplified, equilibrium thermodynamic geochemical model for cement and bentonite compartments using the "in-house" coupled reactive transport code MCOTAC-GEMIPM2K. In a sensitivity study, the diffusion coefficient and the spatial resolution of the numerical grid were found to have a pronounced effect on the rate of skin development. The aim is to extend the system description towards a more sophisticated treatment of mineral dissolution and precipitation processes.

The THM-transport code Rockflow/Geosys has been coupled with the GEMIPM2K chemical solver. The first application of the new THMC-reactive transport code was to model the transport of radium in the bentonite near field for a case where the geochemistry was described by means of a Ra-Sr-Ba sulphate and carbonate solid-solution model. Such reactive transport simulations can describe the retardation of

radium in sulphate rich bentonite in a more realistic way than the traditional $K_d$ approach.

The modelling of Ni diffusion through bentonite using the 2SPNE SC/CE sorption model ported into MCOTAC has been continued with the aim of elucidating the influence of certain cations (Fe, Mn and Zn) known to be present in the bentonite porewater, on the Ni retardation, and to compare these results with the traditional $K_d$ approach. The calculations have shown that with increasing competition the initial arrival times in the breakthrough curves converge close to those calculated for the "reference $K_d$ case". However, the Ni breakthrough always occurs at a higher concentration level.

### 1.5.2 Cement

Iodide ($^{129}I$), chloride ($^{36}Cl$) and $^{14}C$ species largely determine the long term activity release rate from a cementitious near field into the far field. The uptake of $^{125}I$ ($I^-$) and $^{36}Cl$ ($Cl^-$) by carbonate-containing HTS cement was investigated. The uptake of $^{125}I$ and $^{36}Cl$ by cement decreases with increasing concentration of stable $Cl^-$ in solution. The partitioning of $^{36}Cl$ can be interpreted in terms of isotopic exchange of $^{36}Cl$ between the inventories of stable $Cl^-$ bound by cement matrix and in solution. The influence of stable $Cl^-$ on the $^{125}I$ uptake is somewhat weaker but the mechanism is not yet clarified.

First sorption experiments on cement with $^{14}C$ labelled formic and acetic acids as potential "$^{14}C$ containing small organic molecules" arising from the anaerobic corrosion of carbon steels at high pH showed that acetic acid does not sorb onto cement whereas formic acid exhibited a low $R_d$ value of ~$10^{-4}$ $m^3$ $kg^{-1}$.

Investigations into the interaction of trivalent lanthanides (and actinides) with cementitious systems was carried out in the framework of a PhD thesis with the main aims of corroborating the high sorption values determined in earlier studies and the development a molecular-level understanding of the uptake processes. Using a combination of wet chemistry, EXAFS and TRLFS, the high sorption of trivalent metals on C-S-H phases and hardened cement past (HCP) was confirmed. It was further shown that the Eu(III) uptake mechanisms in tobermorite, for example, is by surface complexation in the short term, with later incorporation in the interlayers and/or substitution for Ca in the Ca layers, i.e. the long term fate of trivalent metals is likely to be incorporation into the C-S-H structure in cementitious systems.

The TRLFS and EXAFS spectroscopy based investigations into the uptake of U(VI) by cementitious materials was continued in 2008. Several U(VI) containing minerals, i.e. soddyite, K-boltwoodite and uranophane, needed as reference compounds for the TRLFS and EXAFS studies, were synthesized and characterized by X-ray diffraction. The main finding was that the TRLFS and EXAFS data supported the idea that C-S-H phases are responsible for U(VI) immobilization in HCP.

Within the 7$^{th}$ EU Framework Programme collaborative project "RECOSY", a wet chemistry and spectroscopy study on the uptake of Np(IV/V) by HCP and C-S-H phases under oxidizing and reducing conditions, is being performed. (This is part of a broader programme of work on sorption under controlled redox conditions.) Sorption experiments with Np(V) on C-S-H phases, and on HCP in artificial cement porewater, showed that the uptake of this pentavalent actinide is unexpectedly high, i.e. $R_d$ values between $10^5$ and $10^6$ L $kg^{-1}$, and >$10^5$ L $kg^{-1}$ respectively. Also, Np(V) exhibited linear sorption in both systems in the equilibrium concentration range between $10^{-6}$ and $10^{-9}$ M. Variations in the Ca:Si ratio of the C-S-H phases and pH (~10.5 to 12.5) had no measurable effect on Np(V) uptake. The similarities in behaviour between C-S-H phases and HCP suggest that C-S-H phases could be the uptake-controlling cement phase for Np(V) in the cement matrix. Also, an electrochemical cell was developed and tested, and analytical methods for the determination of Np(IV/V) in concentrated and dilute solutions were established. This will allow sorption experiments with Np(IV) under controlled redox conditions to be carried out in the near future.

HCP contains large quantities of Fe(III), and the influence of reducing conditions on the long term stability of HCP and its mineral composition is unclear. Such aspects are being investigated in a co-operation with EMPA via a joint PhD project.

The laboratory support for the Mont Terri field experiment on cement-Opalinus Clay interaction (CI project) has shifted to focus on the development of an X-ray micro-diffraction (micro-XRD) technique for characterizing cementitious materials and the cement-clay interface with micro-scale resolution within a collaborative project involving EPFL and the Swiss-Norwegian beamline at the ESRF (Grenoble, France). The first measurements have been performed on thin sections prepared from Portland cement at the Swiss-Norwegian beamline and the micro-XAS beamlines at the SLS and have demonstrated that the identification

of crystalline phases within selected regions of the sample is feasible.

Finally, the foreseen investigations into the potential formation of small organic molecules containing $^{14}C$ as a result of the anaerobic corrosion of carbon steels at high pH was delayed. This work has safety relevant implications and it is imperative that a good start on these investigations is made in 2009.

C-S-H phases are very important components in HCP. However, their structure remains unresolved due to their high degree of disorder and wide compositional variations. Ab initio lattice energy optimization and molecular dynamics simulations have been applied to elucidate the structure, the defect formation mechanisms in the tetrahedral chain, and the interaction of $H_2O$ molecules and solvated Ca ions at the interface with C-S-H phases using crystalline C-S-H minerals such as xonotlite, tobermorite and jennite as model phases. Such a molecular level understanding is expected to bring insights into the macroscopic behaviour and contribute to the understanding of the interaction of radioelements with cementitious phases.

### 1.6 Repository far field

In 2008 the focus of the far field work has remained on Opalinus Clay (OPA).

The results from an in-diffusion experiment with $^{152}Eu$ showed a dual porosity type behaviour, i.e. a fast and a slow diffusion process, similar to that previously measured for $^{60}Co$. First estimates of Eu sorption deduced from the apparent diffusion coefficient of the slow process yielded a value of 100 $m^3$ $kg^{-1}$, which is similar to the values measured previously in batch tests on dispersed systems under similar chemical conditions.

First tests on the homogeneity of the OPA as a function of depth with respect to diffusion properties were performed using HTO as tracer on samples taken from the deep bore hole in the Zürcher Weinland. The diffusion coefficient of HTO decreased by a factor of ~1.5 between a depth of -564 m and -651 m. Similar trends were found for $^{36}Cl^-$ and $^{35}SO_4^{2-}$ where the diffusion coefficients decreased by a factor of ~2.7.

In the DINAPOR project the diffusion of 3 types of nano-particles through OPA was studied (G3=3.6 nm, G5=5.4 nm, and G7=8.1 nm). It could be shown that only the G3 particles with a diameter of 3.6 nm were able to diffuse through the OPA. Although having a diameter smaller than the average diameter of the pores in OPA (~15 nm), the G5 and G7 did not migrate. This effect was explained by anisotropic properties of the slot pore structure in OPA.

Illite is important because it is most probably the main clay mineral responsible for the rentention properties of argillaceous rocks. The physico-chemical, titration and sorption characteristics of Na-Illite have been measured. Protolysis constants and site capacities obtained from the titration measurements have been used in the 2SPNE SC/CE sorption model to model sorption edges for 9 metals with valencies between II and VI. A linear relationship between the logarithm of strong site metal binding constants, $^{S}K_{x-1}$, and the logarithm of the corresponding aqueous hydrolysis stability constant, $^{OH}K_x$, extending over nearly 35 orders of magnitude could be established in a similar manner to that which was previously done for montmorillonite. This is considered to be an important milestone on the way to developing thermodynamic sorption databases. As an essential part of this goal the work on the influence of carbonate complexation on the uptake characteristics of Ni(II), Co(II), U(VI) and Eu(III) on Na-illite ($6^{th}$ EU project FUNMIG, and INCA) has been completed. The results of such investigations are essential to test the ability of the 2SPNE SC/CE sorption model to predict the uptake on argillaceous rocks. In fact, sorption isotherms for Ni(II), Co(II), Eu(III) and U(VI) in OPA/groundwater systems have been successfully reproduced in blind modelling exercises.

The MCOTAC reactive transport code, incorporating the "in house" Cs sorption model, has been applied to successfully model Cs through-diffusion, out-diffusion and mass balance data in OPA. The conventional modelling approach using an experimentally determined non-linear isotherm was unsuccessful. The general conclusion from this work is that a rigorous analysis of tracer diffusion experiments may, in many cases, need to include explicit coupling of transport (diffusion), sorption and water chemistry.

Laboratory support for the long-term diffusion/ retention experiment (DR) in Mont Terri has continued in 2008. The radial diffusion experiments with $I^-$, $Br^-$, $^{36}Cl^-$, $^{22}Na^+$, $D_2O$ and $H_2{}^{18}O$ were finished. Good agreement was found with previous measurements on samples taken from a different location at Mont Terri. Further diffusion tests with $^{85}Sr^{2+}$, $^{133}Ba^{2+}$ and $^{134}Cs^+$ were started in 2008 and are continuing. It is planned to start diffusion measurements with $SeO_4^{2-}$ and $TcO_4^-$ at the beginning of 2009. To verify the appropriateness of the computational tools used for modelling the DR results, benchmarking of the Flotran, Crunch, r3t and

Core2D codes for a well-defined set of input parameters has continued. Differences in the results obtained with different codes were mostly related to inappropriate numerical representations of the system used in the past. In the down-hole injection system it has been demonstrated that the filter has a dominant effect on the transport of strongly sorbing tracers. For conservative and weakly sorbing tracers filter effects are not so important.

The activities on colloid research are restricted to a modest but effective contribution to the "Colloid Formation and Migration" (CFM) work carried out at the Grimsel Test Site. The colloid generation approach followed is considered to be a "first" in this area. The generation of colloids at a bentonite bloc / groundwater flow interface with quasi-stagnant water is being studied from a mechanistic point of view, and an "in house" model has been developed which will be used to describe the generation during the main experiment which is in the process of being designed.

***Table 1.2:*** *LES Organigram (December 2008)*

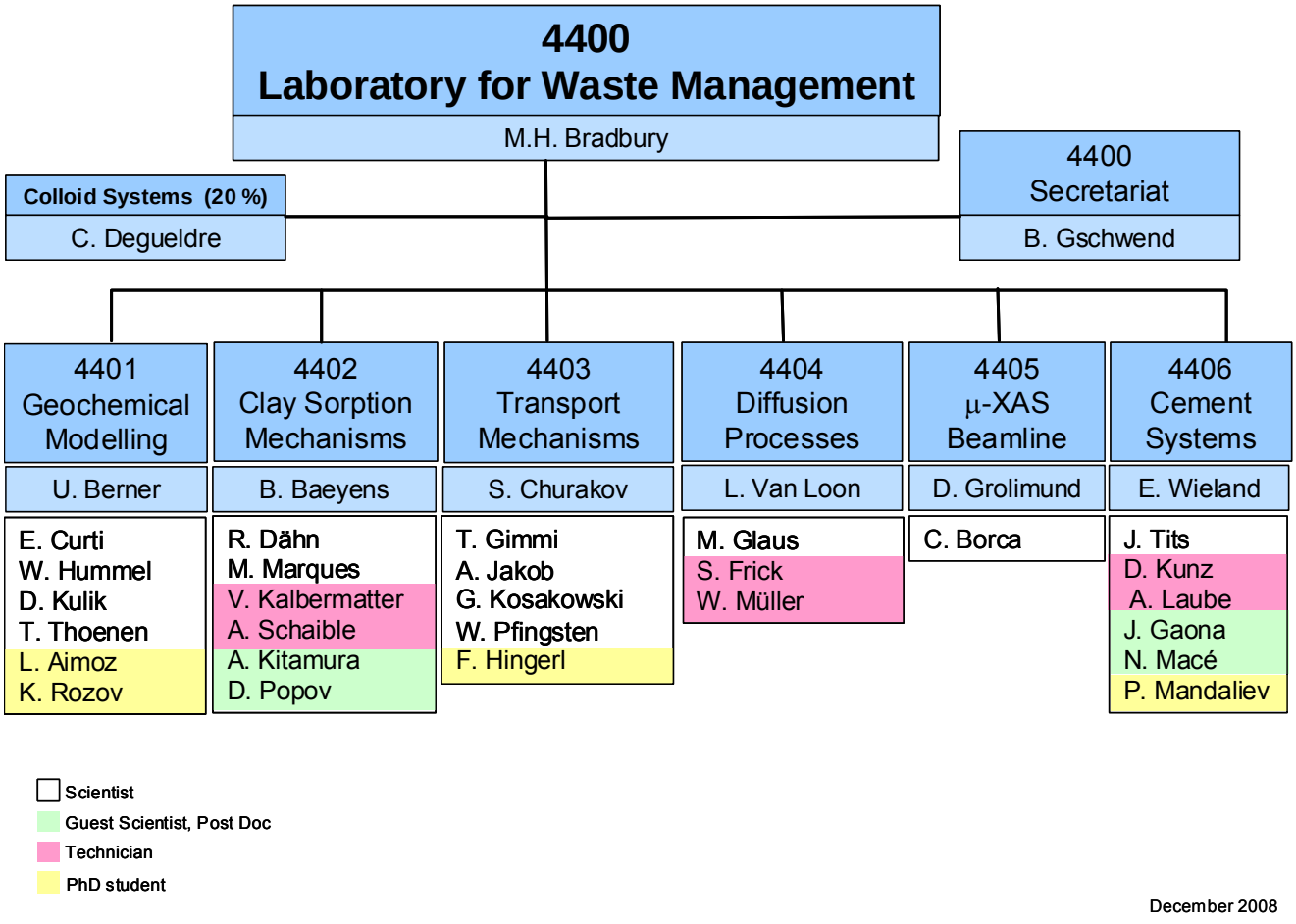

# 2 GEOCHEMICAL MODELLING

*W. Hummel, U. Berner, E. Curti, D. Kulik, T. Thoenen, L. Aimoz, K. Rozov*

## 2.1 Overview

Work related to thermodynamic databases and codes was one important part of our activities.

- Six years after the publication of the Nagra/PSI Chemical Thermodynamic Data Base 01/01 (HUMMEL et al., 2002) an update on the database has begun. The update work started with the actinides, nickel and selected organic ligands.
- Within the scope of the ongoing OECD NEA iron review, a very detailed investigation of Fe(II)-carbonate complexes was performed.
- The numerical kernel of the GEMS-PSI code for coupling with fluid mass transport (FMT) codes has been performance-optimized by introducing a "smart initial approximation" mode with a 10-20 times gain in time. The performance is now comparable with that of PHREEQC.

Characterisation and modelling of solid solution systems was another important part of our activities.

- A PhD study aimed at understanding the thermodynamics of hydrotalcite – pyroaurite solid solution systems is continuing and has yielded estimates of the Gibbs free energies of solids from experimental data.
- Within the scope of the joint JAEA – LES project on radium interaction with clays and minor minerals, work on barite re-crystallisation rates has been performed
- The solid solution model for C-S-H phases (the main phase in hydrated cement paste), which is incorporated in the GEMS-PSI code, has been revised using recent structural and spectroscopic information. A new "semi-rigorous" quaternary solid solution model now provides a better description of solubility data in [Ca]-[Si] and [Si]-C/S space than did the old model.

Activities related to the long-term glass corrosion experiments running at PSI were centred on the evaluation of the X-ray spectroscopic data gathered in 2007.

Teaching duties of W. Hummel as Privatdozent (PD) for "Nuclear Environmental Chemistry" at ETH Zurich included lectures and exercises on nuclear waste management within the scope of the courses "Nuclear Energy Systems" and "Landfilling, Nuclear Repositories and Contaminated Sites".

## 2.2 Thermodynamic databases and software

### 2.2.1 PSI/Nagra Chemical Thermodynamic Data Base 12/07

Six years after the publication of the Nagra/PSI Chemical Thermodynamic Data Base 01/01 (HUMMEL et al., 2002) the update work on the database has begun. December 2007 has been selected as the cut-off date for the inclusion of new published data into the database update. After detailed internal discussions, the authors participating in the update work agreed on guidelines concerning data quality and data categories, inclusion of solid compounds, treatment of weak complexes, and discussion and presentation of the data selection.

Our current concepts concerning data quality and data categories are presented here.

The Nagra TDB version 05/92 (PEARSON & BERNER, 1991, PEARSON et al., 1992) distinguished between two types of data, "core data" and "supplemental data".

Well characterised aqueous species, minerals and gases of elements commonly found in significant quantities in natural waters were included as core data. These data were carefully selected and are widely accepted.

Supplemental, or auxiliary, data were added for elements that are found as minor components in natural waters, or elements that are of interest principally for the safety assessment of nuclear waste facilities. Supplemental aqueous species, and minerals, are usually less well-characterised than those in the core data.

In the Nagra TDB 05/92 the data for the aqueous species and minerals in the core subset were selected individually. In contrast, the supplemental data were selected (imported) in groups, each from one of several existing data sets.

In the Nagra/PSI TDB 01/01 the classification of "core data" and "supplemental data" was retained although the supplemental data were selected individually, either taken from NEA TDB reviews or derived from in-house reviews.

Meanwhile, after 20 years of NEA TDB review projects, currently resulting in the publication of nine volumes of "Chemical Thermodynamics", slowly emerging publications of IUPAC reviews, and our own efforts concerning in-house reviews, as well as our participation in NEA and IUPAC review projects, the historic data categories have to be redefined.

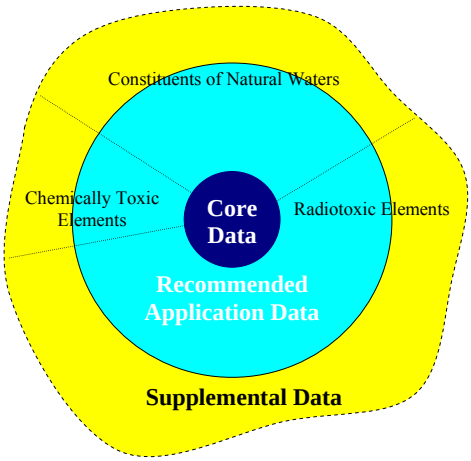


***Fig. 2.1:*** *Data types to be distinguished in the update of the Nagra/PSI TDB 01/01. For a detailed explanation see text.*

**Core Data**: Well characterised aqueous species, minerals and gases of elements involved in almost any type of speciation calculation. These data have been carefully selected and are widely accepted in different fields of application. The core data basically comprise the CODATA key values and some other values of similar quality with almost worldwide acceptance.

**Recommended Application Data:** Well characterised aqueous species, minerals and gases of elements important in different fields of application. These fields of application are (a) modelling of ground and surface waters, (b) safety assessments of nuclear waste repositories and (c) pollution dynamics of chemically toxic substances. The boundaries of the three fields are fuzzy, e.g. Sr is a minor constituent of natural waters but is also of interest as the radiotoxic isotope $^{90}$Sr, and the chemically toxic element Ni has also to be included in safety assessments of nuclear waste facilities as $^{59}$Ni and $^{63}$Ni. The recommended application data are of high quality and well established, but in contrast to the core data, which may not be revised in the foreseeable future, the recommended application data originate from rather active fields of environmental sciences and may be revised and improved over time. Besides the widely used ground and surface water data, high quality data for radiotoxic elements come from the NEA TDB review projects and our in-house reviews, whereas data for chemically toxic elements mainly originate from IUPAC reviews.

**Supplemental Data:** Supplemental aqueous species and minerals are less well-characterised than those in the recommended application data. They comprise of uncertain data, not selected in the NEA TDB and other reviews, but discussed in these reports as suitable for scoping calculations and qualitative modelling. Furthermore, data are included here that are not thermodynamic constants in a strict sense, but which reproduce relevant observations, e.g. the solubility of some tetravalent actinides in neutral and alkaline solutions. Last but not least, estimates are provided for important species where experimental data are missing or unreliable, particularly in cases where omission of such estimated constants would lead to obviously unacceptable results. These estimates are based on chemical analogues, linear free energy relationships or other estimation methods found reliable by the reviewers.

For the elements uranium, neptunium, plutonium, americium and technetium, the Nagra/PSI TDB 01/01 relied on the OECD NEA reviews published before 2002. In the meantime, newer literature on these elements was reviewed by GUILLAUMONT et al. (2003), and these data will serve as a basis for the update of the Nagra/PSI TDB 01/01 to the PSI/Nagra TDB 12/07. The updates for technetium, neptunium, and plutonium have been finished and are documented in PSI Technical Reports.

The update of nickel data is based on the NEA review by GAMSJÄGER et al. (2005). Data on organic ligands were not included in the Nagra/PSI TDB 01/01; these data will now be added based on the NEA review on selected organic ligands by HUMMEL et al. (2005).

### 2.2.2 OECD/NEA TDB iron review

A very detailed investigation of Fe(II)-carbonate complexes was performed in the framework of the OECD/NEA TDB iron review project. One would assume that geochemically important systems such as the ferrous carbonates have been well investigated. Unfortunately, the contrary is the case for the aqueous complexes. Within the last one hundred years very few papers have dealt with the complexation of Fe(II) with carbonate. Only the work of BRUNO et al. (1992), describing the solubility of $FeCO_3$(s) as a function of pH at 298.15 K, provides data that can be evaluated from a quantitative point of view. Fig. 2.2 shows their raw data measured in 1 M $NaClO_4$ at varying pH and $pCO_2$ values.

The measured points suggest three pH-regions, visualized by solid lines in Fig. 2.2, which can be described with the equilibria

$FeCO_3(s) + 2H^+ \leftrightarrows Fe^{2+} + CO_2(g) + H_2O$ ($K_s$)

$FeCO_3(s) \leftrightarrows FeCO_3(aq)$ ($K_1$)

$FeCO_3(s) + H_2O + CO_2(g) \leftrightarrows Fe(CO_3)_2^{2-} + 2H^+$ ($K_2$)

The data in the pH range ~7 to ~8.5 appear to be more or less independent of pH. Considering these data independently of the rest of the experiments, produced $\log_{10}K^0_1 = -(5.39\pm0.18)$. Hence, by using an appropriate value for $K^0_s$, and using the well established carbonate equilibrium for conversion, it should have been possible to derive a formation constant for the reaction $Fe^{2+} + CO_3^{2-} \leftrightarrows FeCO_3(aq)$ ($K_{FeCO3(aq)}$).

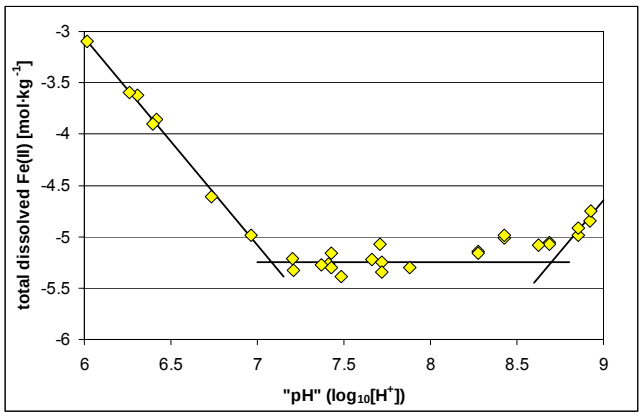


***Fig. 2.2:*** *The solubility of $FeCO_3(s)$ (1 M $NaClO_4$, 298.15 K) as a function of pH at different $CO_2$ partial pressures according to* BRUNO *et al. (1992). The solid lines indicate pH regions where the reactions $K_s$, $K_1$, $K_2$ should dominate the measured Fe(II) concentrations.*

However, it turned out that this assumed simple task included several difficulties related to the determination of $K_s$. Deriving $K_s$ from the data of BRUNO et al. (1992) (which is the most obvious step) revealed that this entity critically depended on the selection of relevant experimental points and on the experimental uncertainties associated with these points. Further, it turned out that a simple regression analysis of the measured Fe(II) concentration against pH produced a slope of 2.027 which is slightly different from the theoretical slope of 2.000. This apparently insignificant difference in slope became critical when attempting to fit the experimental points in the pH range 6 to 8.5 with the chemically correct combined equation $Fe(II)_{tot} = K_s\cdot[H^+]^{2.000}/p(CO_2) + K_1$, because $K_1$ took on meaningless values. Note that the complete equation includes in addition the term $+K_2\cdot p(CO_2)/[H^+]^2$, which defines the constant $K_2$ which arises from an evaluation of the experimental points between pH 8.5 and 9. A further complication is the fact that the fitted solubility product $K_s$ ($\log_{10}K^0_s = 7.32$) from Bruno's data should be consistent with solubility data from other studies and with the finally selected solubility constant for siderite, which in fact it is not. (According to the present state of the TDB project, the selected value for $\log_{10}K^0_s$ will be ~ 7.5±0.2). It is estimated that the formation constant for the reaction $Fe^{2+} + CO_3^{2-} \leftrightarrows FeCO_3(aq)$ will finally be $\log_{10}K^0_{FeCO3(aq)} \sim 4.0\pm0.2$. $\log_{10}K_2$ was found to be -20.86, which converts to $\log_{10}K^0(Fe^{2+} + 2CO_3^{2-} \leftrightarrows Fe(CO_3)_2^{2-}) \sim 4.2\pm0.2$.

Related to the above discussion is the formation constant of the complex $FeHCO_3^+$ which could play a significant role in the pH-range 6.5 to 9 and could substantially complicate the aforementioned evaluation. Indeed, the estimated formation constants reported in the literature range from 10 to about 150 $mol^{-1}\cdot kg$ for this complex. However, a detailed re-analysis of $FeCO_3(s)$ solubility experiments conducted by SMITH (1918) at 30ºC, revealed that this complex most likely does not exist.

It was not expected that an "in principle simple evaluation" would be so sensitive to the uncertainties and to the selection of experimental points. The exercise confirmed that the effort required for evaluating thermodynamic properties from literature data should not be underestimated.

### 2.2.3 GEM-Selektor program package v.2-PSI

The GEMS-PSI code has been under development at LES since June 2000 and this is now mainly being continued through co-operations and collaborations (S. Dmytrieva, Kiev and Th. Wagner, ETHZ). The Nagra/PSI TDB 01/01 and a third-party database Cemdata-07 (http://www.empa.ch/cemdata), have been built into the code making it an excellent tool for advanced geochemical modelling. The GEMS-PSI v.2.2.4 (for Win32, Mac OS X and Linux) is available from http://gems.web.psi.ch (>1100 downloads have been registered so far). More work on the help system, documentation, test examples and tutorials are still necessary.

A further increase in performance of up to 20 times of the numerical kernel GEM IPM2 in coupled codes has been achieved by introducing "smart initial approximation" and "internal mass re-scaling" modes. The former uses the previously calculated equilibrium speciation to start the next GEM IPM2 run, with special criteria for checking its "goodness"; if the

check fails the program switches to the automatic (simplex) initial approximation. The latter mode stabilizes the convergence and numerical behaviour of the GEM IPM2 algorithm by re-setting the internal chemical system definition to a prescribed mass (usually 1 kg). This is crucial for reactive transport problems with nodes of very different sizes. On the other hand, this improvement caused a delay in the preparation of report(s) concerning GEMIPM2K performance optimization, testing, and documentation. Bug-fixing in GEMIPM2K and GEMS-PSI codes was done mainly in connection with the accuracy and stability of fluid mass transport (FMT) – GEM coupling.

In collaboration with Th.Wagner (ETHZ IGMR), the following functionalities were added to the GEMS-PSI code (see http://gems.web.psi.ch):

(1) Modified Ryzhenko-Bryzgalin model for extrapolating equilibrium constants of aqueous complexes to elevated *T,P* (with formation reaction properties $\Delta_r G$, $\Delta_r S$, $\Delta_r H$, $\Delta_r V$, $\Delta_r Cp$).

(2) The Akinfiev-Diamond EoS model for calculating the standard molal properties of aqueous non-electrolyte species at elevated *T,P* ($G^o$, $S^o$, $H^o$, $V^o$, $Cp^o$), was also built into GEMIPM2K.

(3) The Marshall-Franck density model for extrapolating equilibrium constants of aqueous complexes to elevated *T,P* (with the formation reaction properties $\Delta_r G$, $\Delta_r S$, $\Delta_r H$, $\Delta_r V$, $\Delta_r Cp$).

(4) The correlation algorithm PRONSPREP-OH for estimating $S^o$, $Cp^o$ and $V^o$ with HKF EoS parameters for aqueous metal hydroxide complexes.

(5) The NRTL and Wilson mixing models (Phase module) for multicomponent liquid and solid solutions.

(6) Improvement of the Cp-dependent calculations of reaction properties.

### 2.2.4 Sensitivity analysis in the Uncertainty Space

Karpov's concept of pay-off (decision) matrix and functions aimed at identifying the most consistent variant of uncertain GEM input data were tested. The concept was found to be deficient and must be re-formulated for utilizing the available *a priori* information about phase speciation in chemical systems in the context of inverse modelling. This new approach will be used as a generalised fitting procedure to derive Gibbs free energies and their associated uncertainties from experimental data.

## 2.3 Solid Solutions

### 2.3.1 Thermodynamics of hydrotalcites

In the PhD study investigating the thermodynamics of hydrotalcite – pyroaurite solid solution systems, a series of solid phases with compositions $Mg_3Al_xFe(III)_{1-x}(OH)_p(CO_3)_q.zH_2O$ ($p\approx8$; $q\approx0.5$) had been prepared previously. XRD (Rietveld) analysis showed that the lattice parameters $a_0=b_0$ followed Vegard's Law, thus confirming the existence of a solid solution. Chemical analysis of solid phases and their mother solutions have been completed. In order to make a first estimate of the Gibbs free energies of the solids, it was assumed that a true thermodynamic equilibrium exists between the precipitated solid and the mother solution. Individual solutions were modelled using GEMS and the resulting chemical potentials of the solutes, $\mu$, together with the stoichiometric coefficients of the solid composition precipitated from this solution, were used to estimate the Gibbs free energy of the solid according to:

$$\Delta G^0_f = 3\,\mu(Mg^{2+}) + b\,\mu(Al^{3+}) + c\,\mu(Fe^{3+}) + d\,\mu(OH^-) + e\,\mu(CO_3^{2-}) + f\,\mu(H_2O),$$

where b to f correspond to the stoichiometric coefficients of the solid composition. In order to compare the solids on a common basis, the coefficient "f" was set to zero (water free solid). The results are shown in Fig. 2.3, together with the uncertainties. It is evident from Fig. 2.3 that the $\Delta G^0_f$ values are accompanied by huge error bars, which arise mainly from the solid phase analyses.

Each stoichiometric coefficient is associated with an uncertainty originating from the analytical procedure. When the formula is constructed from chemical and TGA results and the analytical uncertainties are included, this leads to a substantially large range of possible stoichiometries. The solid with an Fe mole fraction of $x_{Fe}\approx0.2$ may serve as an example. (Calculated Gibbs free energies are given in parentheses.)

$Mg_3Al_{0.910}Fe_{0.211}(CO_3)_{0.553}(OH)_{8.258}$ (-3802.8 $kJ\cdot mol^{-1}$)
$Mg_3Al_{0.745}Fe_{0.173}(CO_3)_{0.518}(OH)_{7.717}$ (-3577.8 $kJ\cdot mol^{-1}$)

The average of these extremes, i.e., -3690.3 ± 112.5 $kJ\cdot mol^{-1}$, is used as the "experimentally determined value" in Fig. 2.3. Due to the large uncertainties, the present dependency $\Delta G^0_f=f(x_{Fe})$ is still compatible with a mechanical mixture of hydrotalcite and pyroaurite and does not yet allow any conclusions on the solid solution properties to be made. A first step in improving this situation is to improve the quality of the analyses. Work on measuring the solubility behaviour from under saturation (dissolution) using $^{55}Fe$ tracers has begun.

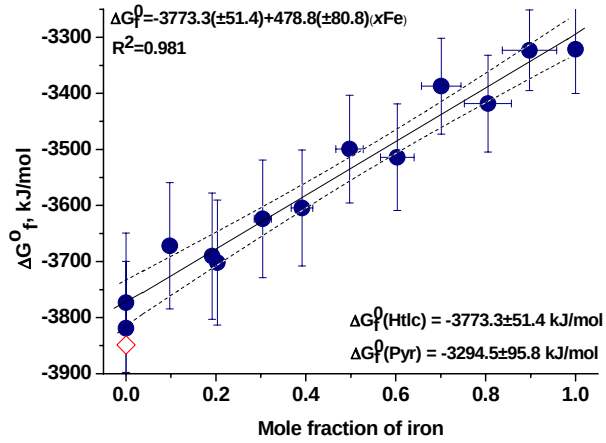


***Fig. 2.3:*** *Plot of the Gibbs free energy of individual solids against the iron mole fraction. The values for the end-members, hydrotalcite and pyroaurite, were calculated from a linear regression analysis and are given in the figure. The only available literature value (ALLADA et al., 2005; calorimetric determinations) is represented by an open red diamond. (See text for uncertainties.)*

### 2.3.2 Radium interaction with clays and minor minerals (JAEA-LES)

In the framework of the co-operation with the Japan Atomic Energy Agency (JAEA) $^{133}$Ba kinetic sorption experiments with barite have been carried out. The goal of these experiments was the determination of barite re-crystallization rates, which are necessary in order to apply thermodynamic solid solution models for the uptake of Ra under saturation conditions. Ra uptake experiments on barite, witherite and calcite, as well as on montmorillonite and illite, are currently being carried out by our Japanese partners.

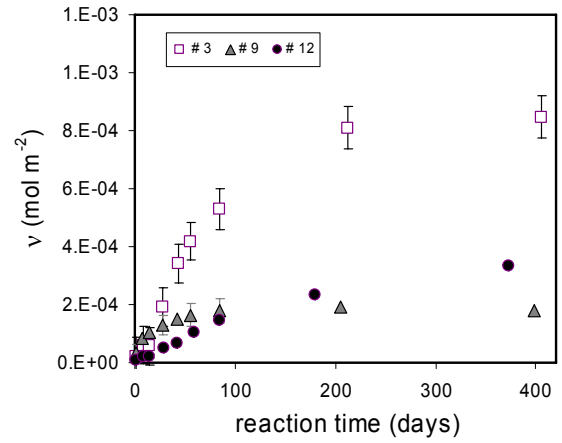


***Fig. 2.4:*** *Re-crystallization kinetics of barite in $10^{-4}$ M $BaCl_2$ (#3), pure water (#9), and $Na_2SO_4$ $10^{-4}$ M (#12). The graph shows the amount of barite re-crystallized per unit surface area as a function of reaction time as calculated from the uptake of $^{133}$Ba tracer.*

The $^{133}$Ba uptake experiments on barite were started in July 2007 and are now almost complete. Currently, a last experiment at pH ~8 is underway. The results so far obtained under slightly acidic conditions (pH~ 5-6) revealed parabolic re-crystallization kinetics with a dependence on solution composition (Fig. 2.4). In $BaCl_2$ and $Na_2SO_4$ solutions, re-crystallization appears to be faster and more prolonged than in pure water. Equilibrium conditions (secession of the re-crystallization reaction) are reached only after 200 days in $BaCl_2$ and $Na_2SO_4$ solutions, whereas in pure water re-crystallization stops already after approximately 90 days. These results are consistent with recent data on the barite precipitation kinetics from oversaturated solutions (KOVACZ et al., 2007).

### 2.3.3 Revision of the C-S-H solid solution model

Quantitative knowledge of the aqueous solubility of C-S-H solid solutions is needed in studies on cement hydration and of waste-cement interactions. Our previous model (KULIK & KERSTEN, 2001, LOTHENBACH et al., 2008) has been useful, but exhibited weaknesses in describing solubility data in the [Ca]-[Si] and C/S – [Si] spaces, which was related, at least in part, to an insufficient connection to the atomistic structures. The improvement of the C-S-H solid solution model is based on the recent structural data supporting the defect-tobermorite-jennite model (RICHARDSON, 2008, CHEN et al., 2004, GARBEV et al., 2008) represented here as a solid solution model with four independent mixing sites:

$$[A^{+2}]_1:[B^{-}]_2:[C^{0}]_2:[D^{0}]_5$$

In our model it is assumed that on the A site the incorporation of a $Ca^{2+}$ ion in the interlayer occurs simultaneously with the removal of a bridging tetrahedron in the silica "dreierketten" chain, and this process is reversible. The excess calcium is incorporated as a $Ca(OH)_2$ moiety, either interstitially in tobermorite, or forming domains of jennite. This was accounted for by the exchange of a vacancy with $Ca(OH)_2$ in the C sites. The occupation of B and D sites was assumed to be fixed as $2CaSiO_{3.5}^{-}$ and $4H_2O$ plus a vacancy, respectively. This led to four end members with stoichiometries depending on the assumed $Ca^{2+}/H^{+}$ ratio in the A sites. Our model has no interlayer $Ca^{2+}$ in a fully polymerized tobermorite TobH (or jennite JenH) and a 1:1 $Ca^{2+}/H^{+}$ ratio in the dimeric TobD (JenD) end member.

The solid solution model was set up in a "semi-rigorous" way as a simple ideal mixture of 4 end members, where $\Delta G_{recip} = 0$ in the reciprocal reaction TobH + JenD = TobD + JenH. This assumption was used to find the $G^{o}_{298}$(TobH) value. No solid solution

at a C/S ratio of < 2/3 was introduced because its existence has not been confirmed by experimental data (CHEN et al., 2004, GARBEV et al., 2008). This system was used in GEM forward modelling of literature solubility data. The JenH end member was insignificant ($x_{JenH}$ < 1%), and the model under-predicted the mean chain length <CL> available from $^{29}$Si NMR measurements (CHEN et al., 2004). Hence, the stability of the JenH end member was increased to fit the <CL> data. This C-S-HQ model (Table 2.1) also provides a good fit to solubility data (CHEN et al., 2004) in [Ca]-[Si], [Ca]-C/S and [Si]-C/S spaces (Fig. 2.5).

The C-S-HQ ideal solid solution model (which also runs on PHREEQC) was fitted to the data of CHEN et al. (2004). It could have been fitted equally well to all other published experimental datasets within the quite moderate $G^{o}_{298}$ brackets shown in Table 2.1, i.e. within 0.2 to 0.6 pK units. Compared to the previous model (KULIK & KERSTEN, 2001), the "semi-rigorous" C-S-HQ model gives a better description of solubility, and it is also consistent with structural/ spectroscopy data such as that for <CL>.

**Table 2.1:** The "semi-rigorous" C-S-HQ ideal model.

| EM | Formula | $G^{o}_{298}$ kJ/mol | $G^{o}_{298}$ range | |
|---|---|---|---|---|
| | | | + | - |
| TobH | $C_{2/3}SH_{1.433}$ | -1652.74 | 1.2 | 2.3 |
| TobD | $C_{5/6}S_{2/3}H_{1.433}$ | -1476.02 | 1.2 | 3.2 |
| JenH | $C_{4/3}SH_{2.4}$ | -2329.35 | 2.9 | 1.8 |
| JenD | $C_{3/2}S_{2/3}H_{2.4}$ | -2145.84 | 1.8 | 1.6 |

Nomenclature: C=CaO; S=$SiO_2$; H=$H_2O$.

Some work still has to be done to make the model "fully rigorous" by properly considering the configurational entropies and ordering around C/S = 1, as well as of density and $H_2O$ content in the C-S-H phases. This provides a way to further extend the model to include Sr, Na, K, Zn, U, REE,… end members.

## 2.4 Glass corrosion, spectroscopy

Activities related to the long-term glass corrosion experiments running at PSI were centred on the evaluation of the X-ray spectroscopic data gathered at beamline X05 (SLS) in August 2007. The behaviour of the redox sensitive elements $Ce^{IV/III}$, $Cr^{III/VI}$, $Fe^{II/III}$ during the long-term corrosion of the MW glass (an inactive simulation of vitrified glass produced at the Sellafield plant, U.K.) was investigated by means of μ-XRF mapping and μ-XAS spectra.

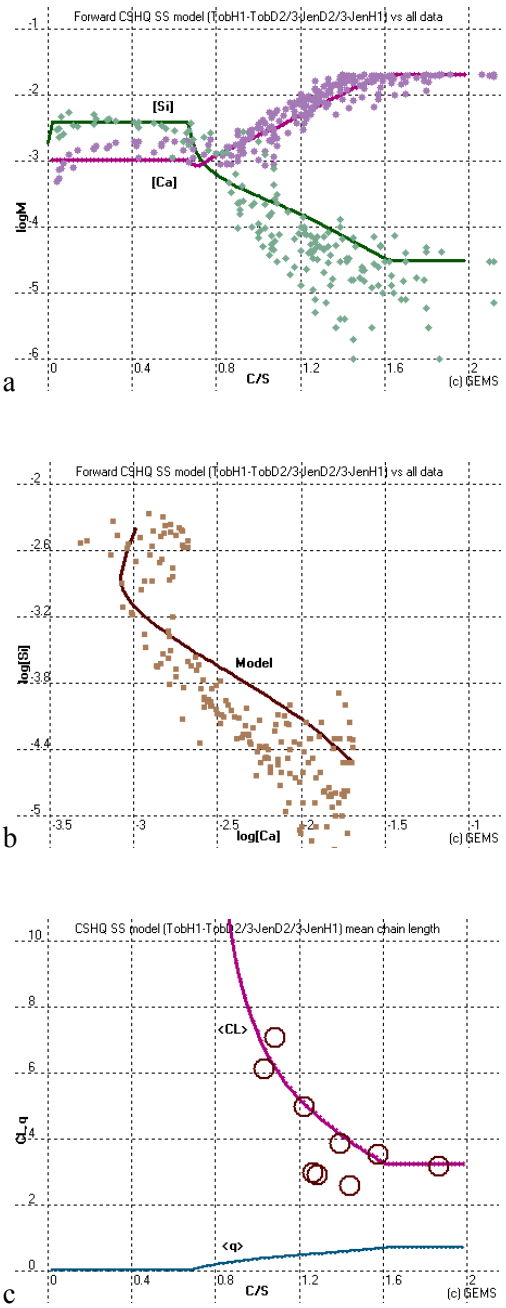


***Fig. 2.5:*** *C-S-HQ model compared with experimental data in [Ca],[Si]-C/S space (a), in [Ca]-[Si] space (b) and in <CL>-C/S coordinates (c). The data are from* CHEN et al. (2004*).*

In the previous annual progress report preliminary results were presented indicating that Ce(IV) from unaltered domains of the glass is reduced to Ce(III) and concentrated in the interstitial secondary phases (Mg-clays). Since cerium was introduced into the glass as a chemical analogue of plutonium, this result suggests that relatively soluble Pu(IV) released from the glass will re-precipitate, almost in-situ, as insoluble Pu(III), thus reducing the mobility of this actinide in the repository system.

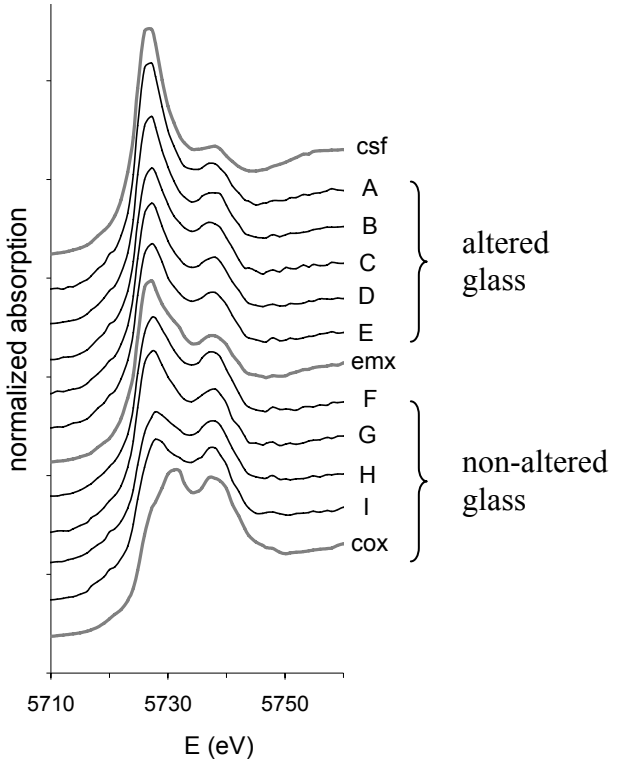


**Fig. 2.6:** *Ce-$L_{III}$ μ-XANES spectra (A to I) collected on the altered MW glass sample compared to Ce(III/IV) reference compounds: csf = $Ce(III)_2(SO_4)_3$, cox=$Ce(IV)O_2$, emx = equimolar mixture of the two latter compounds.*

The μ-XRF results are confirmed by μ-XANES spectra collected in different regions of the glass sample, which show that within the alteration products (clay phases) cerium is predominantly in the reduced form, whereas in the unaltered core regions of the glass the oxidized form predominates (Fig. 2.6).
In order to identify the reducing agents responsible for the Ce(IV) to Ce(III) transformation, other redox sensitive elements present in the glass were investigated, notably Cr and Fe. The collected Fe-K and Cr-K pre-edge spectra (Fig. 2.7) indicate that the predominant oxidation state in the glass sample are Fe(III) and Cr(VI), respectively. In the altered regions, a fraction of the chromium is present as Cr(III). The redox maps shown in Fig. 2.8 indicate that Ce(III) and Cr(III) are spatially correlated, revealing that (in analogy to cerium) Cr(VI) has also been reduced in the course of the glass alteration process. In contrast, no indication for a reduction of Fe(III) was found.

These results indicate that the reducing agent most probably does not originate from the glass, but must be supplied from an external source, probably Fe(0) from the steel container in which the glass leaching experiments were carried out. (Note that in the real system the glass is also surrounded by an iron container.)

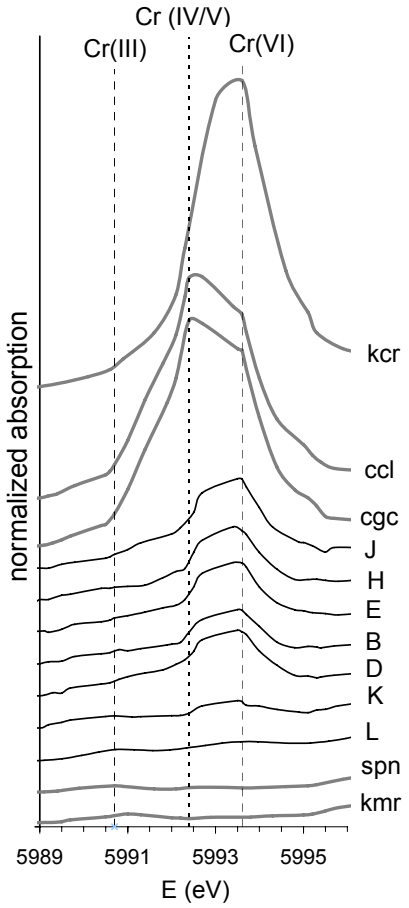


***Fig. 2.7:*** *Cr-K μ-XANES spectra (B to L) collected on the altered MW glass sample compared to Cr(III/IV/V/VI) reference compounds:*
*kmr= kämmererite $(Mg,Fe)_5(Al,Cr^{III})$ $(Si_3Al)O_{10}(OH)_8$*
*spn= Cr-spinel $MgFeCr^{III}$ $O_4$, cgc = $Ca_2(Ge,Cr^{IV})O_4$*
*ccl = $Ca_5(Cr^{V}$ $O_4)_3Cl$, kcr=$K_2Cr^{VI}O_4$.*

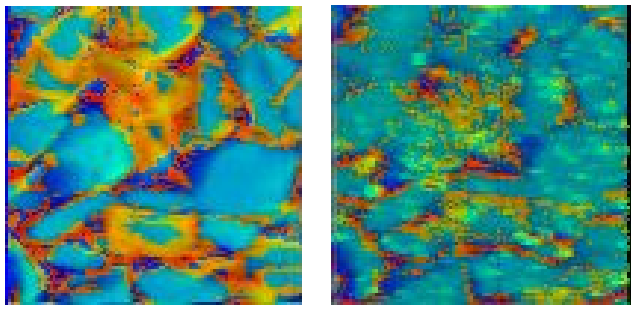

(a) (b)

***Fig. 2.8:*** *Bicolour maps showing the distribution of oxidized (blue) and reduced (orange) species for (a) Ce(IV/III) and (b) Cr(VI/III). In the case of cerium, the colours denote zones with > 50% of either species, whereas for the Cr species the distribution cannot be quantified.*

## 2.5 Other Activities: Teaching at university level

The teaching duties of W. Hummel as Privatdozent (PD) for "Nuclear Environmental Chemistry" at ETHZ included lectures and exercises on nuclear waste management within the scope of the course "Nuclear Energy Systems" (Prasser, Günther, Hirschberg, Hummel, Williams, Zuidema). This course started in the Spring Semester of 2008 with 30 students and will become a compulsory course for the new "Master of Science in Nuclear Engineering" in the Spring Semester of 2009.

In the Autumn Semester of 2008 the yearly course "Landfilling, Nuclear Repositories and Contaminated Sites" given by A. Johnson, W. Hummel and L.M. Plötze were chosen by 31 students. This two hours per week lecture with student's exercises and work on case studies is a "joint venture" of two different departments, i.e. it is eligible for credits for the Majors in Biogeochemistry and Pollutant Dynamics (Master of Environmental Sciences) and compulsory for the Majors in Ecological Systems Design and Waste Management (Master of Environmental Engineering).

## 2.6 References

ALLADA R.K., NAVROTSKY A., BOERIO-GOATES J. (2005)
Thermochemistry of hydrotalcite-like phases in the MgO-Al2O3-CO2-H2O system: A determination of enthalpy, entropy, and free energy. Am. Mineral. 90, 329-335.

BRUNO J., WERSIN P., STUMM W. (1992)
On the influence of carbonate in mineral dissolution: II. The solubility of $FeCO_3$(s) at 25 °C and 1 atm total pressure. Geochim. et Cosmochim. Acta 56, 1149-1155.

CHEN J.J., THOMAS J.J., TAYLOR H.F.W., JENNINGS H.M. (2004)
Solubility and structure of calcium silicate hydrate. Cem. Concr. Res. 34, 1499-1519.

GAMSJÄGER H., BUGAJSKI J., GAJDA T., LEMIRE R.J., PREIS W. (2005)
Chemical Thermodynamics of Nickel. Elsevier, Amsterdam, 617 p.

GARBEV K., BORNEFELD M., BEUCHLE G., STEMMERMANN P. (2008)
Cell dimensions and composition of nanocrystalline calcium silicate hydrate solid solutions. Part 2: X-ray and thermogravimetry study. J. Am. Ceram. Soc. 91, 3015-3023.

GUILLAUMONT R., FANGHÄNEL T., FUGER J., GRENTHE I., NECK V., PALMER D.A., RAND M.A. (2003)
Update on the Chemical Thermodynamics of Uranium, Neptunium, Plutonium, Americium and Technetium. Elsevier, Amsterdam, 763p.

HUMMEL W., ANDEREGG G., PUIGDOMÈNECH I., RAO L., TOCHIYAMA O. (2005)
Chemical Thermodynamics of Compounds and Complexes of U, Np, Pu, Am, Tc, Se, Ni and Zr with Selected Organic Ligands. Elsevier, Amsterdam, 1088p.

HUMMEL W., BERNER U., CURTI E., PEARSON F.J., THOENEN T. (2002)
Nagra/PSI Chemical Thermodynamic Data Base 01/01. Nagra NTB 02-16, Nagra, Wettingen, Switzerland. Also published by Universal Publishers/upublish.com, Parkland, Florida, USA.

KOVACZ M., PUTNIS C.V., PUTNIS A. (2007)
The effect of cation:anion ratio on the mechanism of barite growth at constant supersaturation: Role of the desolvation process on the growth kinetics. Geochim. Cosmochim. Acta 71, 5168-5179.

KULIK D.A., KERSTEN M. (2001)
Aqueous solubility diagrams for cementitious waste stabilization systems: II, End-member stoichiometries of ideal calcium silicate hydrate solid solutions. J. Am. Ceram. Soc. 84, 3017-3026.

LOTHENBACH B., MATSCHEI T., MOSCHNER G., GLASSER F.P. (2008)
Thermodynamic modelling of the effect of temperature on the hydration and porosity of Portland cement. Cem. Concr. Res. 38, 1-18.

PEARSON F.J., BERNER U. (1991)
Nagra Thermochemical Data Base I. Core Data. Nagra Technical Report NTB 91-17, Nagra, Wettingen, Switzerland, 70p.

PEARSON F.J., BERNER U., HUMMEL W. (1992)
Nagra Thermochemical Data Base II. Supplemental Data 05/92. Nagra Technical Report NTB 91-18, Nagra, Wettingen, Switzerland, 284 p.

RICHARDSON I.G. (2008)
The calcium silicate hydrates. Cem. Concr. Res. 38, 137.

SMITH H.J. (1918).
On equilibrium in the system: ferrous carbonate, carbon dioxide and water. J. Am. Chem. Soc. 40, 879-883.

# 3 TRANSPORT MECHANISMS

*S. Churakov, T. Gimmi, A. Jakob, G. Kosakowski, W. Pfingsten*

## 3.1 Overview

Transport modelling in LES is based on an interdisciplinary approach, merging experimental knowledge at the field and laboratory scales, geochemical modelling and mechanistic understanding of transport phenomena in order to assess the performance and evolution of the radioactive waste repository types under consideration in Switzerland. Our research activities in 2008 covered the following areas:

Data acquisition from experiments on the laboratory and field scales (section 3.2)
- Modelling of field experiments in Mont Terri
- Reactive transport modelling of laboratory Cs diffusion experiments
- Design of the experimental setup for laboratory diffusion experiments

Predictive modelling of in-situ repository evolution (section 3.3)
- Reactive transport modelling of porosity evolution in L/ILW repository near field
- Reactive transport modelling of Ra retardation in bentonite

Understanding radionuclide transport mechanisms (section 3.4)
- Reactive transport modelling of Ni in bentonite including competitive sorption
- Molecular modelling of crystalline cement phases

"Know-how" transfer, connection with universities and benchmarking of coupled codes (section 3.5)
- Fluid-rock interaction modelling
- Benchmarking of coupled codes
- Varia

## 3.2 Data acquisition from experiments on the laboratory and field scales

### 3.2.1 Modelling of field experiments in Mont Terri

Diffusion and retention of radionuclides at the field scale are currently being investigated within the frame of the DR project in the Mont Terri Rock Laboratory (Fig. 3.1). We are screening and compiling the transport and sorption data which are then distributed to the other participants. At present, such data are available for HDO, HTO, I, Br, $^{22}$Na, $^{85}$Sr, $^{133}$Ba, $^{137}$Cs, stable Cs, $^{60}$Co, $^{152}$Eu and stable Eu.

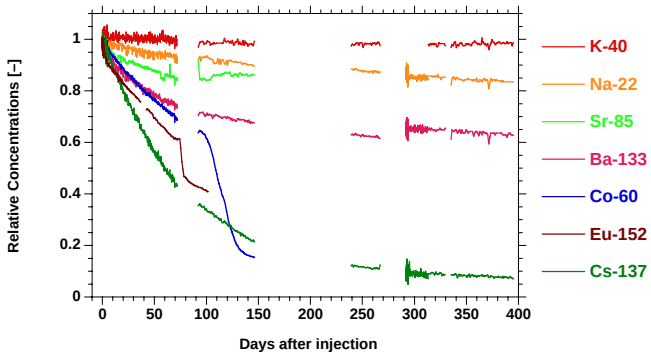


***Fig. 3.1:*** *Decay-corrected, normalised online data of the Mont Terri DR experiment. Note that the Sr and Co data are below the detection limit after about 100 and 150 days, respectively. The sudden decrease of Co concentration after day 90 is probably linked to precipitation effects.*

To verify the appropriateness of the computational tools used for the modelling, we have continued the benchmarking of the Flotran (Gimmi, LES/Uni. Bern), Crunch (J. Soler, CSIC Barcelona), r3t (A. Rübel, GRS Braunschweig) and Core2D (J. Samper und Q. Yang, UDC La Coruña) codes for a well-defined set of input parameters. Some differences were detected between the results obtained with different codes. These differences were mostly related to inappropriate numerical representations of the system used in the past. By explicitly including the filter and the gap of the down-hole injection system into our model we were able to demonstrate that the filter has a dominant effect on the transport of strongly sorbing tracers (Fig. 3.2). First comparisons between measured and simulated data have corroborated these conclusions. For conservative and weakly sorbing tracers the measured borehole data agree reasonably well with the simulation results obtained whether the filter effects are included or not. As DR field-experiment work package leader within the European FUNMIG project we issue progress reports and summaries for the annual meetings.

A draft status report critically assessing the available geochemical data, past and ongoing pore water modelling and transport simulations have been provided within the Geochemical Data project (GD). Together with U. Maeder, Uni Bern, we made a contribution to the chapter on reactive transport modelling (MÄDER & GIMMI, 2008).

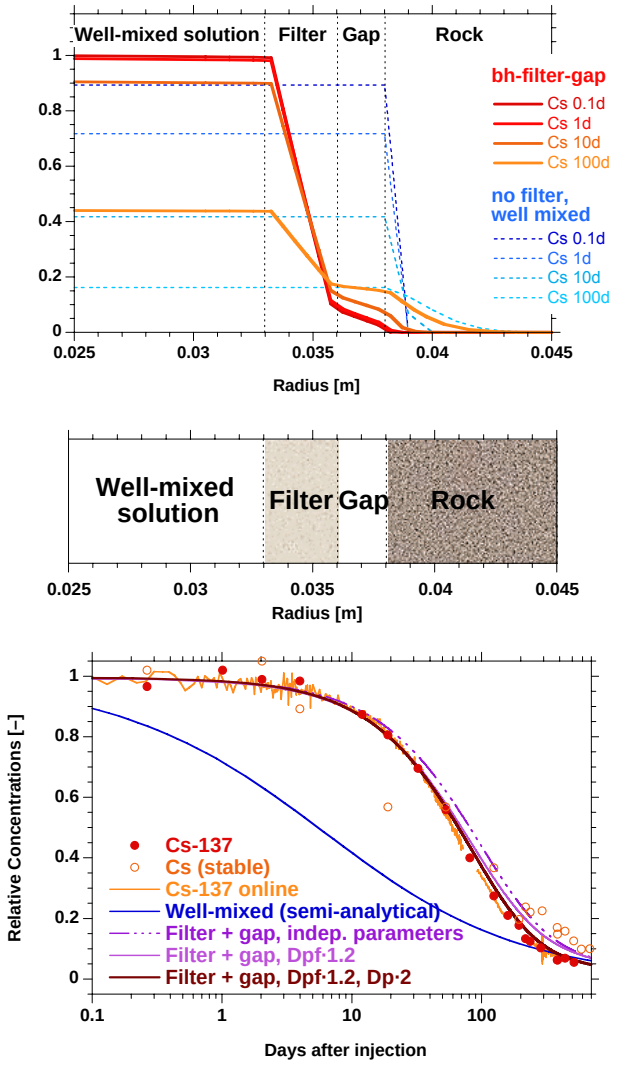


***Fig. 3.2:*** *DR experiment Mont Terri: Data (stable Cs and $^{137}$Cs) and simulations for $^{137}$Cs using different representations of the borehole interval and varying the transport parameters. Top: Concentration profiles. Bottom: Borehole concentration versus time. Well-mixed: parameters obtained independently, but effects of filter and gap ignored. Filter + gap: accounting for effects of filter and gap. The corresponding parameters were either obtained independently (dashed-dotted curve), or the pore diffusion coefficient of the filter Dpf was increased by 20% (Dpf·1.2), and the pore diffusion coefficient for Cs was increased by a factor of 2 (Dp·2).*

### 3.2.2 Reactive transport modelling of laboratory Cs diffusion experiments

In the past, Cs diffusion through Opalinus Clay had been modeled using a nonlinear $K_d$ approach based on sorption isotherms derived form batch experiments. In this approach sorption processes were incorporated into the diffusion equation via a rock capacity factor including a non-linear single-species Cs sorption isotherm. Recent simulations have revealed that this model fails to reproduce the experimental Cs break through curve. A reasonable fit could only be obtained by reducing the experimentally measured sorption isotherm for Cs by a factor of five. Even so, the out-diffusion results and mass balance could not be reproduced using the transport parameters derived from the through diffusion data. Moreover, there is no reasonable explanation for such a sizeable reduction of sorption in the through diffusion experiments. Actually, recent Cs sorption studies on compacted systems indicated that the sorption capacity of dispersed and compacted Opalinus Clay is essentially the same. These conceptual inconsistencies indicated that the coupling of sorption and transport was inadequate.

The flaw in the modelling procedure was eliminated by incorporating a mechanistic sorption model for Cs sorption on illite (BRADBURY & BAEYENS, 2000) into the MCOTAC reactive transport code. In the mechanistic sorption model, contrary to the single sorption isotherm approach, the Cs sorption depends on the composition of the background electrolyte, and so allows any changes in the pore water chemistry to be accounted for in the Cs sorption. Using this approach both the through- and out-diffusion data could be reproduced consistently and in addition the mass balance constraints were satisfied (Fig. 3.3). The value of the Cs diffusion coefficient obtained from the modelling was in good agreement with the results of molecular dynamic simulations (KOSAKOWSKI et al., 2008).

By calculating the concentration profiles in the pore water through the samples we were able to reveal the interplay of the sorption and transport phenomena. When caesium migrates through the Opalinus Clay sample, the cations potassium, sodium calcium, etc. are released into the aqueous phase through cation exchange as the caesium sorbs (Source Cs concentration $10^{-3}$ M). The displaced cations create local gradients which induce fluxes of these major pore water cations in the direction of lower concentration. The increase of potassium, sodium, calcium, etc concentrations due to local diffusive fluxes in the pore water increases the sorption of these cations and in turn influences the retardation of caesium. Thereby the migration and retardation of caesium is fully coupled with the diffusion and sorption of other aqueous species, and thus cannot be addressed by the formalism of a single non-linear sorption isotherm where this coupling is not taken into account.

We conclude that a rigorous analysis of the single tracer diffusion experiments requires an explicit coupling of transport (diffusion), sorption and water chemistry for all of the cations in the system and – last but not least – relies on a state-of-the-art mechanistic sorption model. Single-species sorption models are thus deemed to be inappropriate.

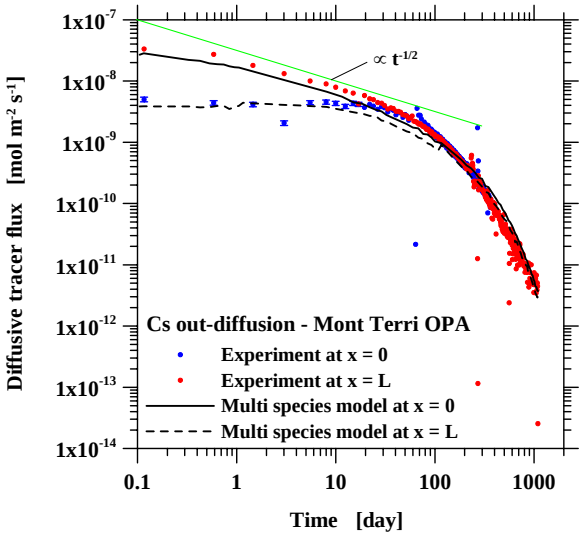


***Fig. 3.3:*** *Blind prediction of caesium out-diffusion measurements in compacted Opalinus Clay based on the MCOTAC code incorporating a mechanistic Cs sorption model and the best-fit value for the effective Cs diffusion coefficient from through-diffusion experiment, obtained using the same model. The $t^{-1/2}$ dependency of the temporal evolution of the flux at the high-concentration side at early times (green line) is indicative of diffusive transport in which the downstream boundary plays only a minor role.*

### 3.2.3 Design of the experimental setup for laboratory diffusion experiments

Diffusion experiments in compacted clay samples require confining filters of sintered stainless steel. Investigations in the past have shown that for very thin clay samples, as needed when studying the diffusion of strongly sorbing tracers, radionuclide transport may be dominated by such filters. The filter effects are especially evident in the transient phase where the diffusive flux is evolving. A potential technique to reduce such effects is to rapidly saturate the filter plates with tracer ("flushed filters") Fig. 3.4. Unlike the conventional experimental setup, a flushed filter on the high concentration side of the diffusion cell maintains a constant source concentration in contact with the sample, thus imposing a steep tracer concentration gradient through the clay sample right from the start of the experiment.

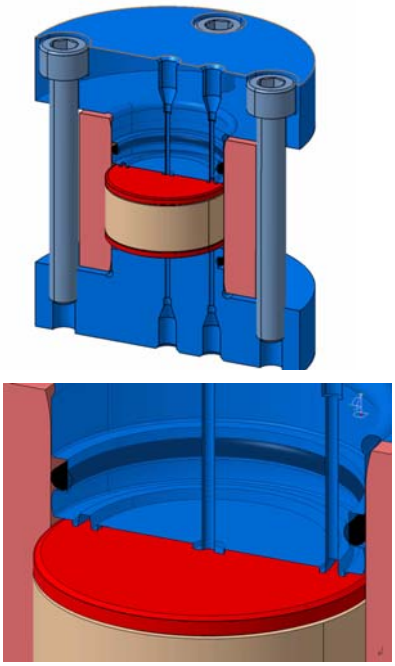

***3.4:*** *Cross-section through the diffusion cell using flushed porous filter plates (top). The filters are drawn in red; the clay sample sandwiched by two filters is shown in brown. In the lower figure an enlarged section of the central part of the equipment is shown. On the right hand side of this figure there is the inlet port on top of a peripheral water-conducting channel distributing the tracer efficiently to the filter plate; in the middle is the outlet port. Steel components are given in blue and pink. The filter diameter is 2.54 cm with a thickness 1.58 mm.*

In order to minimise the number of freely adjustable parameters in the analysis of subsequent diffusion experiments using compacted clay samples, the transport properties of the filters need to be known precisely. 3D-calculations using COMSOL-Multiphysics were carried out in order to investigate the filter's transport properties, to optimise the filter's geometry (i.e. length of necessary tubing, position of inlet- and outlet-ports, etc.) and to justify the use of one dimensional model in the analysis of diffusion experiments. The analysis showed that the transient distribution of the tracer in the filter due to the slow saturation via advection and diffusion is not homogeneous and will have an effect on tracer break-through if thin (~1 mm) clay samples are used. Evolution of the tracer concentration in the filter and at the outlet is illustrated in Figs 3.5 and 3.6, respectively. The first picture shows the steady-state flow field in terms of streamlines. Two subsequent snapshots show the non-uniformity of the tracer distribution in the filter plate after 10 and 25 seconds since tracer injection was initialised.

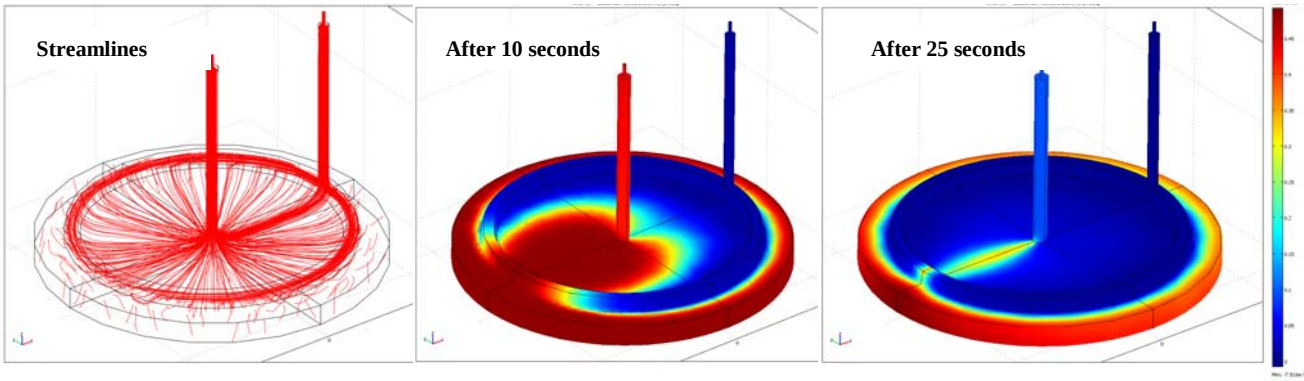


***Fig. 3.5:*** *Distribution of NaCl in a porous stainless steel filter initially saturated with a 0.495 M NaCl solution 10 and 25 seconds after starting to pump pure water into the inlet port (right) which is sitting on top of a peripheral water-conducting channel. The NaCl concentration was monitored at the outlet – the central port. Red means high and blue low NaCl concentrations. The left figure shows the flow field represented by a set of streamlines (red lines) leading from the inlet via the water-conducting channel towards the central outlet.*

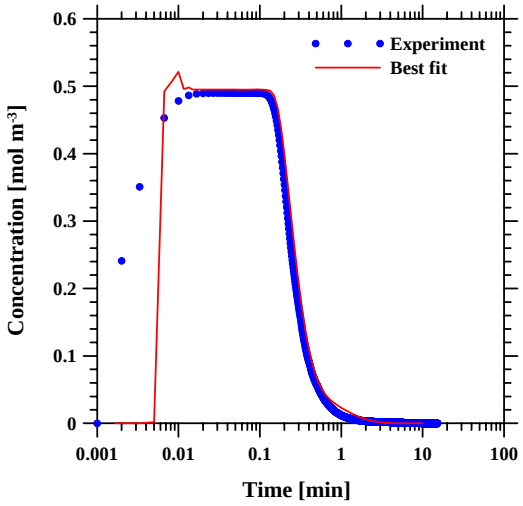


***Fig. 3.6:*** *A comparison of measured (dots) and calculated (solid line) tracer concentrations at the outlet versus time. The tubing attached to both ports was also taken into account in the calculation but is not show in Fig. 3.5). The jagged overshoot in the rising edge of the calculated breakthrough curve is caused by a numerical artefact. The presented best fit is indicative of a small but non-zero mechanical dispersion resulting in a certain tailing of the trailing edge of the breakthrough curve.*

## 3.3 Predictive modelling of in-situ repository evolution

### 3.3.1 Reactive transport modelling of porosity evolution in a L/ILW repository near field

Mineralogical transformations at interfaces between cement and clay rocks where strong geochemical gradients are present, are of prime importance for the safety of a radioactive waste repository. The reason is that mineralogical transformations may lead to the formation of thin layers of precipitated material, so called "skins", which may influence the transport of radionuclides through the system of engineered and geological barriers. Preliminary investigations of the mineralogical evolution at generic clay–cement interfaces were carrier out within the framework of an MSc thesis. The evolution of the cement-bentonite interface was described based on a simplified, but still realistic, equilibrium thermodynamic geochemical model for cement and bentonite compartments using the "in-house" coupled reactive transport code MCOTAC-GEMIPM2K. Advection (Fig. 3.7) and diffusion controlled scenarios were modeled. All simulation scenarios predicted a complex sequence of precipitation/dissolution reactions resulting in a rapid porosity reduction at the interface. In a sensitivity study, the diffusion coefficient and the spatial resolution of the numerical grid were found to have a pronounced effect on the rate of skin development. The aim is to extend the system description towards a more sophisticated treatment of mineral dissolution and precipitations processes. It is planned to introduce kinetic constraints into the geochemical computational module. Similar to the findings of de WINDT et al. (2008), the expectation is that the system evolution will depend strongly on the reaction rates.

The clogging times and porosity evolution obtained in the reactive transport simulation of cement – bentonite interfaces are important parameters for the safety assessment of the repository. The growth and extension of "skins" may control gas and solute transport within the repository. Using empirical porosity-permeability relationships this data will be used by Nagra as input parameters for probabilistic safety assessment calculations (KOSAKOWSKI et al., 2008a, 2008b).

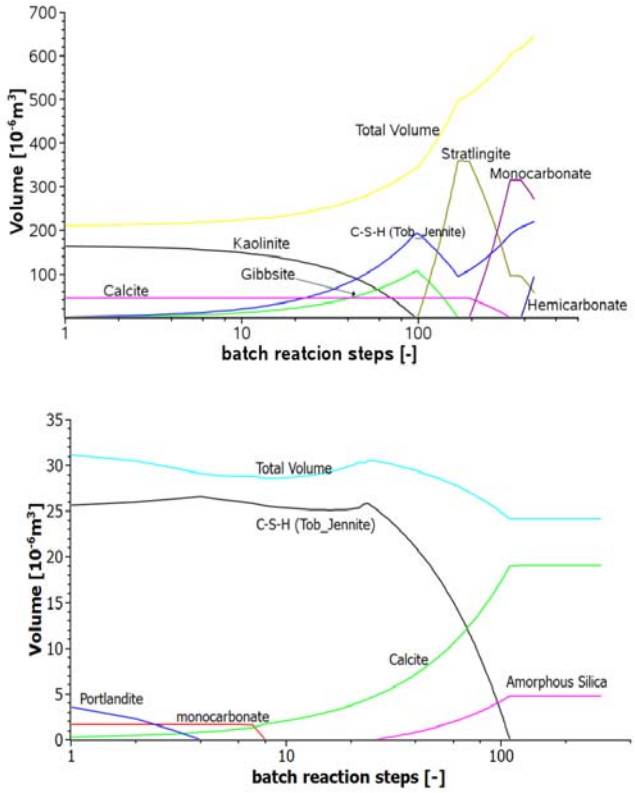


***Fig. 3.7:*** *The evolution of the mineral phase compositions and specific volumes of solid phases in bentonite (top) and cement (bottom) at their interface, is modelled with a batch reaction method. In each batch reaction step the bentonite sample is equilibrated with a fresh amount of cement pore water. In the cement compartment, a batch of cement is equilibrated with bentonite pore water. The equilibrium fluid phase is removed and fresh fluid is introduced to perform a new batch step. The simulations predict increasing cement porosity due to dissolution of portlandite and C-S-H phases, and clogging in bentonite due to the neo-formation of carbonate minerals and C-S-H phases.*

### 3.3.2 Reactive transport modelling of Ra retardation in bentonite

Reactive transport calculations are used to increase the understanding of the influence of competitive chemical processes on radionuclide transport in the complex poly-mineral environment of an underground waste repository. Within a joint PhD project with the Department of Environmental Informatics at the Helmholtz Centre for Environmental Research – UFZ Halle-Leipzig, Germany (Prof. Kolditz), the coupling of the THM-transport code Rockflow/Geosys, developed at the UFZ, with GEMIPM2K chemical solver, developed at LES, was implemented. As a first application of the new THMC-reactive transport code, the transport of radium in the bentonite near field of a nuclear waste repository was calculated. The system geochemistry was described by means of a Ra-Sr-Ba sulphate and carbonate solid-solution model. Depending on the initial inventories of Sr, Ba and sulphate, the non-ideal sulphate and carbonate solid solutions can fix mobile radium cations. Thanks to an improved treatment of the geochemistry, the reactive transport simulations can describe the retardation of radium in sulphate rich bentonite in a more realistic way than the traditional linear $K_d$ approach (Fig. 3.8). In a next step the plan is to incorporate other sorption processes such as cation exchange and surface complexation reactions to investigate competitive sorption effects on Ra transport.

## 3.4 Understanding radionuclide transport mechanisms

### 3.4.1 Reactive transport modelling of Ni competitive sorption in bentonite

The modelling of Ni diffusion through bentonite using the 2SPNE SC/CE model ported into MCOTAC has been continued with the aim of elucidating the influence of certain cations (Fe, Mn and Zn) known to be present in the bentonite pore water on the Ni retardation and to compare the results with the traditional $K_d$ approach. Fig. 3.9 shows the calculated Ni breakthrough in the bentonite for increasing sorption competition resulting from the sequential inclusion of Fe, Fe + Mn and Fe + Mn + Zn into the bentonite water at different concentration levels. The Ni breakthrough without competition occurs earlier than when the "optimistic value for $K_d$" (NTB-02-05) is used, but is much later than for the "pessimistic $K_d$ value". However, with increasing competition, the initial arrival times in the breakthrough curves converge close to the one calculated for the "reference $K_d$ case". However, the Ni breakthrough always occurs at a higher concentration level. The reference $K_d$ value stems from batch sorption experiments in which Fe, Mn and Zn were present, and therefore this sorption value for Ni implicitly includes competitive effects from these metals. The break-through curves are very similar with respect to the initial arrival time but not with respect to the maximum Ni concentration level. The $K_d$ approach includes an "unlimited" sorption capacity, whereas the finite site capacities in the mechanistic sorption model are responsible for the Ni breakthrough at a higher level.

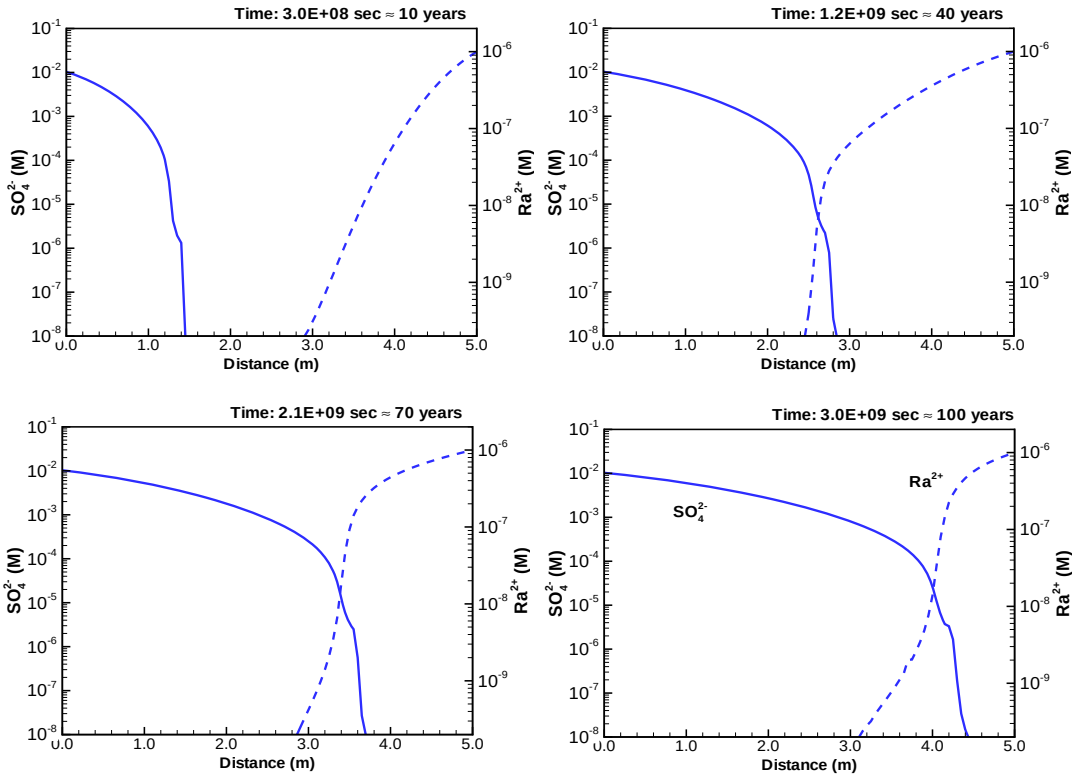


***Fig. 3.8:*** *The temporal evolution of sulphate and radium aqueous concentration profiles in a one-dimensional bentonite column after 10, 40, 70 and 100 years; solid lines are $SO_4^{2-}$ and dashed lines are $Ra^{2+}$ concentrations. Sulphate is entering the column from the left and $Ra^{2+}$ from the right.*

It must be realised that if the concentrations of Fe, Mn and Zn are different in the real system from those in the batch measurements then the batch tests will yield a false $K_d$ value whereas the mechanistic sorption model in MCOTAC will automatically take care of the changing system chemistry. Thus the sorption $K_d$ data from batch tests are only valid for a fixed water and solid chemistry and would not be applicable for cases in which the bentonite is degrading and the water chemistry is changing. Preliminary calculations show that the sorption site capacity has the largest effect on the Ni breakthrough amongst all competitive effects. Therefore, the temporal evolution of the bentonite degradation and other precipitation and dissolution reactions at the canister-bentonite interface could be important for Ni migration and will need to be investigated in more detail. Calculations for an appropriate spatial resolution of the simulation grid take as long as several weeks when repository specific transport parameters are used, even for one-dimensional problems. Therefore, parallelisation of MCOTAC is becoming urgent.

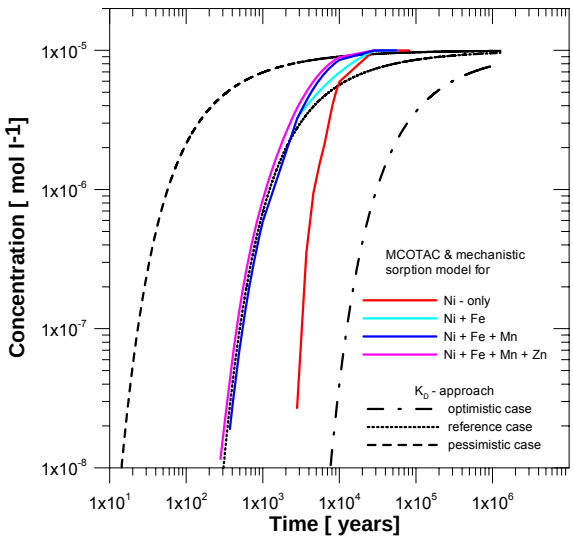


***Fig. 3.9:*** *Calculated Ni concentration in the bentonite buffer 46 cm away from the canister surface (red line). Further calculations account for the effects of sorption competition between Ni and Fe, (Ni, Fe and Mn), and (Ni, Fe, Mn and Zn). The mechanistic sorption model of BRADBURY & BAEYENS (2005), ported into MCOTAC, was used to capture the competitive effects. For comparison, results from calculations based on the simple $K_d$ approach using bounding pessimistic and optimistic $K_d$ values for nickel (NTB-02-05) are also shown.*

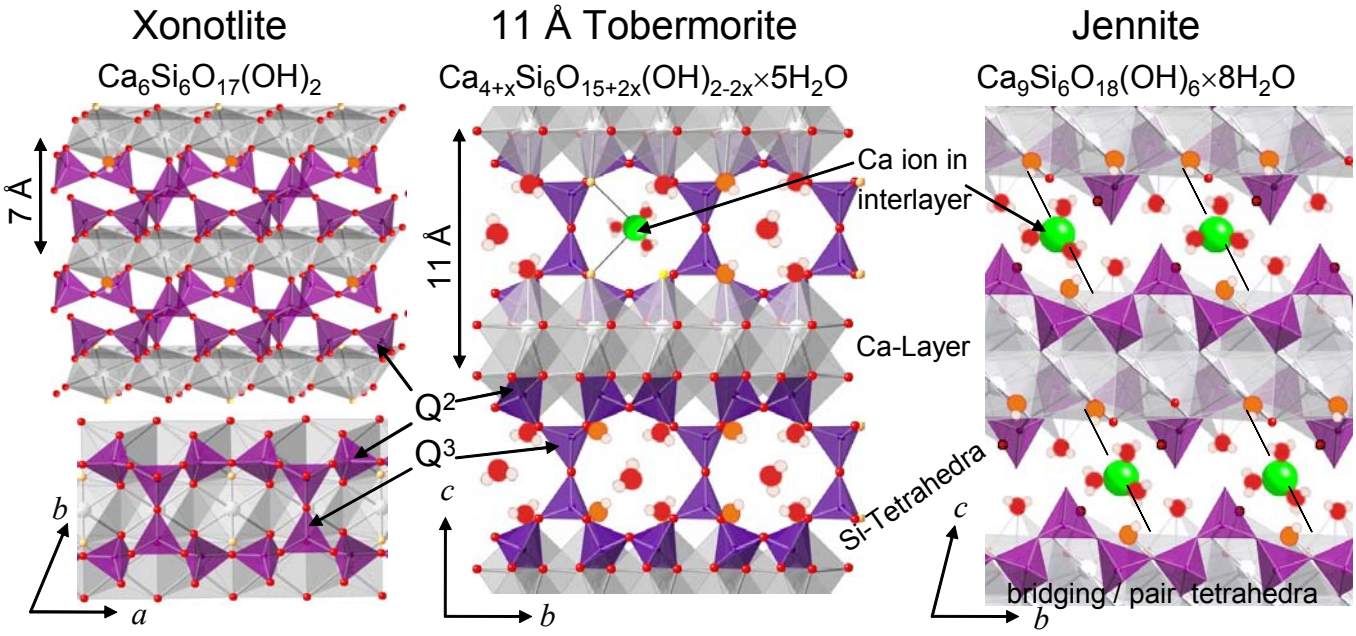


***Fig. 3.10:*** *Basic structural elements of xonotlite, 11 Å tobermorite, and jennite. The Ca layers are shown as gray shaded polyhedra. Chains of Si tetrahedra are violet-blue. Oxygen sites within the Ca layer are shown as small red spheres. $H_2O$ molecules and OH groups are schematically shown as large red spheres - oxygen and small light pink spheres – hydrogen. Ca ions in the interlayer of 11 Å tobermorite and jennite are shown as large green spheres.*

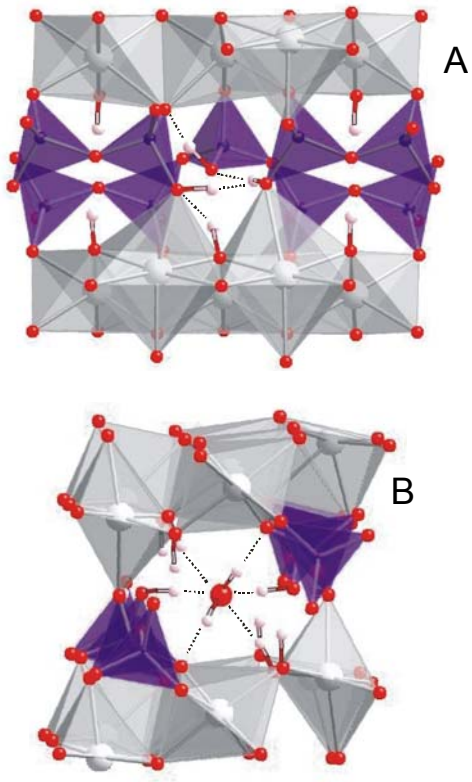


***Fig. 3.11:*** *Distribution of OH groups in the $Q^3$ defects of the tetrahedral chain in xonotlite. A single $Q^3$ defect (A). A coupled defect in neighbouring $Q^3$ sites (B).*

### 3.4.2 Molecular modelling of crystalline cement phases

Amorphous calcium silicate hydrate (C-S-H) phases are important components in cement materials. Their structure remains unresolved due to their high degree of disorder and wide compositional variations. Crystalline C-S-H minerals such as tobermorite and jennite are considered as structural analogues for amorphous C-S-H phases. The $SiO_2$-tobermorite and tobermorite-jennite solid solutions, for example, have been proposed to describe the thermodynamic properties of the so called C-S-H-I and C-S-H-II phases, respectively. Ab initio lattice energy optimization and molecular dynamics simulations have been applied to elucidate the structure, the defect formation mechanisms in the tetrahedral chain, and the interaction of $H_2O$ molecules and solvated Ca ions at the interface with C-S-H phases.

The basic structural elements of the studied crystalline C-S-H phases - xonotlite, 11 Å tobermorite, and jennite - are shown in Fig. 3.10. All three phases are built up of layers of six and seven coordinated calcium polyhedra. Wollastonite-like chains of Si tetrahedra are attached to both sides of the Ca-layers. In xonotlite and 11 Å tobermorite, neighbouring tetrahedral chains are joined to form a double chain. The framework of the Si-double chain holds the Ca layer together and constrains the interlayer distance in tobermorite at 11 Å.

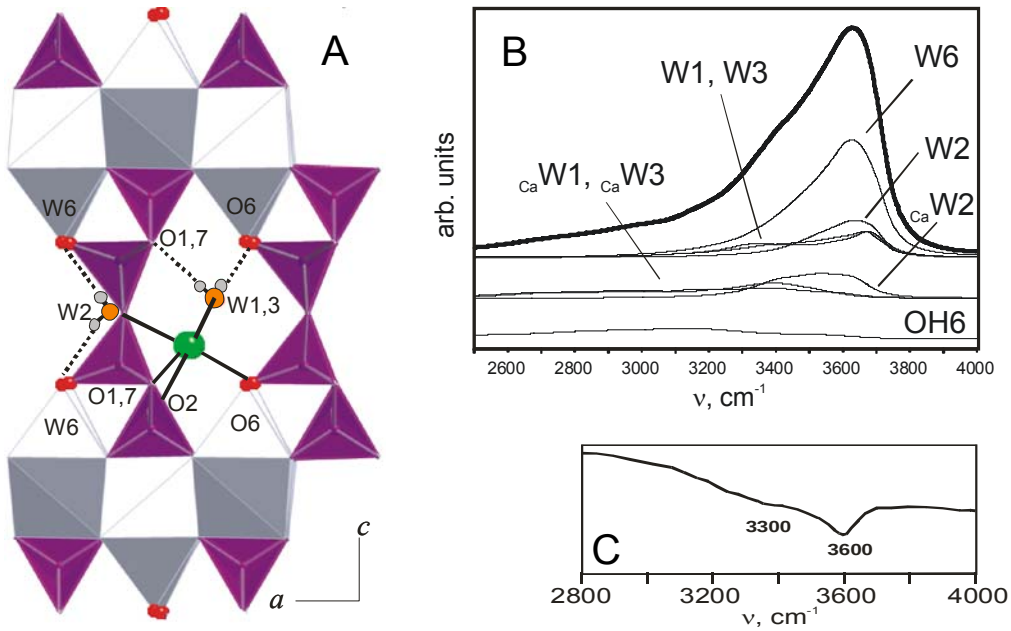


***Fig. 3.12:*** *Structure of the hydration sphere and the optimal position of the Ca ion in the interlayer of 11 Å tobermorite (A). Calculated vibrational density of state in 2500-4000 $cm^{-1}$ frequency range (B, thick solid line). Individual contributions of distinct crystallographic sites to the total vibrational density of states are given by the thin solid lines. The subscript "Ca" in front of "W" (B) indicates water molecules in the coordination sphere of the interlayer Ca ion. The measured IR absorption spectra of 11 Å tobermorite (C) are taken from YU et al.,1999.*

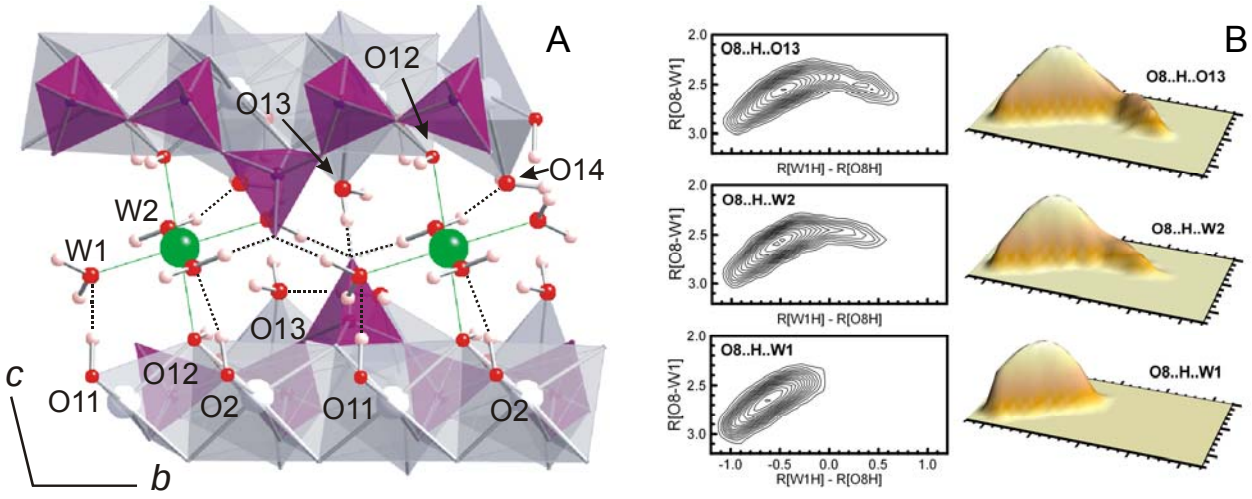


***Fig. 3.13:*** *Equilibrium distribution of $H_2O$ molecules, OH groups and interlayer Ca ions in the structure of jennite (A). Free energy landscapes ($-F^*(kT)^{-1}$) for proton transfer reactions among O8…H-OX contacts (where OH is W1,W2,W3; k is the Boltzmann constant and T is temperature) as a function of O8-OX distances and O8H-OXH distance differences. The contour lines of the free energy profile are shown for every 0.5 units of the reduced energy.*

In jennite, neighbouring layers are attached through the interlayer Ca ions. Based on NMR studies, it was suggested that the disordered crystallite C-S-H phases, with defects in the tetrahedral chain, resemble the basic structural elements of the amorphous C-S-H phases.
The defect formation mechanism in the tetrahedral double chain of C-S-H phases was investigated using xonotlite. It was found that Si defects in $Q^3$ tetrahedra positions (Fig. 3.10) are energetically more stable compared to the $Q^2$ sites. Moreover, coupled defects in neighbouring $Q^3$ sites are more stable than isolated $Q^3$ defects. The structure of single and coupled defects in the tetrahedral double chain of xonotlite is shown in Fig. 3.11.
The simulations suggest that coupled $Q^3$ defects are able to incorporate water molecules even in an anhydrous phase such as xonotlite. Interlayer space in 11 Å tobermorite is occupied by water molecules and Ca ions. The interlayer Ca ions are readily substituted by other cations making tobermorite an efficient cation exchanger and a sorbent for radionuclides. The hydration mechanism and the distribution of water molecules in the interlayer of 11 Å tobermorite were studied using ab initio molecular dynamics simulations. Fig. 3.12 (A) illustrates the equilibrium orientation of a Ca ion on the surface of 11 Å tobermorite.

The calculated vibrational density of states is in good agreement with measured IR spectra (Fig. 3.12 (B,C)). The analysis of the individual contributions to the vibrational density of states helps to explain the nature of distinct absorption bands in the IR spectra of tobermorite. Based on bond valence calculations it was argued that the dangling oxygen sites (O8, Fig. 3.13) of the bridging tetrahedra in the jennite structure are de-protonated. Such a de-protonated oxygen site should behave as a strong acceptor of hydrogen bonds and a strong sorption site for foreign cations in the jennite interlayer. Free energy profiles for the proton exchange reactions between water molecules and the O8 site of the bridging tetrahedra derived from ab initio molecular dynamic trajectory at 300 K are shown in Fig. 3.13. The results indicate that water molecules in the interlayer of jennite occasionally donate protons to the dangling O8 sites. The free energy barriers for such proton transfers are of the order of 12-30 kJ $mol^{-1}$ (Fig. 3.13, (B)).

By considering the disordered structure of the crystalline C-S-H phases, the chemical behaviour of the structural fragments in amorphous C-S-H phases can be accessed. Calculated defect formation energies in xonotlite suggest that the defects in C-S-H phases are preferentially formed in the $Q^3$ sites of the double chain or bridging tetrahedra of a single chain, while the paired tetrahedra (the $Q^2$ sites in the double chain) are undisturbed. Such a conclusion is consistent with experimental observations of fully depolymerised paired Si tetrahedra in the structure of C-S-H phases at Ca to Si ratios above 1.5. The calculations suggest that the dangling oxygen sites on the bridging tetrahedra are strong acceptors of protons on the surface of C-S-H phases. In an aqueous solution the de-protonated oxygen sites on the Si tetrahedra are the primary sorption sites for cations.

## 3.5 "Know-how" transfer, connection with universities and benchmarking of coupled codes

### 3.5.1 Fluid-rock interaction modelling

In November 2008 a joint PhD project on the simulation of geochemical processes in Enhanced Geothermal Systems (EGS) was started between LES and the Institut für Isotopengeologie und Mineralische Rohstoffe of the ETH Zürich. The project is fully funded by the Competence Centre for Environment and Sustainability, ETHZ. The project is aimed at developing a geochemical model for hydrothermal water-rock interactions at elevated temperatures and studying the effects of geometrical heterogeneities on the large-scale permeability, heat and solute transport. The thermodynamic database and modelling expertise developed within this project can be used later in the reactive transport modelling of the evolution of the repository near field at realistic (elevated) temperatures.

### 3.5.2 Benchmarking of coupled codes

The benchmarking studies belong to ongoing long term activities in the group. In co-operation with ENSI, formerly HSK, the benchmarking of several transport codes used in performance assessment calculations was initiated. Several codes are also being benchmarked in the Mont Terri field diffusion experiments (see section 3.2.1).

### 3.5.3 Varia

In order to extend our expertise in the field of reactive transport modelling, a post doc proposal entitled "Two dimensional investigations of reactive transport processes at heterogeneous interfaces" was submitted to the NES department’s competition for financial support. The proposal focuses on a case study of clogging processes at chemically and mineralogicaly heterogeneous interfaces. Included are also design calculations for future experiments at the laboratory scale to measure/confirm model parameters and

predictions of the system evolution such as "skin thickness" and "skin propagation" at cement/ bentonite/clay interfaces. We are very pleased to report that we won this competition and plan to have a post doc in position by April 2009.

A joint experimental-theoretical post doc proposal entitled "Accessing heterogeneities on the microscopic scale and implementation of such structures in a 3D transport models for compacted argillaceous materials" was submitted to the PSI FoKo. The project is aimed at tomographic investigations of 3D heterogeneities in clays materials on the micro- and meso-scales. The 3D-porosity/connectivity models derived from tomography measurements will be ported into the COMSOL/Multiphysics code. Again, we have pleasure in reporting that this post doc position (in co-operation with CEA) has been approved and the candidate is expected to begin in March 2009.

During the open day celebrating the 20th anniversary of PSI, the Geosphere Transport Group produced a DVD covering some of the experimental and modelling activities within LES ("multiscale research") in order to increase the visibility and the public acceptance of the work carried out in LES.

In co-operation with the Laboratory for Neutron Scattering (Dr. F. Juranyi) a PhD proposal entitled "Water Dynamics in Clays", dealing with diffusion of water through clays, measured at different scales, has been submitted to the Swiss National Science Foundation. The proposal was successful and we are starting the search for a new PhD candidate. This PhD work is a follow up to the work recently completed by Dr. González-Sánchez.

## 3.6 References

KOSAKOWSKI G., MÄDER U., PFINGSTEN W. (2008)
A proposal for inclusion of geochemical FEPs in the Integrated Flow Code. PSI internal report AN-44-08-01, Paul Scherrer Institut, Villigen PSI, Switzerland.

KOSAKOWSKI G., MÄDER U., PFINGSTEN W. (2008)
Progress report of the expert group on the "Implementation of geochemical FEPs in the Integrated Flow Code". PSI internal report AN-44-08-02, Paul Scherrer Institut, Villigen Switzerland.

MÄDER U., GIMMI T. (2008)
Reactive Transport and Tracer Transport Modelling. In: P. Wersin, Th. Gimmi, O. Leupin, U. Mäder, J. Pearson, T. Thönen, Ch. Tournassat, Mont Terri Geochemical Data (GD) Project – Geochemistry of pore waters in Opalinus Clay at Mont Terri: experimental data and modelling, In preparation, Mont Terri Technical Note.

DE WINDT L., MARSAL F., TINSEAU E., PELLEGRINI D.
Reactive transport modelling of a geochemical interaction at a concrete/argillite interface, Tournemire site (France), Physics and Chemistry of the Earth, in press, doi: 10.1016/j.pce.2008.10.035.

YU P.; KIRKPATRICK R.J.; POE B.; MCMILLAN P.F., CONG X.D (2008)
Structure of calcium silicate hydrate (C-S-H) : Near-, mid-, and far-infrared spectroscopy.
Journal of the American Ceramic Society 1999, vol. 82, no 3, 742-748.

# 4 CLAY SYSTEMS

*B. Baeyens, M. Bradbury, R. Dähn, M. Marques-Fernandes, V. Kalbermatter, A. Schaible*

## 4.1 Summary

Within the framework of the Sachplan Geologische Tiefenlagerung (Sectoral Plan) a report has been written in which generic sorption databases (SDBs) were generated for argillaceous, crystalline and calcareous rocks for groundwater compositions covering the ranges measured in the corresponding systems in Switzerland.

The clay minerals montmorillonite and illite are important with respect to the sorption characteristics of bentonite and Opalinus Clay respectively. The main aim of the investigations into these clay minerals is to elucidate their sorption properties and develop (quasi) mechanistic sorption models to quantitatively describe the uptake of radionuclides over a wide range of conditions (pH, Eh, water chemistry, radionuclide concentration). A milestone was reached in the current year in that a linear free energy relationship (LFER) between surface complexation constants and the corresponding hydrolysis constant was established for illite. Such a relationship is regarded as an important component in the development of sorption databases founded on thermodynamic principles.

In natural systems, the predominant aqueous phase reactions of radionuclides are hydrolysis and complexation with dissolved inorganic ligands e.g. carbonates. The formation of carbonate complexes in solution can influence the sorption of radionuclides in natural systems. Investigations relating to this topic were embedded within the 6$^{th}$ EU Framework Programme.

The work carried out during 2007 in the integrated project FUNMIG was focussed on the modelling of isotherm measurements of Eu(III) on Opalinus Clay in a realistic water composition. The surface species formed by the uptake of Am(III) and U(VI) on montmorillonite and illite in the presence of inorganic carbon were studied using TRLFS and XAS spectroscopic methods at KIT (at the INE and ANKA facilities) and at FZD (IFR). These investigations were carried out within the framework of two EU projects, i.e. INCA and ACTINET. EXAFS measurements on Np(V) sorption on montmorillonite in the absence and presence of inorganic carbon were carried out at the Rossendorf Beamline (ROBL, ESRF, Grenoble).

Maria Marques joined the Clay Sorption Mechanisms Group in November 2008.

## 4.2 Performance assessment

The sorption of radionuclides on materials in the near field (bentonite) and the far field (host rock) of a radioactive waste repository is one of the main pillars upon which the safety case for a deep geological repository is founded (NAGRA, 2002). One of the primary tasks of the Clay Sorption Mechanisms Group is to ensure that near- and far field sorption databases (SDBs) for performance assessment are "state of the art". Within the framework of the Sectoral Plan generic sorption databases for the main host rock types in Switzerland (crystalline, argillaceous and calcareous) have been developed (BRADBURY et al., 2008). The groundwater compositions used in this study covered the ranges of experimental data measured for the corresponding rocks. These SDBs provided part of the information required to enable a transparent, defensible and robust selection of the regions in Switzerland suitable for sighting radioactive waste repositories to be made (NAGRA, 2008).

One of the main features of this work was it's generic nature. For crystalline and argillaceous rocks, arguments were presented that the main factor influencing sorption is the phyllosilicate (clay minerals and micas) content. The magnitude of sorption is directly correlated with the phyllosilicate content and the parameter which best reflects the sorption potential of a mineral assembly is the cation exchange capacity (CEC).

The second component essential to the development of the SDBs is water chemistry. Generic water compositions were extracted from numerous analyses of different deep groundwaters from various geological formations in Switzerland. In order to cover the range of ionic strength (I) and pH values of Swiss groundwaters for argillaceous and crystalline rocks, 4 types of generic groundwaters were defined for each rock type, high I /high pH, low I / high pH, high I / low pH and low I /low pH.

As a starting point for developing generic SDBs, the existing Opalinus Clay (OPA) reference SDB (BRADBURY & BAEYENS, 2003) and crystalline SDB (STENHOUSE, 1995) were taken. These two SDBs were modified and updated to yield an argillaceous reference SDB and a crystalline reference SDB. These two SDBs were then used to create generic in situ SDBs for crystalline/argillaceous rock types using

"conversion factors". The aim was to convert the sorption values in the reference SDBs into sorption values appropriate to the mineralogical and water chemistry conditions for the particular generic case considered. Conversion factors were used to account for (i) mineralogy, (ii) pH and (iii) radionuclide speciation. Further, to account for the fact that the sorption data used was measured in batch tests on dispersed systems, and the in situ conditions relate to intact rock, a Lab→Field conversion factor was applied in the generic SDBs for crystalline/ argillaceous rocks.

Calcareous rock types were treated separately. Sorption data on calcite are extremely sparse and there is a general lack of understanding on the uptake mechanisms. However, from the pool of existing sorption data an acceptable linear correlation was obtained if the log $R_d$ values were plotted against the ionic radii of the respective metals, i.e. a sort of linear free energy relationship (LFER). Many of the sorption values given in the SDB for calcareous systems were taken from this LFER and complemented the sparse experimental data.

### 4.3 Sorption studies on illite

The physico-chemical, titration and sorption characteristics of Na-illite have been measured and modelled. Samples of illite, collected in the region of le Puy-en-Velay, France, were purified and conditioned to the Na-form and physico-chemically characterised. Some of the previous measurements (BRADBURY & BAEYENS, 2005), particularly the titration experiments, were repeated with Na-illite that was "acid treated" in order to remove a Ca phase which was shown to influence titration and sorption data in the low pH range.

Potentiometric titrations on suspensions of the Na-illite were carried out from pH ~3 to ~11.5 in an inert atmosphere glove box. A batch titration technique with backtitration was used to measure the acid/base characteristics of conditioned Na-illite at three background $NaClO_4$ concentrations (0.01, 0.1 and 0.5 M). The data are shown in Fig.4.1 as symbols. The purpose of the backtitration approach chosen was to take into account the effects of the clay dissolution as a function of pH and thus obtain a net titration curve reflecting the protolysis behaviour of the amphoteric edge sites only. In addition, the influence of cation exchange reactions, principally $H^+$-$Na^+$ exchange and $Al^{3+}$-$Na^+$ (pH < 5) exchange, on the titration curve were included in the analysis of the data.

The titration data were modelled in terms of the protolysis of two amphoteric edge sites ($\equiv S^{W1}OH$ and $\equiv S^{W2}OH$) without an electrostatic term. The model parameters are summarised in Table 4.1 and were used to calculate the continuous curve in Fig. 4.1.

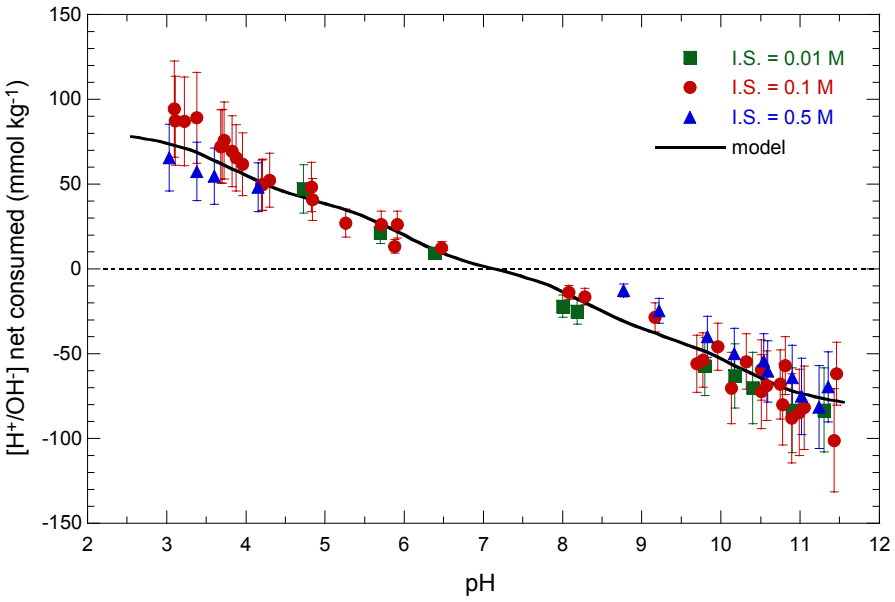


***Fig. 4.1:*** *Titration data for Na-illite at 0.01 M, 0.1 M and 0.5 M $NaClO_4$. The continuous line is calculated with the 2-site protolysis non electrostatic (2SPNE) model and the parameters given in Table 4.1 for the $\equiv S^{W1}OH$ and $\equiv S^{W2}OH$ edge sites.*

***Table 4.1:*** *Summary of site types, site capacities and protolysis constants determined for Na-illite using the 2SPNE model.*

| Amphotheric edge sites | | Protolysis reactions | Constants (log K) | | |
|---|---|---|---|---|---|
| Type | Capacity (mol/kg) | | $\equiv S^{S}OH$ | $\equiv S^{W1}OH$ | $\equiv S^{W2}OH$ |
| $\equiv S^{S}OH$ | $2 \times 10^{-3}$ | $\equiv SOH + H^{+} \Leftrightarrow \equiv SOH_2^{+}$ | 4.0 | 4.0 | 8.5 |
| $\equiv S^{W1}OH$ | $4 \times 10^{-2}$ | $\equiv SOH \Leftrightarrow \equiv SO^{-} + H^{+}$ | -6.2 | -6.2 | -10.5 |
| $\equiv S^{W2}OH$ | $4 \times 10^{-2}$ | | | | |

Cation exchange capacity for Na-illite = 225 meq/kg (BAEYENS & BRADBURY, 2004)

Sorption edges for Ni(II), Co(II), Eu(III), Sn(IV) at trace concentrations have been determined on Na-illite suspensions. All experiments were carried out in inert atmosphere glove boxes ($CO_2 \leq 2$ ppm, $O_2 \leq 2$ ppm.). The site types, their capacities and protolysis constants obtained from the modelling of the titration results were fixed in the modelling of the sorption edge data. The uptake at trace concentrations in such experiments could be described very well for all of the metals investigated in terms of surface complexation on a set of strong sites, $\equiv S^{S}OH$, with a fixed capacity, and cation exchange on planar exchange sites. It is interesting to note that the sorption model developed for montmorillonite i.e. a 2 site protolysis non electrostatic surface complexation and cation exchange (2SPNE SC/CE) model, was used to describe the titration and sorption data obtained for illite. This work has been accepted for publication in Geochimica et Cosmochimica Acta (BRADBURY & BAEYENS, 2008a).

Sorption edge measurements were extended to include Am(III), Th(IV), Pa(V) and U(VI) and the uptake of these actinides on Na-illitte was also modelled with the 2SPNE SC/CE sorption model. In addition, two further data sets for the sorption of Am(III) and Np(V) on Illite du Puy obtained from the literature (GORGEON, 1994), could also be modelled. Thus, surface complexation constants for the strong sites in the 2SPNE SC/CE sorption model for 9 metals with valence states from II to VI have been obtained. A linear relationship between the logarithm of strong site metal binding constants, $^{S}K_{x-1}$, and the logarithm of the corresponding aqueous hydrolysis stability constant, $^{OH}K_x$, could be established for illite for these 9 metals (BRADBURY & BAEYENS, 2008b). This correlation is presented in Fig. 4.2.

Such correlations are often termed Linear Free Energy Relationships (LFER), and although they are quite common in aqueous phase chemistry, they are much less so in surface chemistry, especially over this large range, nearly 35 orders of magnitude. The LFER for illite could be described by the equation:

$$\log {}^{S}K_{x-1} = 8.0 \pm 0.4 + (0.83 \pm 0.02) \log {}^{OH}K_x$$

where "x" is an integer.

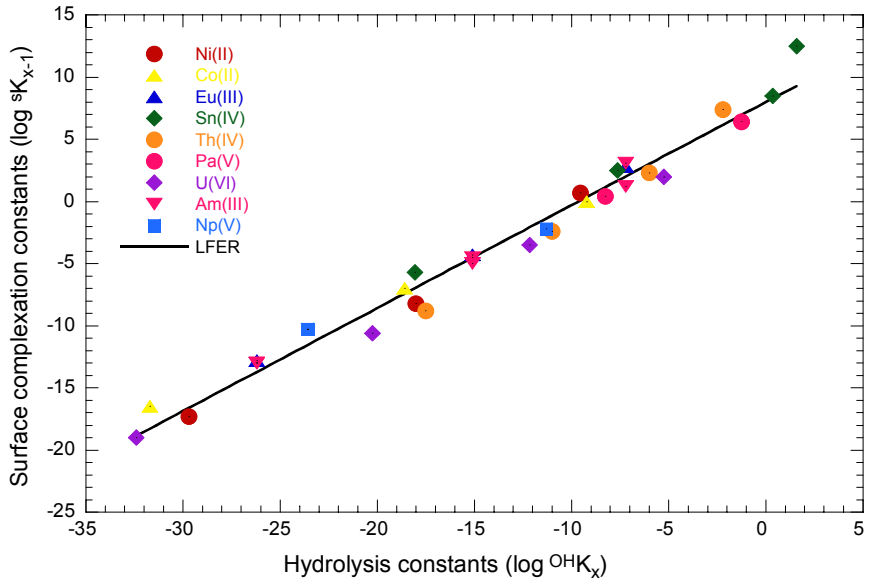


***Fig. 4.2:*** *Correlation of surface complexation constants of metal species sorbing on the strong sites of illite ($^{S}K_{x-1}$) with the corresponding aqueous hydrolysis constants ($^{OH}K_x$), Linear Free Energy Relation. The least squares relation between log $^{S}K_{x-1}$ and log $^{OH}K_x$ is given by: log $^{S}K_{x-1}$ = 8.0 ±0.4 + (0.83 ±0.02) log $^{OH}K_x$.*

A similar relationship has been previously obtained for montmorillonite. Thus LFERs relating to sorption on two of the most important clay minerals present in natural systems have been established. Such an LFER approach is an extremely useful tool for estimating surface complexation constants for metals in a chemically consistent manner. It provides a means of obtaining sorption values for radionuclides for which there are no measured values and hence allows gaps in missing sorption data to be filled. An ultimate goal of this approach is to develop a thermodynamic sorption database. This could then be used in radioactive waste management performance assessment studies to calculate sorption in natural systems for any given water chemistry, and thereby replace the current usage of single solid/liquid distribution coefficients ($K_d$ values) to describe radionuclide uptake.

## 4.4 6th EU Framework Projects

In natural systems, the predominant aqueous phase reactions of radionuclides are hydrolysis and complexation with dissolved inorganic ligands e.g. carbonates. When attempting to model radionuclide sorption in natural systems it is important to be able to quantify the influence of such complexation reactions.

Within the framework of various 6th EU framework programme, the effect of dissolved inorganic carbon on the sorption behaviour of metals onto montmorillonite and illite has been quantified, and the 2SPNE SC/CE sorption model applied to derive ternary surface complexation constants where appropriate. The main goal was to extend this (quasi) mechanistic sorption model to radionuclide sorption onto clay minerals by including the influence of carbonate complexation.

### 4.4.1 FUNMIG IP

Sorption edge and isotherms for Eu(III) on purified Na-illite in the absence of inorganic carbon had already been measured and modelled previously using the 2SPNE SC/CE sorption model (red symbols and solid line in Fig. 4.3). The influence of inorganic carbon on Na-illite has been studied and the effect is shown by the blue symbols in Fig. 4.3. An important outcome from the modelling was that the sorption data in the presence of inorganic carbon (p-$CO_2$ = $10^{-3.5}$ bar) could only be quantitatively described if ternary Eu(III) carbonate surface complexes ($\equiv SOEuCO_3^0$ and $\equiv SOEuOHCO_3^-$) were included in the modelling (solid blue line).

A sorption isotherm at Eu(III) equilibrium concentrations between $10^{-10}$ and $10^{-7}$ M was determined in a synthetic porewater at pH 8 on an Opalinus Clay sample from Mont Terri.

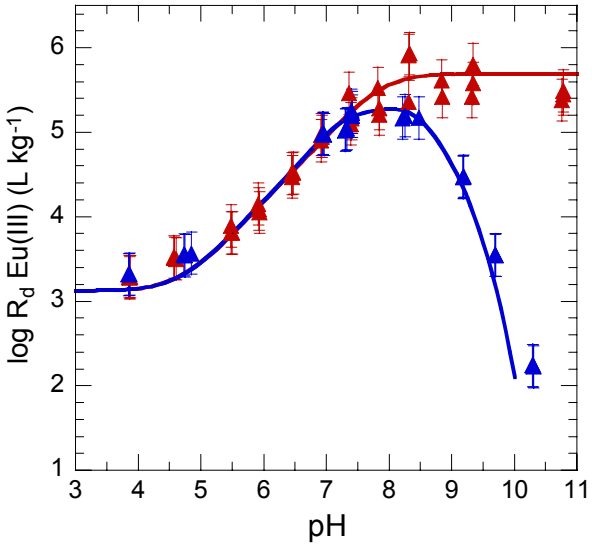


***Fig. 4.3:*** *Sorption edge of Eu(III) on Na-illite in the absence (▲) and presence (▲) of inorganic carbon. Experimental and modelling*

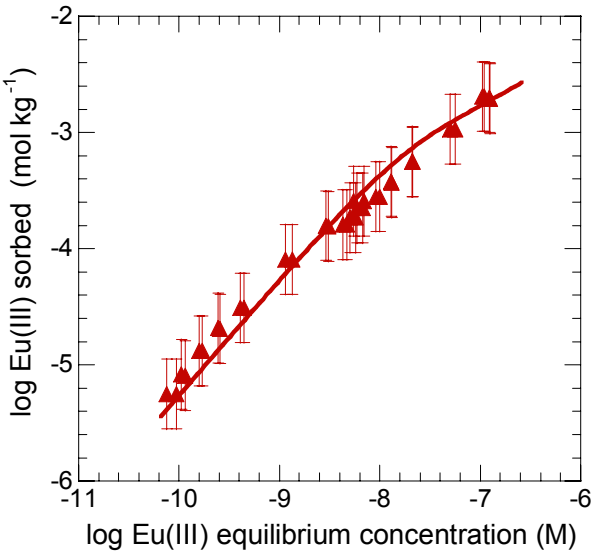


***Fig. 4.4:*** *Sorption isotherm of Eu(III) on Opalinus Clay in a synthetic porewater (pH 8). Experimental and modelling results.*

Fig. 4.4 shows the experimental data together with the modelling (solid red line). Clearly, the predicted sorption data agreed very well with the measured data. In this "bottom-up" exercise the modelling was carried out under the assumption that the illite present in the Opalinus Clay is the main sorbate and that ternary Eu(III) carbonate complexes are formed on the edge sites of illite.

The successful modelling of sorption isotherms on Opalinus Clay for Eu(III) (trivalent actinide analogue) together with the previous modelling results for Ni(II), Co(II) and U(VI) using the 2SPNE SC/CE sorption model are strong indicators that the approach used here can be applied for calculating sorption values in performance assessment.

### 4.4.2 INCA

The influence of dissolved inorganic carbon on the sorption behaviour of actinides (Am(III), U(VI)) onto clay minerals was investigated by applying Time Resolved Laser Fluorescence Spectroscopy (TRLFS) and Extended X-ray Absorption Fine Structure (EXAFS) measurements. The EXAFS measurements were performed at the Rossendorf Beamline (ESRF, Grenoble) at the uranium $L_{III}$ edge at 17166 eV. Cm(III) TRLFS measurements were performed at the Institut für Nukleare Entsorgung (KIT, Karlsruhe).

*Sorption of trivalent actinides on clay minerals: TRLFS studies*

TRLFS measurements were performed on Cm(III), loaded kaolinite (Na-KGa-1, 0.13 wt.% structural Fe) and γ-$Al_2O_3$ (iron free reference compound) in the presence (20 mM $NaHCO_3$) and absence of inorganic carbon at 17 K. In a preliminary step iron poor minerals were chosen to investigate the influence of carbonate on the sorption of Cm(III) in order to avoid any fluorescence quenching by Fe.

The Cm(III) TRLFS measurements were carried out on wet clay pastes (0.1 M $NaClO_4$ background electrolyte, Cm(III) loading ~ 0.06 µmol/g).

The excitation spectra of the Cm(III) kaolinite samples were measured by scanning the excitation wavelength in the range of the $^6D_{7/2} \rightarrow {}^8S_{7/2}$ transition [595–625nm] and recording simultaneously the corresponding Cm(III) emission spectra. Fig. 4.5a shows the excitation spectra of Cm(III)/kaolinite in the absence (black line) and presence of carbonate (red line). Fig. 4.5b shows the fluorescence emission decay curves of Cm(III) obtained for both systems by exciting at two different wavelength. A similar behaviour was observed in the γ-$Al_2O_3$ system.

The fluorescence features (red-shift and the shape of the excitation spectra, increase of the fluorescence lifetime) of the Cm(III)-carbonate-mineral systems differ strongly from those of the carbonate free systems. This is indicative of different coordination environments for Cm(III), supporting the formation of ternary An(III)-$CO_3$/(hydroxy)$CO_3$ complexes at the clay surface postulated in the macroscopic studies.

*Sorption of U(VI) on clay minerals: EXAFS studies*

Macroscopic sorption experiments have shown that the presence of inorganic carbon leads to a strong decrease of the sorption of U(VI) on montmorillonite. EXAFS measurements were performed on U(VI) loaded self supporting clay films. The investigated samples were prepared at pH ~8 in the absence and presence of 1 mM $NaHCO_3$. Table 4.2 summarizes the experimental conditions used for the U(VI) sorption on Na-SWy-1.

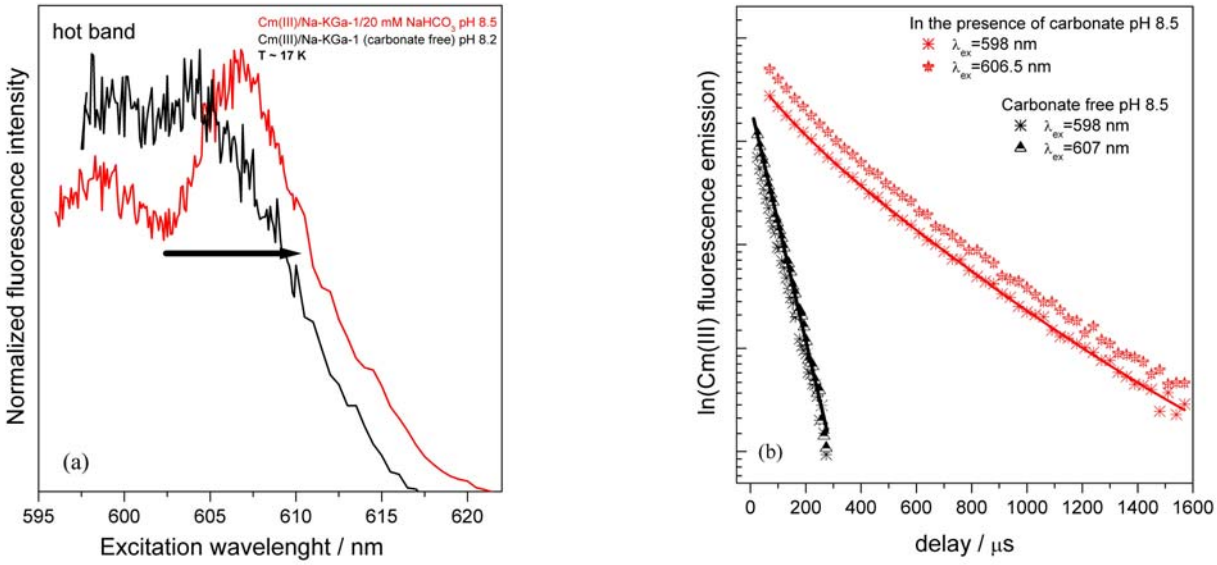


***Fig. 4.5:*** *a) Excitation spectrum of Cm(III) loaded Na-KGa-1 in the presence (red line) and absence(black line) of carbonate b) fluorescence lifetime of Cm(III) loaded Na-KGa-1 in the presence(red line) and absence (black line)of carbonate.*

***Table 4.2:*** *Summary of experimental conditions, 0.1 M $NaClO_4$, pH= 7.9, S/L ratio = 2 g $L^{-1}$.*

| Sample | Conditions | Initial U | log $R_d$ ($L.kg^{-1}$) | U loading ($\mu mol\ g^{-1}$) |
|---|---|---|---|---|
| A | carbonate free | $1.5.10^{-5}$ | 3.97 | 7.1 |
| B | 1 mM $NaHCO_3$ | $2.0.10^{-5}$ | 2.7 | 5.0 |

Fig. 4.6 shows the radial structure functions of U(VI) loaded Na-montmorillonite at pH 8 in the absence (A) and presence (B) of carbonate measured at a beam incidence angle of 35°. EXAFS spectra were analyzed and fitted using the IFEFFIT software package (NEWVILLE et al., 1995). Back-scattering phases and amplitudes were obtained from FEFF8.0 calculations using the structure of soddyite. The EXAFS parameters obtained by fitting the spectra of both samples are summarized in Table 4.3. Structural data for both systems (with and without carbonate) show unambiguously that U(VI) forms inner-sphere complexes at the clay surface (Si shell, Fe shell and splitting of the $O_{eq}$ shell,). However, no pronounced difference is observed for these two samples (no C shell ~ 2.90 Å, no distant O-shell). This might be an indication that under the given experimental conditions no measurable U(VI)-carbonate ternary complexes forms at the montmorillonite surface or the backscatter amplitude of carbon C (z=6) is too weak compared to Si (z=14) to make a significant contribution on the spectra.

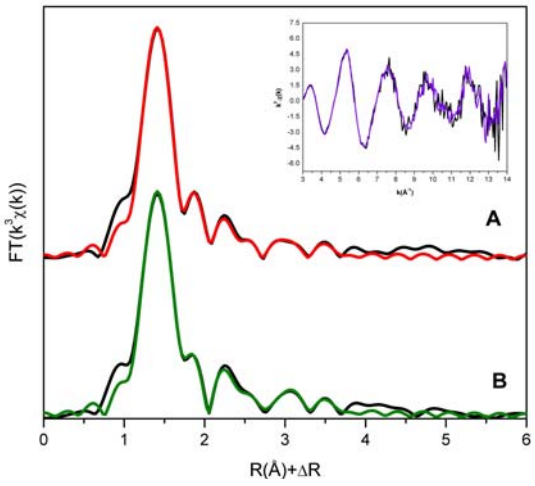


***Fig. 4.6:*** *Radial structure functions of U(VI) loaded self-supporting montmorillonite films. A) in the absence of carbonate, B) in the presence of carbonate. Black line: experimental data, red and green dotted line: modelled data.*

***Table 4.3:*** *Structural information derived from the EXAFS analysis of U(VI) loaded self-supporting montmorillonite films prepared in the absence and in the presence of carbonate at pH ~8.*

| Sample | Shell | N | R (Å) | $\sigma^2(Å^2)$ | $E_0$ |
|---|---|---|---|---|---|
| A | U-$O_{ax}$ | 2* | 1.80 | 0.002 | 8.4 |
| | U-$O_{eq1}$ | 3.6 | 2.29 | 0.008 | |
| | U-$O_{eq2}$ | 3.1 | 2.48 | 0.008 | |
| | U-Si/Al | 0.5 | 3.09 | 0.003* | |
| | U-Fe | 0.3 | 3.41 | 0.003* | |
| | U-Si/Al | 2.3 | 3.84 | 0.013 | |
| B | U-$O_{ax}$ | 2* | 1.80 | 0.002 | 9.6 |
| | U-$O_{eq1}$ | 3.5 | 2.29 | 0.007 | |
| | U-$O_{eq2}$ | 2.9 | 2.50 | 0.007 | |
| | U-Si/Al | 0.8 | 3.10 | 0.003* | |
| | U-Si/Al | 0.5 | 3.43 | 0.003* | |
| | | 1.6 | 3.86 | 0.011 | |

* Fixed values, fitting range: k: 3.6-12.6 $Å^{-1}$, MS path of the uranyl moiety was linked to U-$O_{ax}$ scattering as described in HUDSON et al. (1996)

### 4.4.3 Np(V) investigations on clay: Macroscopic and microscopic analysis

Within the framework of an ACTINET joint research project with the Johannes Gutenberg-University Mainz, FZD (ROBL) and LES the sorption of Np(V) on montmorillonite in the absence of inorganic carbon and under air-equilibrated conditions is being investigated. The results of batch sorption measurements together with the modelling are summarised in Fig. 4.7.

As can be seen in Fig. 4.7b the presence of inorganic carbon has a large impact on the sorption behaviour of Np(V) at pH > 8 because of aqueous complexation with carbonates. The data could be modelled using the 2SPNE SC/CE sorption model under the condition that for the data in equilibrium with air the following additional surface complex was required.

$$\equiv SOH + NpO_2^+ + CO_3^{2-} \Leftrightarrow \equiv SONpO_2CO_3^0 + H^+$$

EXAFS measurements were carried out at the Rossendorf Beamline (ESRF, Grenoble) with the aim of checking that the postulated surface complexes in the macroscopic studies, both in the absence and presence of inorganic carbon, are consistent with the EXAFS spectra. Np $L_{III}$-edge EXAFS spectra for the Np(V)/montmorillonite system at pH 9 equilibrated for 3 days in the absence of inorganic carbon, and in the presence of inorganic carbon (equilibrium with air, p-$CO_2$ = $10^{-3.5}$ bar) have been measured.

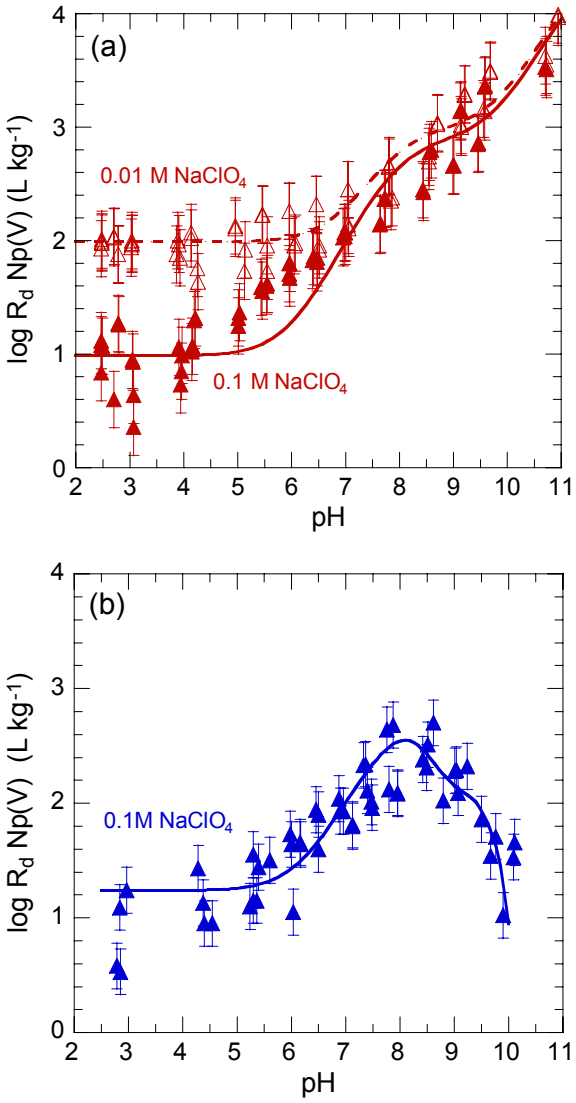


***Fig. 4.7:*** *Np(V) sorption on Na montmorillonite (a) in the absence of inorganic carbon and (b) in the presence of inorganic carbon (p-$CO_2$ = $10^{-3.5}$ bar). The curves are calculated with the 2SPNE SC/CE sorption model.*

The Np loadings for the samples prepared in air and in $CO_2$-free conditions were 2 µmol/g and 3.5 µmol/g respectively.

The radial structure functions (RSFs) corresponding to the recorded EXAFS spectra are shown in Fig. 4.8. The amplitude and position of the first RSFs peaks (peaks A, Np-O axial backscattering pairs) are invariant with reaction conditions. The second RSFs peak (peak B), however, increases in amplitude and the position slightly shifts to higher values (R + ΔR ~2.13 Å vs. ~2.15 Å) for the sample prepared in the presence of carbonate. This is caused by the Np-O backscattering pairs of the carbonate complexes. The origin of peak C is mainly caused by Np-Al/Si and multiple scattering contributions from the Np-$O_{ax}$ backscattering pairs. The strongest indication for the formation of Np-carbonate complexes at the montmorillonite surface is given by the presence of peak D in the sample equilibrated with air. This feature is caused by the multiple scattering paths of the Np-O-C entity.

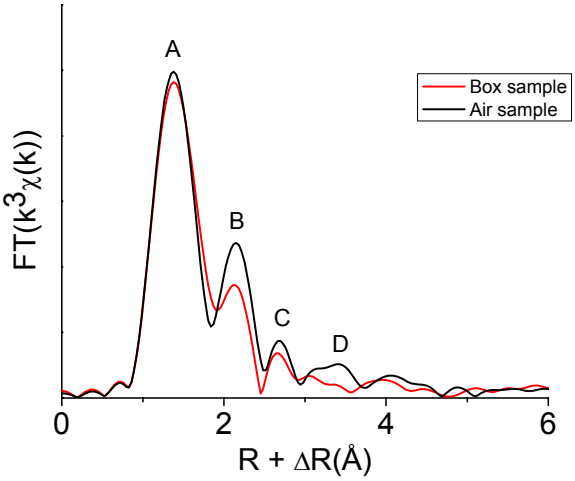


***Fig. 4.8:*** *Np $L_{III}$-edge radial structure functions (RSF) of montmorillonite reacted with Np(V) in the absence (red) and presence (black) of inorganic carbon (p-$CO_2$ = $10^{-3.5}$ bar).*

## 4.5 References

BRADBURY M.H., BAEYENS B. (2003)
Far field sorption databases for performance assessment of a HLW repository in an undisturbed Opalinus Clay host rock. PSI Bericht Nr. 03-08 and Nagra NTB 02-19, Nagra, Wettingen, Switzerland.

BRADBURY M.H., BAEYENS B. (2005)
Experimental and modelling investigations on Na-illite: Acid-base behaviour and the sorption of strontium, nickel, europium and uranyl. PSI Bericht Nr. 05-02 and Nagra NTB 04-02, Nagra, Wettingen, Switzerland.

BRADBURY M.H., BAEYENS B. (2008a)
Sorption modelling on illite. Part I: Titration measurements and sorption of Ni, Co, Eu and Sn. Geochim. Cosmochim Acta (in press).

BRADBURY M.H., BAEYENS B. (2008b)
Sorption modelling on illite. Part II: Actinide sorption and Linear Free Energy Relationships. Geochim. Cosmochim. Acta (in press).

BRADBURY M.H., BAEYENS B., THOENEN T. (2008)
Sorption Data Bases for Generic Swiss Argillaceous, Crystalline and Calcareous Rock Systems, Nagra NAB 08-50, Nagra, Wettingen, Switzerland.

GORGEON L. (1994)
Contribution à la modélisation physico-chimique de la retention de radioeléments à vie longue par des materiaux argileux. Unpublished PhD Thesis. Université Paris 6.

HUDSON E.A., ALLEN P.G., TERMINELLO L.J., DENECKE M.A., REICH T. (1996)
Polarized X-ray-absorption spectroscopy of the uranyl ion: Comparison of experiment and theory. Phys. Rev. B, 54(1), 156.

NAGRA (2002)
Project Opalinus Clay: Safety Report. Demonstration of disposal feasibility (Entsorgungsnachweis) for spent fuel, vitrified high-level waste and long-lived intermediate-level waste. Nagra NTB 02-05, Nagra, Wettingen, Switzerland.

NAGRA (2008)
Vorschlag geologischer Standortgebiete für das SMA- und das HAA-Lager: Darlegung der Anforderungen, des Vorgehens und der Ergebnisse. Nagra NTB 08-03, Nagra, Wettingen, Switzerland.

NEWVILLE M., RAVEL B., HASKEL D., REHR J.J., STERN E.A., YACOBY Y. (1995)
Analysis of multiple-scattering XAFS data using theoretical standards. Physica B 208 & 209, 154-155.

STENHOUSE M. (1995)
Sorption databases for crystalline, marl and bentonite for performance assessment. Nagra NTB 93-06, Nagra, Wettingen, Switzerland.

# 5 CEMENT SYSTEMS

*E. Wieland, J. Tits, X. Gaona, D. Kunz, A. Laube, N. Macé, P. Mandaliev, D. Popov, B. Dilnesa (Empa)*

## 5.1 Overview

Cement-based materials play an important role in multi-barrier concepts developed worldwide for the safe disposal of low- and intermediate-level radioactive waste. In the proposed Swiss disposal concept, cement is used to condition (solidify and stabilize) the waste materials, and further, cementitious materials will be used for the construction of the cavern (lining, backfill material) of the planned deep geological repositories. The cement-based near field controls radionuclide solubilities and retards their release into the far field. Therefore, knowledge of the chemical mechanisms by which radionuclides are sorbed onto cement minerals is essential for long-term assessments of the safe disposal of radioactive waste.

The long-term aim of the Cement Systems Group is to develop mechanistic models for the interaction of safety relevant radionuclides with cementitious materials and to improve current knowledge on the chemical processes in the near field of the planned Swiss ILW and L/ILW repositories. The research programme is directed towards better source term descriptions and strengthening the credibility of the sorption values used in performance assessment studies. The cement used for the experimental studies is a sulphate-resisting Portland cement CEM I 52.5 N HTS (Lafarge, France), which is currently employed for the conditioning of ILW and L/ILW radioactive waste in Switzerland. Hydrated cement or hardened cement paste (HCP) was prepared and used for wet chemistry (sorption, diffusion) and spectroscopic studies with the safety relevant radionuclides. HCP is a heterogeneous matrix consisting mainly of calcium (aluminium) silicate hydrates (C-(A)-S-H), portlandite ($Ca(OH)_2$) and calcium aluminates (AFt- and AFm-type phases). Among the different cement phases, C-S-H phases are considered to be the most important constituent of HCP as they are abundant and exhibit a wide diversity of structural sites for cation and anion binding. For this reason studies using C-S-H phases have been carried out with the aim of gaining a sufficiently detailed mechanistic understanding of the radionuclide uptake by cementitious materials.

The main lines in our research activities in 2008 were:

- Sorption studies with the dose-determining radionuclides $^{14}C$, $^{129}I$ and $^{36}Cl$ on HCP
- Sorption studies and spectroscopic investigations on the interaction of Np(V) and U(VI) with HCP and C-S-H phases
- Determination of the binding mechanisms of Nd(III) and Eu(III) in cementitious materials using spectroscopic techniques
- Development of a methodology for phase identification in cement and at the clay-cement interface using micro-diffraction
- Determination of the Fe speciation in cementitious materials.

Sorption under reducing conditions is one of the main subjects in the 7th EU Framework Programme collaborative project "RECOSY" (REdox phenomena COntrolling SYstems), which started in April 2008. The wet chemistry and spectroscopic investigations of Np(IV/V) uptake by cementitious materials are being carried out in the framework of RECOSY.

The studies on U(VI) immobilization in cement, performed by Dr. N. Macé, are fully financed by the EU in the framework of a Marie-Curie Fellowship ("MISUC" project) and are partly carried out as an ACTINET joint project with the Institute of Radiochemistry, Forschungszentrum Dresden-Rossendorf (Dresden, Germany), the Rossendorf beamline (ROBL-BM20) at the European Synchrotron Radiation Facility (ESRF, Grenoble, France), the Micro-XAS beamline of the Swiss Light Source (SLS) and the Commisariat à l'Energie Atomique (CEA) (Saclay, France).

The Ph.D. project on the binding mechanisms of trivalent lanthanides (Nd(III), Eu(III)) carried out by P. Mandaliev was brought to a close with the final Ph.D. examination in November 2008. In the last year of this project the main activities focused on completing the spectroscopic studies and preparing the papers required for the submission of the Ph.D. work.

The joint Ph.D. project with Empa on the Fe speciation in cement being carried out by B. Dilnesa was successfully started. In addition, the following collaborators joined the sub-programme in 2008: A. Laube (technician) on July 1st, 2008 and Dr. J. Gaona (guest scientist) on September 1st, 2008. Dr. D. Popov (post doc) joined the "XAFS" sub-programme on May 1st, 2008. His research activities in 2008 will be presented in the framework of this programme.

## 5.2 Uptake of dose-determining radionuclides

Iodide ($^{129}I$), chloride ($^{36}Cl$) and $^{14}C$ species are safety relevant radionuclides which largely determine the long-term activity release rate (mSv per year) from the cementitious near field into the far field. The uptake of $^{125}I$ ($I^-$) and $^{36}Cl$ ($Cl^-$) by carbonate-containing HTS cement was investigated as a function of the solid-to-liquid (S/L) ratio of the cement suspensions. In earlier studies it was observed that the uptake of $I^-$ strongly depends on the amount of HCP in contact with solution (WIELAND & VAN LOON, 2002). In particular, the sorption value ($R_d$) for $I^-$ as determined from diffusion experiments on compact cement systems was found to be significantly lower than that obtained in dispersed (batch-type) systems (JAKOB et al., 1999). The investigations carried out in 2008 showed that the total concentration of chloride in the cementitious systems is the key to a detailed understanding of the above discrepancies in the measured sorption values. Fig. 5.1a shows that the concentration of stable $Cl^-$ in solution increases with increasing S/L ratio due to the release of stable $Cl^-$ bound by the cement matrix. Further, the uptake of both tracers, i.e., $^{125}I$ and $^{36}Cl$, by cement decreases with increasing concentration of stable $Cl^-$ in solution (Fig. 5.1b). Adding $10^{-4}$ M $Cl^-$ to artificial cement pore water (ACW) led to constant $R_d$ values at low S/L ratios, i.e., under conditions where the concentration of added $Cl^-$ was significantly higher than the $Cl^-$ concentration in equilibrium with the cement paste. Mass balance calculations further revealed that the partitioning of $^{36}Cl$ can be interpreted in terms of isotopic exchange of $^{36}Cl$ between the inventories of stable $Cl^-$ bound by cement matrix and in solution. The influence of stable $Cl^-$ on the $^{125}I$ uptake is weaker than on $^{36}Cl$.

In 2008 a first series of sorption tests were performed using $^{14}C$ labeled formic and acetic acids as potential "$^{14}C$ containing small organic molecules" arising from the anaerobic corrosion of carbon steels at high pH. The sorption kinetics of these molecules had to be investigated at very high ratios S/L due to their very weak interaction with HCP. In addition, the stability of the compounds under the highly alkaline conditions in cementitious systems was checked using High Performance Ion Exchange Chromatography (HP-IEC). It was observed that acetic acid does not sorb onto cement. However, very weak sorption was observed in the case of formic acid, i.e., distribution ratios ($R_d$) were determined to be about $10^{-4}$ $m^3$ $kg^{-1}$.

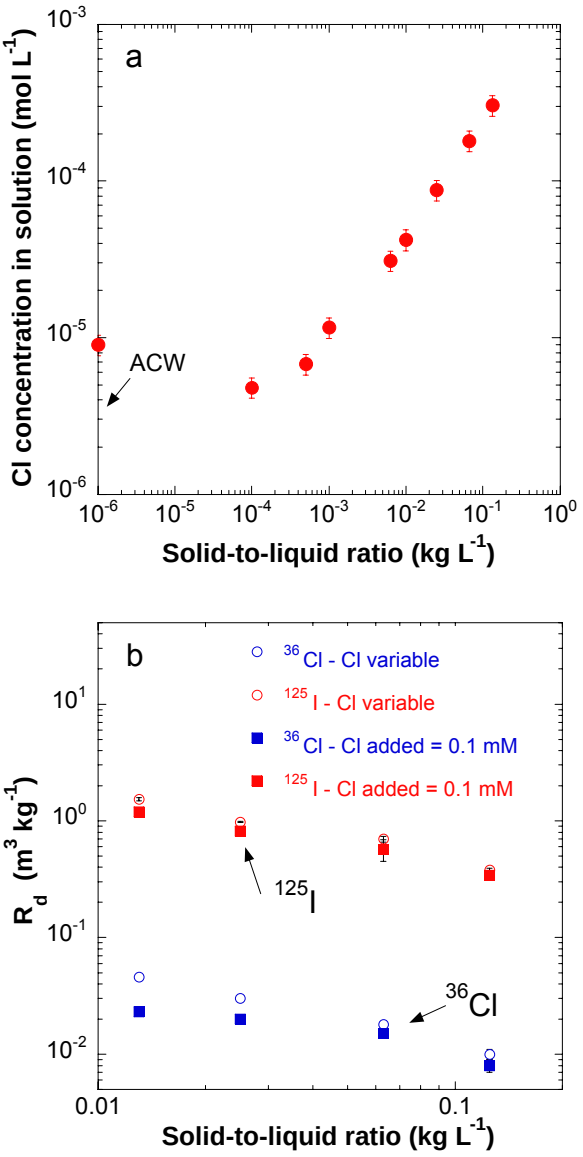


***Fig. 5.1:*** *Influence of stable $Cl^-$ on the uptake of $^{125}I$ and $^{36}Cl$ by "modern" HTS cement (CEM I 52.5 N HTS). a) Concentration of stable $Cl^-$ as a function of the S/L ratio; b) Distribution ratios of $^{125}I$ and $^{36}Cl$ for two different sets of experiments; Open circles: $Cl^-$ concentration varied according to the S/L ratio (Fig. 5.1a); Closed squares: $10^{-4}$ M $Cl^-$ was added to the solution.*

## 5.3 Redox chemistry in cementitious systems

### 5.3.1 Neptunium (V) sorption studies

The uptake of redox sensitive actinides under the reducing conditions of a cementitious near field is poorly characterized (WIELAND & VAN LOON, 2002). In most sorption databases it is assumed that the sorption behavior of tetravalent actinides, such as Np(IV) and Pu(IV), is similar to that of Th(IV). To

verify this assumption, a study on the uptake of Np(IV/V) by HCP and C-S-H phases under oxidizing and reducing conditions was started.

Sorption experiments with Np(V) on C-S-H phases carried out over the past years showed that the uptake of this pentavalent actinide is unexpectedly high, i.e., $R_d$ ranges in value between $10^5$ L kg$^{-1}$ and $2\times10^6$ L kg$^{-1}$ (Fig. 5.2a; exp. 1 and 2). However, the reproducibility of the sorption values determined using $^{237}$Np as tracer was rather poor. For this reason, the analytical technique applied to quantify $^{237}$Np activities in strongly alkaline solution (liquid scintillation counting with alpha-beta discrimination) was optimized. This allowed uncertainties to be reduced significantly (Fig. 5.2a, exp. 3). The average $R_d$ value obtained from these measurements was $3\pm2\times10^5$ L kg$^{-1}$, thus corroborating the high $R_d$ values determined earlier. Np(V) uptake by C-S-H phases was found to be linear in the investigated concentration range (Fig. 5.2a). Variations in the Ca:Si (C/S) ratio of the C-S-H phases and pH (pH = 10.5 for C/S = 0.65; pH = 12.5 for C/S = 1.65) had no measurable effect on Np(V) uptake (Fig. 5.2a). The latter finding is in contrast to earlier studies on the U(VI)/C-S-H system, which showed an increase in the U(VI) uptake with increasing C/S ratio under similar conditions (TITS et al., 2008). Studies with Np(V) on HCP in ACW (pH = 13.3) further corroborate the strong uptake of Np(V) by cementitious materials ($R_d$=3±1×10$^5$ L kg$^{-1}$) and linear sorption (Fig. 5.2b). The latter findings suggest that C-S-H phases could be the uptake-controlling cement phase for Np(V) in the cement matrix.

In 2008 an electrochemical cell was developed and tested, and analytical methods for the determination of Np(IV/V) in concentrated and dilute solutions were established. This will allow sorption experiments with Np(IV) to be carried out under highly alkaline conditions in the future.

### 5.3.2 Fe speciation in cement

In the long term, the reducing conditions prevailing in repositories for radioactive waste may have an influence on the retention properties of cement. The mineral composition and stability of the cement under these conditions is still poorly known, mainly due to lack of knowledge on the speciation of iron in cement. For this reason, a Ph.D. project on this topic is being jointly carried out with the Laboratory for Concrete and Construction Chemistry at Empa. The project is funded by the Swiss National Science Foundation and started in February 2008.

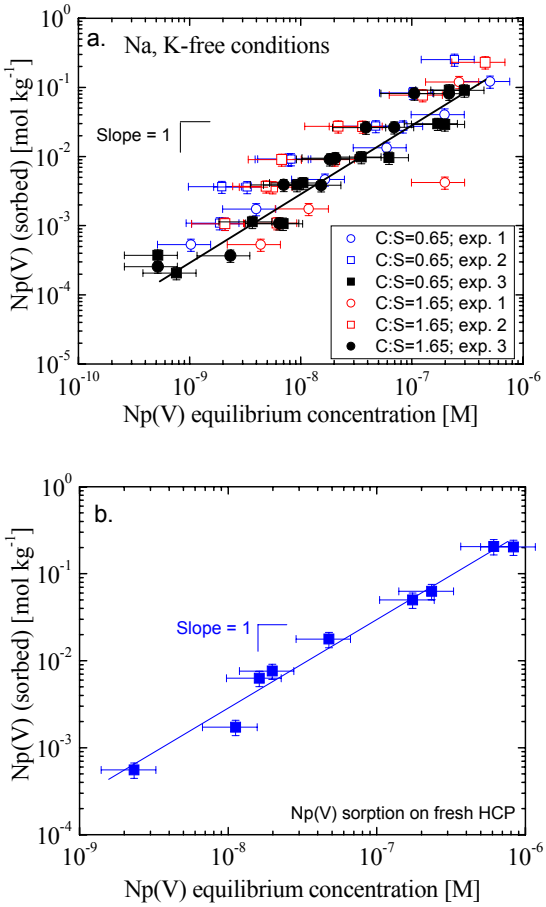


***Fig. 5.2:*** *Uptake of Np(V) by cementitious materials: a) C-S-H phases with different C:S ratios under alkali ion (Na,K) free conditions (pH= 10.5 at C/S=0.65; pH = 12.5 at C/S = 1.65). b) HCP in ACW (pH = 13.3).*

Fe(III) is the dominant oxidation state in ordinary Portland cement. Fe(III) is expected to be reduced to Fe(II) under the reducing conditions of a repository. Important Fe(III)-containing cement minerals such as Fe-ettringite, Fe-monosulphate, Fe-monocarbonate and Fe-hydrogarnet, which are potentially present in hydrated cement, were synthesized in 2008 and characterized using X-ray diffraction (XRD) and thermogravimetric analysis (TGA). Kinetic studies of the formation of theses minerals were carried out, and the solid solution series with their aluminium analogues were synthesized. The solubility products for the Fe minerals and their solid solutions with Al were determined, which allowed the set of thermodynamic data for cement systems to be further enlarged. The above-mentioned Fe-containing cement minerals are considered to be important reference compounds in future EXAFS investigations on the Fe speciation in cement.

## 5.4 Uptake of lanthanides and actinides by cementitious materials

### 5.4.1 Nd(III) and Eu(III) uptake processes

This project on the interaction of Nd(III) and Eu(III) was carried out in the framework of a Ph.D. project launched with the aim of further corroborating the high sorption values determined in earlier studies (WIELAND et al., 1998, TITS et al., 2000). A further aim was to develop a molecular-level understanding of the uptake processes of lanthanides with a view to assessing the retention of trivalent actinides in cement-based repositories. In previous studies it was shown that after equilibrating Nd with crystalline and amorphous C-S-H phases over a few months, Nd was completely taken up within the structure of these phases (Progress report, 2007; MANDALIEV, 2008). Nd incorporation was indicated in EXAFS investigations by increasing Nd-Ca and Nd-Si distances and increasing co-ordination numbers of neighboring Si and Ca atoms in the aged samples (MANDALIEV et al., 2008 a/b).

In 2008, it was checked whether Nd immobilization in the cement matrix can be explained by the proposed uptake mechanism. It should be noted that C-S-H phases constitute about 50 weight (wt) % of HCP.

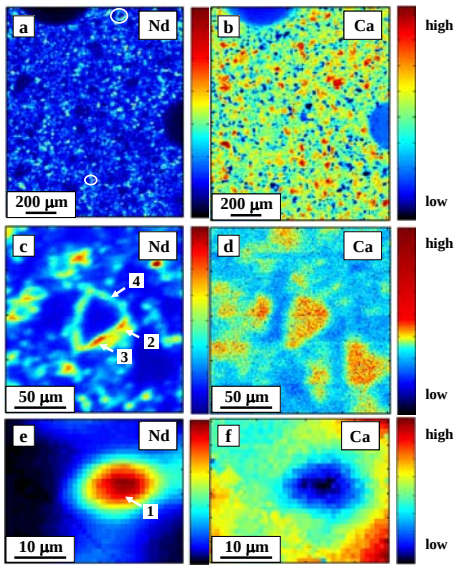


***Fig. 5.3:*** *µ-XRF elemental distribution maps of Nd and Ca in the HCP sample CEMHYD_28 (hydration time = 28 days; metal concentration = 4000 ppm). Selected regions for µ-EXAFS measurement are labeled 1-4. The color bar represents relative metal enrichments in each sample.*

Compact Nd doped cement samples were prepared and investigated using µ-X-ray fluorescence (µ-XRF) and extended µ-X-ray absorption fine structure spectroscopy (µ-EXAFS). The µ-XRF/EXAFS investigations were carried out on thin sections prepared from compact Nd doped cement samples which had been reacted for 28 and 200 days and had loadings of ~4000 ppm (CEMHYD_28 and CEMHYD_200 samples in Fig. 5.3 and 5.4 respectively). The µ-XRF investigations showed that Nd-containing phases formed rims around inner C-S-H phases. This is illustrated for the CEMHYD_28 sample in Fig. 5.3. The speciation of Nd was determined on selected spots in the cement matrix using µ-EXAFS spectroscopy.

The EXAFS spectra, the corresponding radial structure functions (RSF) and the Fourier-back transform spectra for the different spots in the two samples CEMHYD_28 and CEMHYD_200 are shown in Fig. 5.4. The coordination environment of Nd taken up by HCP was found to depend on reaction time. For example, the coordination number of Si was found to vary between $N_{Si}$ = 2.8 and 5.6, while the Nd-Si distances ranged from $R_{Nd\text{-}Si}$ = 3.78 Å to 3.85 Å for the different spots in the sample reacted for 28 days (MANDALIEV et al., 2008c).

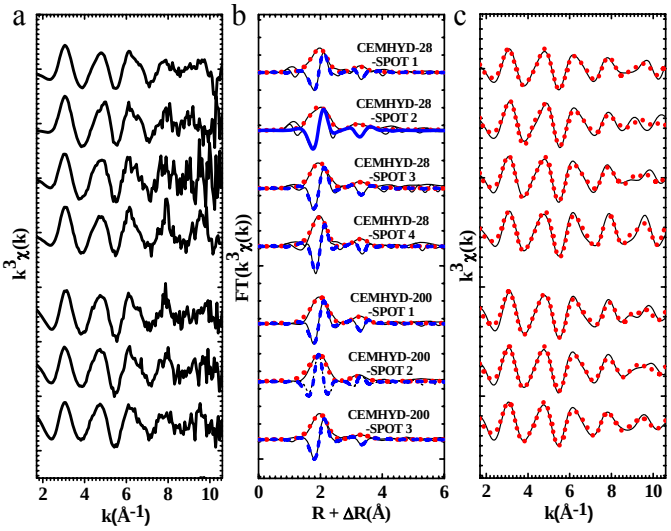


***Fig. 5.4:*** *Selected Nd $L_{III}$-µ-EXAFS measurements for the Nd doped HCP samples (reaction time = 28 and 200 days; metal concentrations = 4000 ppm); a) $k^3$ -weighted spectra and b) experimental (solid line) and fitted (dashed and doted lines for the imaginary and the real part, respectively) RSFs; c) $k^3$-weighted EXAFS function for the Fourier backtransform spectra obtained from Fig. 5.4b ($R + \Delta R$ = 1.7-4.0).*

In the sample reacted for 200 days, variations in the coordination number of Si were smaller ($N_{Si}$ = 5.5 – 6.6) and the Nd-Si distances ranged from $R_{Nd-Si}$ = 3.85 - 3.87 Å. Note that the differences between the corresponding two sets of data are larger than the expected uncertainties, i.e. ± 20% for N and ± 0.02 Å for R. Similar variations were observed for the structural parameters of the neighboring Ca atoms. The results showed in particular that the Nd-Si and Nd-Ca distances increased with increasing reaction time, indicating structural incorporation of Nd into C-S-H phases as observed in previous studies on Nd doped crystalline and amorphous C-S-H phases (MANDALIEV et al., 2008 a/b).

TRLFS investigations on the Eu(III) doped crystalline C-S-H phases, 11 Å tobermorite and xonotlite, were carried out to assess whether or not the incorporation of trivalent lanthanides into the C-S-H structures previously revealed from EXAFS investigations with Nd at high metal loadings, could be confirmed for low metal loadings. (Note that TRLFS is more sensitive than EXAFS spectroscopy.) However, TRLFS requires fluorescing properties of an element, such as Eu, while Nd is non-fluorescing. Eu doped tobermorite and xonotlite samples with a Eu loading of 60 ppm and reaction times of 1 day and 310 days were studied (MANDALIEV et al., 2008d/e). Fig. 5.5a shows the fluorescence emission spectra of Eu doped tobermorite measured at 20 K (excitation at 579.5 nm). The splitting into two crystal field levels of the $^5D_0 \rightarrow {}^7F_2$ emission band, which is more pronounced after 310 days equilibration than that for the one day sample, indicates an increase in structural order with time. The observed emission decay was found to be bi-exponential in both samples (Fig. 5.5b), and the lifetimes of each of the two species in both cases were similar, i.e., $\tau_1$ = 580 +/- 60 µs and $\tau_2$ = 1567 +/- 100 µs, and $\tau_1$ = 540 +/- 60 µs and $\tau_2$ = 2036 +/- 200 µs, respectively. The number of water molecules in the coordination sphere of Eu was estimated to be 1.1 +/- 0.2 and zero water molecules after one day and 310 days, respectively, based on the relationship proposed by HORROCKS & SUDNICK (1979). This indicates that the local structure of Eu did not change significantly with time, and further, that Eu is bound in the structure of tobermorite in a fashion similar to that of Nd(III) in samples at higher Nd loadings (MANDALIEV et al., 2008a).

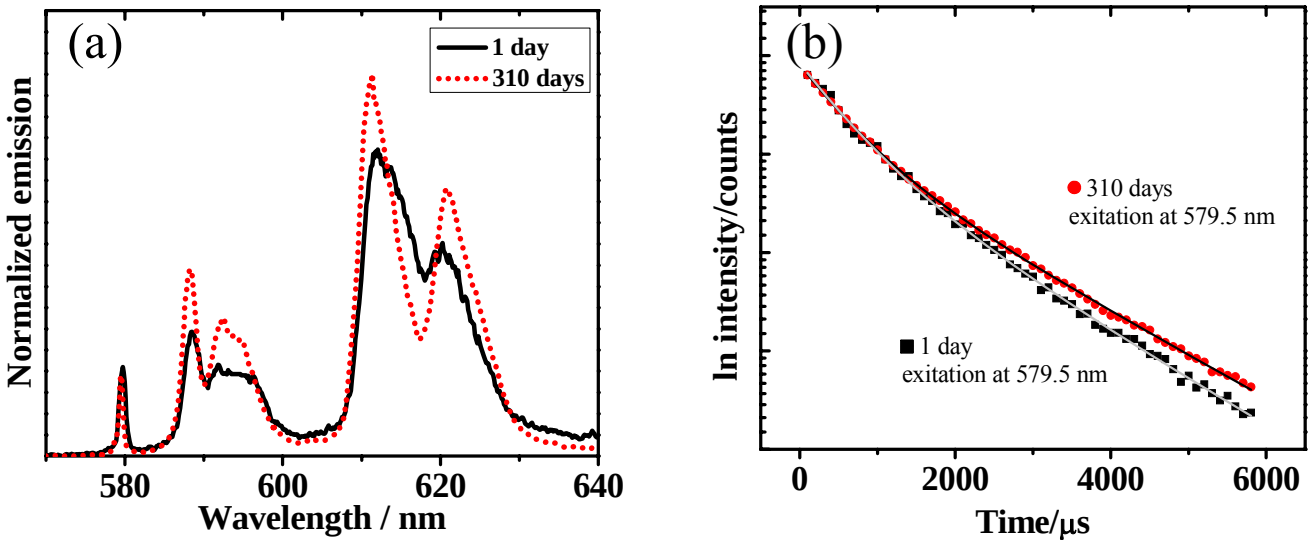


***Fig. 5.5:*** *a) Fluorescence emission spectra and b) the time dependency of Eu(III) emission decay by selective excitation of Eu(III) taken up by 11 Å tobermorite (60 ppm) after 1 and 310 days reaction time measured at 20 K.*

### 5.4.2 Spectroscopic investigations of U(VI) uptake processes

The uptake of U(VI) by cementitious materials was investigated using TRLFS and EXAFS spectroscopy. In 2008 several U(VI) containing minerals, i.e., soddyite, K-boltwoodite and uranophane, needed as reference compounds for the TRLFS and EXAFS studies, were synthesized and characterized by XRD. A key question addressed in 2008 was whether or not the coordination environment of U(VI) in HCP is similar to that in the U(VI)/C-S-H systems. To this aim, U(VI) TRLFS spectra were collected at 150 K using a MOPO laser and an excitation wavelength of 410 nm for cement pastes and supernatant solutions and compared with the corresponding U(VI)/C-S-H spectra. Cryogenic conditions were used to improve the resolution of the spectra by reducing thermal effects.

Fig. 5.6 shows the fluorescence emission spectra for the U(VI)/HCP/ACW, U(VI)/C-S-H/ACW and U(VI)/C-S-H/$H_2O$ systems. The C-S-H phases used had a C/S ratio of 1.07, but the pH values in the equilibrium solutions were different, .i.e. pH=12 for the C-S-H phase synthesized in $H_2O$, and pH = 13.3 in the case of the synthesis in ACW. Fig. 5.6 shows that the spectra determined for the supernatant solutions and the U(VI) doped C-S-H and HCP pastes are different in all systems. There is a shift in the emission wavelength maxima (~10 nm) for the systems in ACW, indicating that the species present in solution and taken up by the paste have different fluorescence characteristics. This suggests that different U(VI) species are present. At pH ~ 12, no fluorescence emission spectra could be determined for the supernatant solution due to the low U(VI) concentration under these conditions, as already observed in wet chemistry experiments (TITS et al., 2008). By comparison of the emission spectra, Fig 5.6b and 5.6c, the same U(VI) species were concluded to sorb in the C-S-H/ACW and the C-S-H/$H_2O$ systems. Furthermore, the chemical environment of U(VI) in HCP and C-S-H phases were similar as indicated by the position of the emission bands. This finding suggests that C-S-H phases are the uptake-controlling phases for U(VI) in the cement matrix.

The TRLFS results could be further substantiated using EXAFS spectroscopy on U(VI) doped C-S-H and HCP samples. Fig. 5.7a shows EXAFS spectra for the most important U(VI) reference compounds ($CaUO_4.xH_2O$, uranophane and soddyite) together with U(VI) doped C-S-H and HCP samples equilibrated for 30 days. The EXAFS spectra of the latter samples agree well, suggesting that the chemical environment of U(VI) bound to C-S-H and HCP are identical. This finding further supports the idea that C-S-H phases are responsible for U(VI) immobilization in HCP.

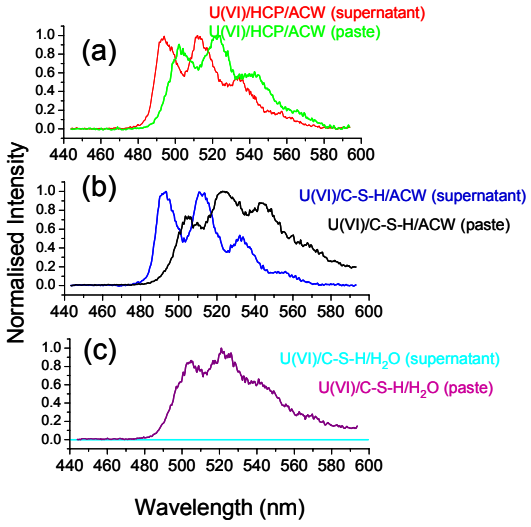


***Fig. 5.6:*** *Emission spectra ($\lambda_{ex}$ = 410 nm, T = 150 K) of supernatant and paste samples a) for U(VI)/HCP in ACW b) for U(VI)/C-S-H (C/S =1.07) in ACW and c) for U(VI)/C-S-H(C/S =1.07) in $H_2O$.*

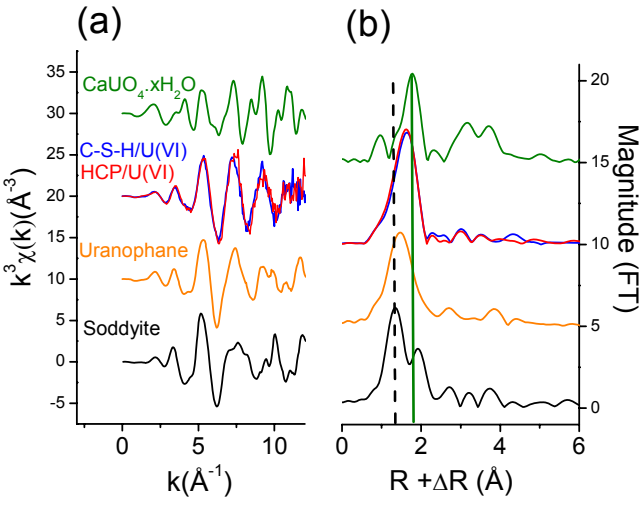


***Fig. 5.7:*** *a) $k^3$-weighted experimental EXAFS data for selected U(VI) reference compounds and U(VI)/HCP and U(VI)/C-S-H samples (3000 ppm); b) the corresponding RSFs with the k range taken between 2 and 11 Å.*

## 5.5 CI project

LES is contributing to the laboratory programme supporting the Mt. Terri field experiment on cement-Opalinus Clay interaction (CI project). In 2008, the contribution mainly involved development of an X-ray micro-diffraction (µ-XRD) technique for characterizing cementitious materials and the cement-clay interface with micro-scale resolution. µ-XRD is potentially a powerful tool to investigate the inherent heterogeneity of these materials because it provides structural information on selected micron-sized crystals within the whole matrix. The aim of this research is to develop a methodology for the collection and reduction of µ-XRD data, including in situ crystal structure refinement, identification of crystalline phases via a search in the powder diffraction database and 3D phase mapping. This project, which is carried out in co-operation with EPFL and the Swiss-Norwegian beamline at the ESRF (Grenoble, France), aims at identifying all of the phases present in the area of interest of the cement or cement-clay interface samples with micro-scale resolution.

In 2008 the first measurements performed on thin sections prepared from Portland cement was carried out at the Swiss-Norwegian beamline and the micro-XAS beamlines at the SLS. These measurements showed that identification of crystalline phases within selected regions of the sample is feasible (Fig. 5.8).
Due to the rather small beam spot sizes (~ 100 µm at the Swiss-Norwegian beamline and ~8.5 µm at the SLS micro-XAS beamline) it was possible to limit the number of different crystals in the beam during data collection, which simplified the signal pattern. The file format of the MAR-CCD used by the Swiss-Norwegian beamline is compatible with the CrysAlis software, which is being used for analysis of diffraction patterns collected on polycrystalline samples at this beamline. Application of the CrysAlis program to the collected data allowed crystals of Portlandite ($Ca(OH)_2$) and Alite ($Ca_3SiO_5$) to be unequivocally determined based on single crystal refinement without any a priori knowledge of the phases or their compositions. The structures of both minerals could be refined using the anisotropic approach of thermal parameters and collected in situ intensity data having 0.9 Å highest resolutions. The typical crystal size was several tens of microns in this setup.

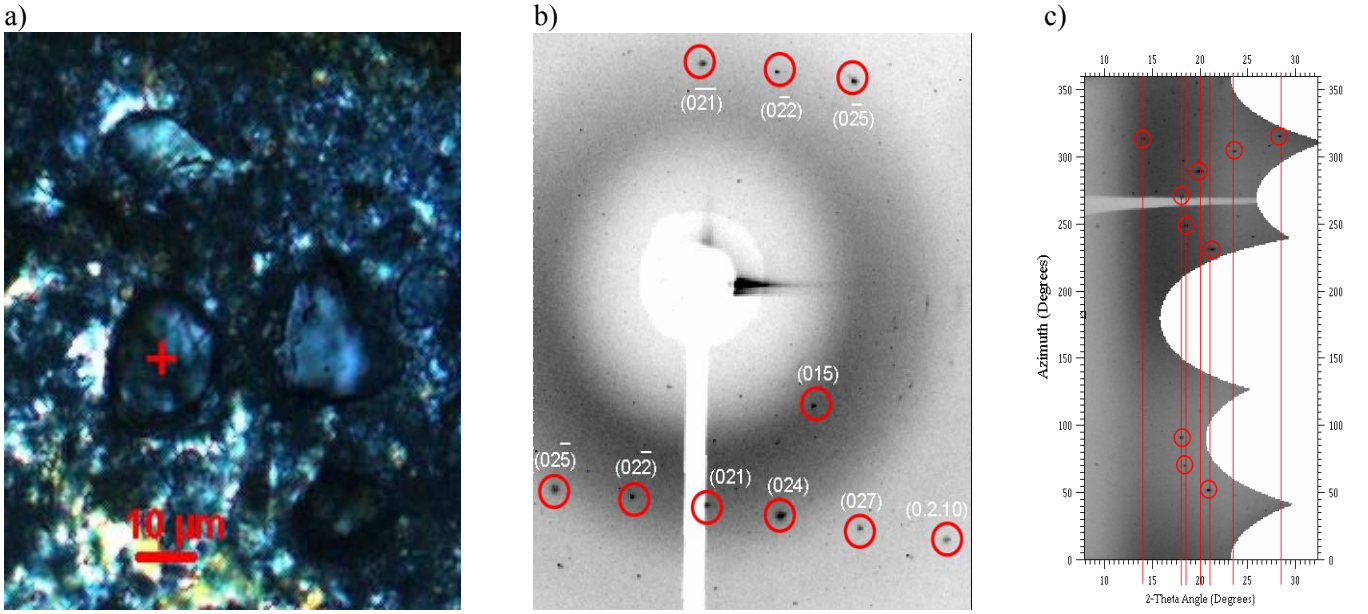


***Fig. 5.8:*** *An example of crystalline phase identification from data collected at the micro-XAS beamline, a) Polarized light optical image of selected area of the cement thin section. The X-ray beam was focused on the point denoted by the red cross. The X-ray beam size was 8.5×8.5 µm with a total flux of $1.3\times10^{11}$ photons/second. Energy used 13 keV. b) Average frame of a series of X-ray images collected in the continuous mode within 30˚ of total angular range. The strongest diffraction spots (circled in red) represent a regular lattice belonging to a crystalline grain. c) The image B presentation in axis of 2-theta angle and azimuth angle. Diffraction spots circled in red correspond to those from the image B. 2θ-angles of these spots (denoted by red vertical lines) coincide with positions of the strongest lines of $Ca_3SiO_5$ powder diagrams. Unit cell parameters of $Ca_3SiO_5$ a=7.057, b=24.97Å (space group R3m).*

At the present time, the CrysAlis software cannot be used as a routine operation for phase identification using the data collected at the micro-XAS beamline due to incompatibility of the data format of the Photonic Science CCD with this software. A programme is currently being developed which allows X-ray images written in the format of the Photonic Science CCD detector to be transformed into the Mar345 format, which is compatible with the CrysAlis software. Successful transformation of formats will finally allow in situ structure refinements on even smaller crystals than previously characterized using the ESRF setup.

### 5.6 References

HORROCKS W. D., SUDNICK D. R. (1979)
Lanthanide ion probes of structure in biology - laser-induced luminescence decay constants provide a direct measure of the number of metal-coordinated water-molecules. J. Am. Chem. Soc.101, 334-340.

JAKOB A., SAROTT F.A., SPIELER P. (1999)
Diffusion and sorption on hardened cement pastes – experiments and modelling results, PSI Bericht 99-05, Paul Scherrer Institut, Villigen, Switzerland.

MANDALIEV P. (2008)
Mechanisms of Nd(III) and Eu(III) uptake by cementitious materials, Swiss Federal Institute of Technology Zürich (ETH), Diss. ETH Nr. 18095, Zürich.

MANDALIEV P., WIELAND E., DÄHN R., TITS J., CHURAKOV S.V., ZAHARKO O. (2008a)
Mechanisms of Nd (III) uptake by 11 Å tobermorite and xonotlite. Geochim. Cosmochim. Acta (submitted).

MANDALIEV P., DÄHN R., TITS J., WEHRLI B., WIELAND E. (2008b)
EXAFS study of Nd (III) uptake by amorphous calcium silicate hydrates (C-S-H). J. Colloid Interface Sci. (submitted).

MANDALIEV P., DÄHN R., TITS J., WEHRLI B., WIELAND E. (2008c)
Macro- and micro-spectroscopic study of Nd (III) uptake mechanisms in hardened cement paste. Environ. Sci. Technol. (submitted).

MANDALIEV P., STUMPF T., TITS J., DÄHN R., WALTHER C., WIELAND E. (2008d)
A combined TRLFS and EXAFS study of Eu(III) uptake by 11 Å tobermorite. Environ. Sci. Technol. (submitted).

MANDALIEV P., STUMPF T., TITS J., DÄHN R., WALTHER C., WIELAND E. (2008e)
Uptake of Eu(III) by xonotlite: A TRLFS and EXAFS study. Radiochim. Acta (submitted).

TITS J., WIELAND E., BRADBURY M.H., DOBLER J.P. (2000)
The uptake of Eu(III) and Th(IV) by cement-type minerals in the alkaline disturbed zone of a nuclear repository, In "Applied Mineralogy" (D. Rammelmair et al. (eds)), Vol 2, 691-694.

TITS J., FUJITA T., TSUKAMOTO M., WIELAND E. (2008)
Uranium(VI) uptake by synthetic calcium silicate hydrates. In: Scientific Basis for Nuclear waste Management XXXI. MRS proceedings Volume 1107. Eds.: W.E. Lee, J.W Roberts, N.C. Hyatt, R.W. Grimes, p 467-474.

WIELAND E., VAN LOON L.R. (2002)
Cementitious near field sorption database for performance assessment of an ILW repository in Opalinus clay. PSI Bericht 03-06, Paul Scherrer Institut, Villigen, Switzerland, 2003, and Nagra Technical Report NTB 02-20, Wettingen, Switzerland.

WIELAND E., TITS J., SPIELER P., DOBLER J.P. (1998)
Interaction of Eu(III) and Th(IV) with sulfate-resisting Portland cement. Mater. Res. Soc. Symp. Proc. 506, 573-578.

# 6 COLLOID CHEMISTRY

*C. Degueldre, K. Bessho*[*]*, S. Frick*
**Visiting scientist from KEK, Tsukuba, Japan*

## 6.1 Introduction

The aim of the colloid sub-program is to understand the role of colloids in the migration of radionuclides in the geosphere. The colloid properties studied are concentration, size distribution and behaviour under safety relevant conditions. This report summarises our activities over the past year within the framework of the Grimsel colloid project: "Colloid Formation and Migration" (CFM). The focus continues to remain on colloid generation using single particle counting (SPC) techniques. The colloid generation approach followed is a "first" in this area with the possibility of evaluating clay colloid size distributions not only in batch systems but also under the quasi-stagnant conditions of the CFM system.

## 6.2 Activities in the CFM project

The Colloid Formation and Migration (CFM) project is conducted in the framework of Phase VI of the research program of the Grimsel Test Site (GTS). GTS Phase VI runs from 2004 to 2013 and is dedicated to repository-relevant (i.e. large-scale, long-term) in-situ experiments.

The CFM project is the latest project in a series of experiments conducted within the Radionuclide Retardation Program (RRP) of the GTS over the past 20+ years. It is divided into 2 Phases. Phase 1 began in 2004 and lasted for 3 years. The main tasks were related to preparatory studies concerning in-situ boundary conditions and predictive modelling and to carry out supporting laboratory experiments. Phase 2 of the CFM project will run for 4 to 6 years, from 2008 to 2011/13**,** with the aim of studying the in-situ generation and migration of colloids in the Grimsel migration zone environment.

The Phase 1 experiment partners were: Andra, JNC (now JAEA), KIT, AIST (joined in 2006), SKB (joined in 2007), CRIEPI (joined in 2007) and NAGRA; with CIEMAT and PSI/LES as associate members. In Phase 2 the partners are likely to be: JAEA, KIT, KAERI, SKB, CRIEPI, POSIVA and NAGRA. Within the last year work has continued on the field, laboratory and modelling programmes to complete Phase 1 and initiate Phase 2.

The main aim of this project is to understand the generation of colloids in quasi-stagnant water at a bentonic block / groundwater flow interface. The LES task is sub-divided into two parts: participation in the in situ colloid measurement campaigns and studying colloid generation mechanisms.

The breakthrough curve recorded in February 2008 (homologue test run 08 - 01) for the clay colloids in a 6.08 m long dipole flow field is shown in Fig. 6.1. The clay colloid peak maximum occurs after about 300 min which is well before the uranine maximum (after 544 min). There is no colloid size effect in the range 50 – 200 nm. LES found that the maximum colloid size was between 100 - 150 nm (single particle counting, SPC, before injection and during breakthrough) and INE colloid size of 153±33 nm during breakthrough, while the injected colloids had similar average size of 144±33 nm (LIBD). The Al (indicator element for clay particles) peaked after 303 min, and the Th, Tb and Hf (homologue elements absorbed on the clay) peaks were found 239-300 min after the injection in the dipole.

In the laboratory, both generation and sedimentation processes of bentonite colloids in NaCl solutions were examined using SPC technique. A colloid-population from Ca-type (FEBEX, Spain) or Na-type (Kunigel, Japan) bentonite pellets formed quickly (within one hour) in batch type tests. This process may be attributed to the detachment of colloids accompanied by structural change of the hydrated clay pellet and colloid self-diffusion.

After the initial particle creation period, colloid size-distributions varied over several hundreds of hours in the batch tests, in which colloids were populated by spontaneous diffusion after detachment (mostly small colloids) from the colloid-bed followed by aggregation of these small colloids in the suspension.

Colloid generation from the bentonite pellets was reduced in higher salinity solutions since the tendency to agglomerate is increased. The sedimentation process was highly dependent on particle size. Whether the starting point was a clay pellet or a concentrated clay suspension, the colloid size-distributions reached similar pseudo-equilibrium states (see Fig. 6.2).

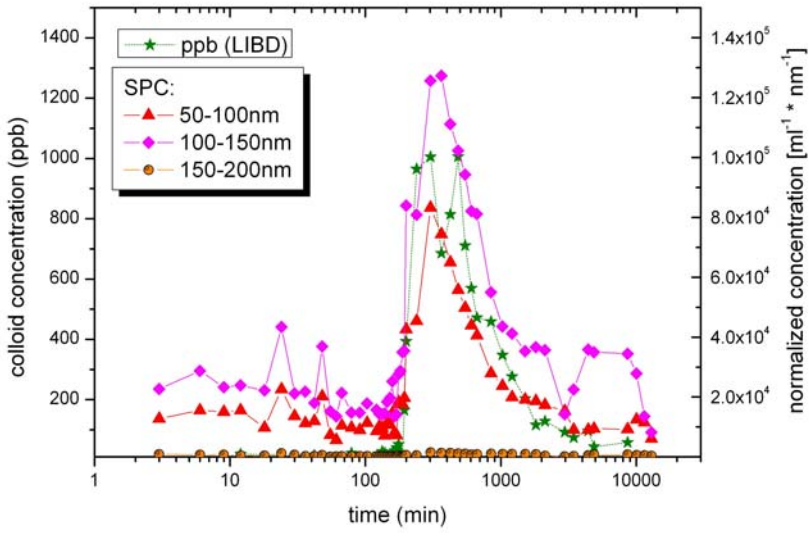


***Fig. 6.1:*** *Comparison of the PSI SPC and INE/KIT, LIBD data. The scales for the SPC and the laser induced breakdown, LIBD, data are on the right and left ordinates respectively. The size analysis shows no apparent chromatographic effect for the larger fraction (30 – 200 nm) of the clay colloids.*

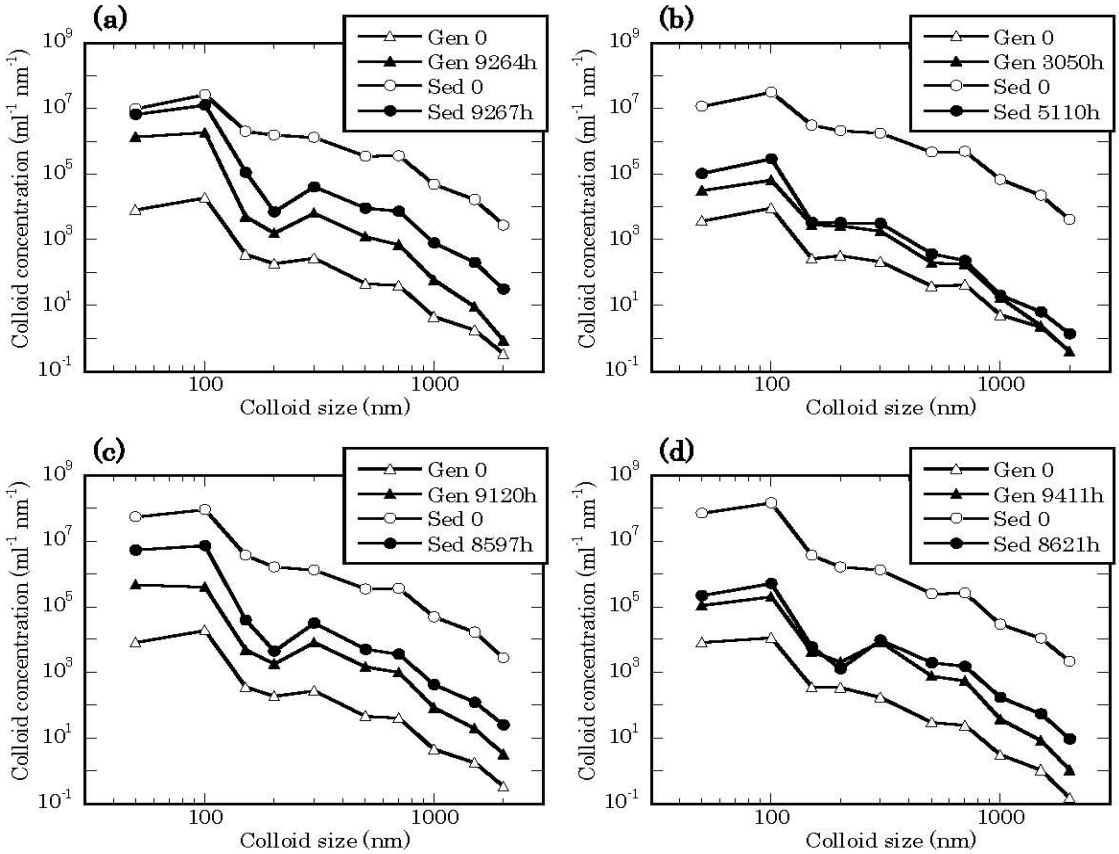


***Fig. 6.2:*** *Size distribution of FEBEX and Kunigel colloids per unit size and volume for the initial and final recorded stages in the colloid generation and sedimentation experiments. (a) FEBEX; 0.001 M NaCl, (b) FEBEX; 0.01 M NaCl, (c) Kunigel; 0.001 M NaCl, (d) Kunigel 0.01 M NaCl. Generation (Gen) and sedimentation (Sed) tests:Gen 0 (t=0) and Sed 0 (t=0). Gen 9120h and Sed 8621h are the values recorded after 9120 h and 8621 h contact times respectively.*

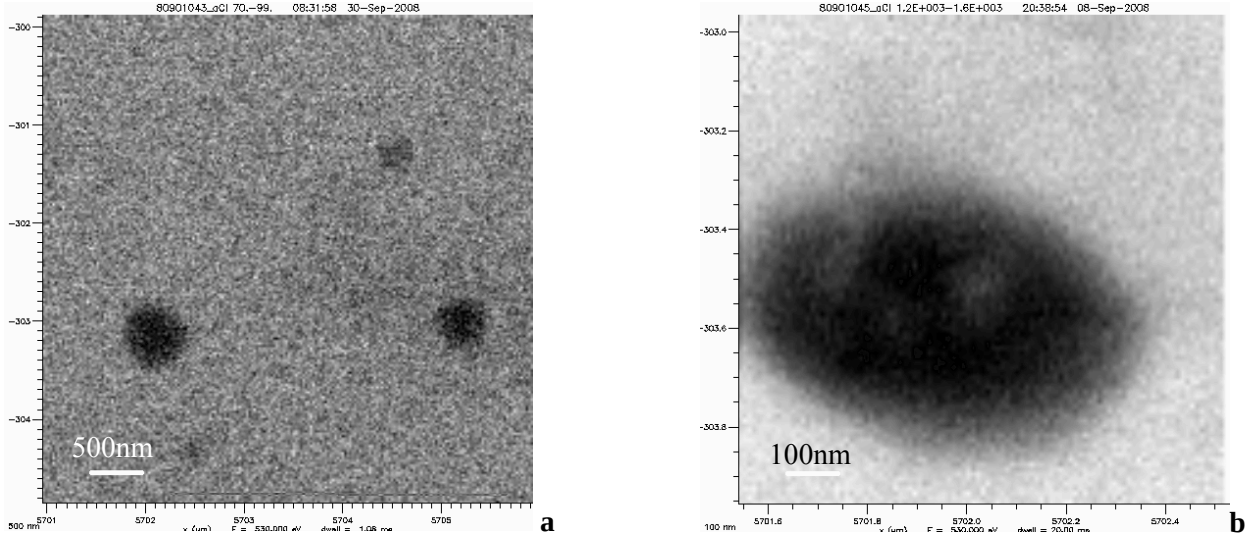


***Fig. 6.3:*** **a** X-ray micrograph of colloidal clay aggregates. **b** X-ray micrograph of a colloidal clay aggregate. Note: detection at 530 eV.

The pseudo-equilibrium size distributions depended on the salinity of the solution and were found not to be significantly dependent of the major initial cation ($Ca^{2+}$ or $Na^{+}$) loading of the montmorillonite. However, the colloid mass concentration for sizes ranging from 50 to 1000 nm was 1.5 mg $L^{-1}$ with a density of 1.2 g $cm^{-3}$ (corresponding to gel like aggregates, see section 3) in 0.001 and 0.01 M NaCl solutions.

Colloid generation and sedimentation experiments were also carried out on Na- and Ca- montmorillonite (Wyoming) in order to verify whether pseudo-equilibrium is reached at the same level for the treated (Ca-montmorillonite) or non-treated clay (Na-montmorillonite). The size and concentration of montmorillonite colloids were again monitored as a function of time and distance from the colloid source in different ionic strength solutions. A stable pseudo-equilibrium concentration was reached in generation and sedimentation experiments. The colloid concentration decreased with increasing distance from the source. At a distance of ~7 cm from the colloid source, the pseudo-equilibrium Na-montmorillonite mass concentration was 4, 0.4 and 0.2 (±0.1) mg $L^{-1}$ in 0.001, 0.01 and 0.1 M NaCl respectively for a density of 1.2 g $cm^{-3}$ (corresponding to gel like aggregates). For Ca- montmorillonite the mass concentration was 0.3 mg $L^{-1}$ in 0.001 M NaCl for sizes ranging from 50-1000 nm for a density of 1.2 g $cm^{-3}$.

## 6.3 Other colloid activities

The environmental behaviour of colloidal clay in aquatic systems is linked to the properties of their aggregates. Earlier investigations of clay colloids were performed with electron microscope techniques which caused dehydration of the particles. These images are not representative of clay colloids occurring in aqueous systems because of this. Information on the structure of clay colloid aggregates is needed to understand their sedimentation behaviour, as well as colloid contaminant transport in natural systems. By using scanning transmission X-ray microspectroscopy, images of montmorillonite colloid aggregates in a pseudo equilibrium state in a mM NaCl suspension after more than one year have been successfully produced for the first time (see Fig. 6.3). These clay aggregates were revealed at photon energies below the oxygen absorption edges of clay and water. They were spherical or ellipsoidal in shape with diameters or major axes of ~100 to ~800 nm (For the elliptical particles the major to minor axes ratio was a maximum of ~2). The aggregates looked porous, with densities lower than the clay mineral. Aggregates with cores of higher density material surrounded by a lower density gel like material were observed. These investigations are important for colloid generation modelling of clay aggregates in aqueous environments because colloids with sizes larger than 50 nm would be readily eliminated for a clay density of 2 g $cm^{-3}$.

The association of Th onto colloids was studied earlier with emphasis on Th polymers. This work has now been published. The study will be completed by EELS investigations aimed at verifying Th polymerisation, or not. EELS will also be used in the characterization of the in the CFM cocktail.

A granitic groundwater sampling and characterisation study (KFM11A, KLX17A and KLX15A) was carried out in the framework of a co-operation with Scandinavian groups and has been published. This study completes our former activities on granitic groundwater colloids.

### 6.4 Future work

New homologue tests are foreseen in early 2009, and SPC will be used together with other techniques to characterise the colloids during breakthrough. During these tests the flow rate will be varied from one experiment to the next.

For the CFM project the generation of colloids at a bentonite bloc/groundwater flow interface with quasi-stagnant water is being studied from a mechanistic point of view, and our model will be used systematically to describe the generation during the main experiment which is in the process of being designed on the basis of mock-up tests performed at INE. Colloid size distributions from the bentonite source will be compared with those from the groundwater system sampled at the exit borehole as a function of time.

### 6.5 References

BESSHO K., DEGUELDRE C. (2008)
Generation and sedimentation of colloidal bentonite particles in water. Applied Clay Science, in Press, Corrected Proof, available online 3 September 2008.

# 7 DIFFUSION PROCESSES

*L.R. Van Loon, M.A. Glaus, F. González, W. Müller, R. Rossé*

## 7.1 General

The "Diffusion Processes" group is studying the diffusion of radioelements in different argillaceous porous media in order to obtain a detailed understanding of the diffusion processes in such materials. The clay systems under investigation are Opalinus Clay (OPA), and compacted clay minerals such as montmorillonite, illite and kaolinite.

The work on pure clay minerals (TRAPHICCS) was continued. So far diffusion data for $^{85}Sr^{2+}$, $^{22}Na^{+}$, $^{134}Cs^{+}$, $^{36}Cl^{-}$ and $^{35}SO_4^{2-}$ in Na-montmorillonite, Na-illite and kaolinite under different chemical conditions and for different degrees of compaction ($\rho_b$= 1300; 1600 and 1900 kg $m^{-3}$) are available. The main challenge is now the interpretation of the diffusion results and the development of a model to describe them.

The work for the EU Integrated project NF-PRO (Near Field Processes) finished at the end of 2007. No further diffusion experiments on compacted bentonite were performed. Within the framework of the EU Integrated Project FUNMIG (Fundamentals of Migration), the focus was on the in-diffusion of $^{152}$Eu(III) in Opalinus Clay. Also, diffusion studies in support of the long-term field experiments in Mont Terri (DR) formed an important part of the experimental work in 2008.

The DINAPOR project (Diffusion of Nanoparticles in Argillaceous Media: Assessment of the Pore Structure; Euratom Training Fellowships: Marie-Curie Euratom Fellowship) was completed at the end of Octobre 2008.

The PhD thesis work of F. González: "Water diffusion through compacted clays analyzed by neutron scattering and tracer experiments" yielded four publications

A new PhD proposal: " Quantitative Analysis of Micro Heterogeneous Systems: A joint employment of complementary microbeam techniques", prepared in co-operation with D. Grolimund, µ-XAS beamline, was accepted by the Swiss National Science Foundation. The focus of the proposal is the application of microbeam techniques to measure narrow diffusion profiles of strongly sorbing tracers in heterogeneous systems. A second PhD proposal: "Water Dynamics in Clays", was prepared in co-operation with the Laboratory for Neutron Scattering (Dr. F. Juranyi) and was also accepted by the Swiss National Science Foundation. This work is a continuation of the PhD work of F. Gonzalez.

## 7.2 Diffusion in Opalinus Clay

The in-diffusion experiments of $^{152}$Eu(III) in Opalinus Clay were repeated. In order to avoid the problems associated with sorption on equipment, the tracer was directly applied onto the surface of the sample. This was achieved by opening the diffusion cell after the resaturation phase, and contacting one side of the sample with a solution containing the $^{152}$Eu(III) tracer. After 5 minutes, the solution was removed, and the diffusion cell was closed. After 1 year of in-diffusion, the profile was measured by the abrasive peeling technique (VAN LOON AND EIKENBERG, 2005). Similar to $^{60}$Co(II), $^{152}$Eu(III) showed a dual porosity type behaviour, i.e. a fast and a slow diffusion process was observed. The majority of the $^{152}$Eu(III) diffused by the slow process. First estimates revealed an apparent diffusion coefficient of $1x10^{-16}$ $m^2$ $s^{-1}$ for the slow process. Taking an effective diffusion coefficient of $1x10^{-11}$ $m^2$ $s^{-1}$, a $K_d$ value of ~100 $m^3$ $kg^{-1}$ was obtained.

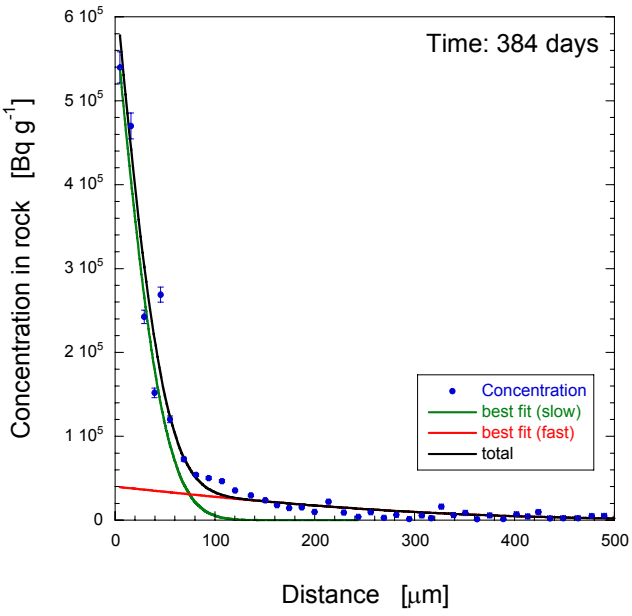


***Fig. 7.1:*** *Diffusion profile of $^{152}$Eu in Opalinus Clay after 384 days of in-diffusion.*

This is in agreement with the high $K_d$ values for Eu(III) measured in batch sorption experiments (LAUBER et al., 2000) and supports the high $K_d$ values for trivalent lanthanides and actinides used in geochemical databases for safety assessment (BRADBURY & BAEYENS, 2003).

In the framework of the long-term diffusion/retention experiment (DR) in Mont Terri, a set of 5 radial diffusion experiments (VAN LOON et al. 2004) have been ongoing since 2007. The diffusion of HTO, $D_2O$, $H_2{}^{18}O$ $I^-$, $Br^-$, $^{36}Cl^-$ and $^{22}Na^+$ were finished. There is good agreement with previous measurements on samples from a different location at Mont Terri, DI-A (Table 7.1). Diffusion tests with $^{85}Sr^{2+}$, $^{133}Ba^{2+}$ and $^{134}Cs^+$ were started in 2008 and are continuing. It is planned to start diffusion measurements with $SeO_4^{2-}$ and $TcO_4^-$ at the beginning of 2009. Before beginning these experiments, some analytical and speciation procedures have to be optimised. A separation technique (based on anion exchange chromatography) was developed in 2008 to distinguish between $SeO_4^{2-}$ and $SeO_3^{2-}$.

***Table 7.1 :*** *Effective diffusion coefficient (De) and rock capacity factors (α) for the diffusion of different radionuclides in samples of Opalinus Clay from two different locations in the Mont Terri underground research laboratoy. The artificial pore water is slightly different for the two locations (DI-A: I = 0.39 M; DR: I = 0.22 M.*

| **Isotop** | **DR** | | **[1)]DI-A** | |
|---|---|---|---|---|
| | $D_e$ ($m^2s^{-1}$) | α (–) | $D_e$ ($m^2s^{-1}$) | α (–) |
| HTO | $5.6x10^{-11}$ | 0.19 | $6.1x10^{-11}$ | 0.16 |
| $D_2O$ | $5.4x10^{-11}$ | 0.18 | n.m. | n.m. |
| $H_2O^{18}$ | $5.8x10^{-11}$ | 0.18 | n.m. | n.m. |
| $^{36}Cl$ | $1.3x10^{-11}$ | 0.09 | $1.7x10^{-11}$ | 0.083 |
| I [2)] | $9.5x10^{-12}$ | 0.10 | $1.7x10^{-11}$ | 0.088 |
| Br [2)] | $1.0x10^{-11}$ | 0.09 | $1.4x10^{-11}$ | 0.085 |
| $^{22}Na$ | $3.8x10^{-11}$ | 0.74 | $8.4x10^{-11}$ | 0.63 |
| $^{85}Sr$ | ongoing | - | $6.8x10^{-11}$ | 6.10 |
| $^{134}Cs$ | ongoing | - | $4.5x10^{-10}$ | isotherm |

[1)] APPELO & VAN LOON (2008).
[2)] stable isotopes

In order to obtain information on the homegeneity of the Opalinus Clay with respect to diffusion properties, several diffusion experiments were performed on samples taken at different depths from the deep bore hole in the Zürcher Weinland (-651m; -589m; -564m). The diffusion coefficient of HTO decreased by a factor of 1.5 over a distance of ~100 m. A similar picture was obtained for $^{36}Cl^-$ and $^{35}SO_4^{2-}$ where the diffusion coefficients decreased by a factor of ~2.7 (Fig. 7.2). For both locations, i.e. Mont Terri and the Zürcher Weinland, the Opalinus Clay formation is very homogeneous with respect to diffusion properties, i.e. the effective diffusion coefficients do not vary more than a factor of maximum 5 within the formation.

The out-diffusion of the $^{14}C$ labelled acetate ($^{14}CH_3COO^-$: a potential product from the anaerobic corrosion of carbon steel) was measured after finishing the through-diffusion studies (see the annual report from 2007).

The out-diffusion showed an unexplained behaviour, i.e. the out-diffusion flux vs time curve was characterised by a long tailing going on for almost 450 days (Fig. 7.3). This slow out-diffusion behaviour of $^{14}C$ labelled acetate indicates that an interaction between acetate and OPA is taking place. At the moment no information on this interaction is available.

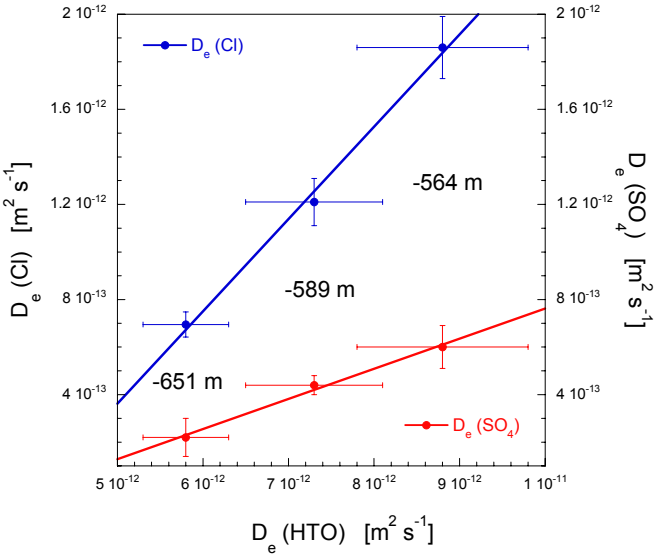


***Fig. 7.2:*** *Relationship between the diffusion coefficient of HTO and $^{36}Cl^-$, and HTO and $^{35}SO_4^{2-}$ for Opalinus Clay samples from the deep borehole in the Zürcher Weinland. The samples were taken at different depths as indicated in the figure.*

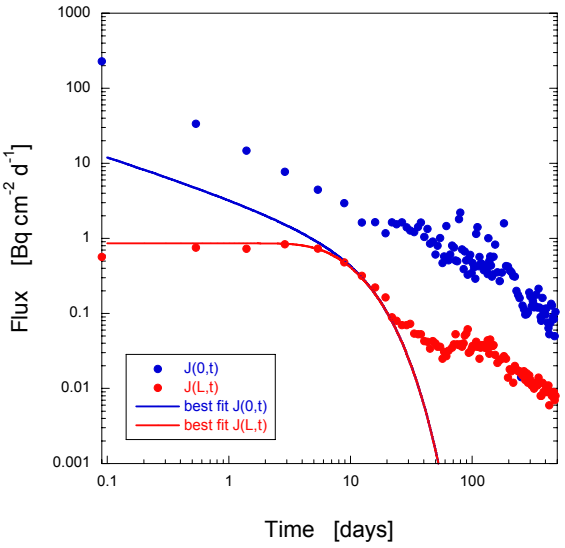


***Fig. 7.3:*** *Out-diffusion behaviour of $^{14}CH_3COO^-$ in Opalinus Clay from Mont Terri. The blue and red dots represent the results from the sample faces in contact with the high and low concentraton sides in the diffusion cell respectively.*

## 7.3 Transport phenomena in compacted clay systems (TRAPHICCS)

The activities within the frame of the TRAPHICCS project focused on the following topics:

1. Tracer diffusion studies with Na-montmorillonite compacted to dry bulk densities of 1300 and 1600 kg $m^{-3}$ for different tracers at variable external salt concentrations.
2. Investigations related to heterogeneities in the boundary zones of compacted clay samples.
3. Designing and testing of experimental equipment for the measurement of through-diffusion in compacted clay samples using gradient-free confining porous filters.

Through-diffusion data of HTO, $^{22}Na^+$, $^{36}Cl^-$ and $^{85}Sr^{2+}$ in Na-montmorillonite (Table 7.2) at dry bulk densities of 1300 and 1600 kg $m^{-3}$ indicated that the measured effective diffusion coefficients depend on the external salt concentration (the salinity of the solution in contact with the clay in the diffusion experiments). The observed dependence appears to be similar to that previously measured for bulk dry densities of 1900 kg $m^{-3}$: Increasing fluxes of cations with decreasing external salt concentrations were observed.

***Table 7.2 :*** *Effective diffusion coefficient ($D_e$) and rock capacity factors ($\alpha$) for the diffusion of different radionuclides in compacted samples of Na-montmorillonite.*

| Tracer | [A][1)] | 1300 kg $m^{-3}$ | | 1600 kg $m^{-3}$ | |
|---|---|---|---|---|---|
| | | $D_e$ ($m^2s^{-1}$) | $\alpha$ (–) | $D_e$ ($m^2s^{-1}$) | $\alpha$ (–) |
| HTO | 0.5 | $7.6x10^{-11}$ | 0.6 | $3.3x10^{-11}$ | 0.5 |
| | 1 | $7.8x10^{-11}$ | 0.8 | $3.3x10^{-11}$ | 0.5 |
| $^{36}Cl$ | 0.5 | $1.3x10^{-11}$ | 0.2 | $2.0x10^{-12}$ | 0.10 |
| | 1 | $1.5x10^{-11}$ | 0.35 | $3.0x10^{-12}$ | 0.13 |
| $^{22}Na$ [2)] | 0.5 | $1.1x10^{-10}$ | 3.5 | $7.0x10^{-11}$ | 3.7 |
| | 1 | $7.0x10^{-11}$ | 2.0 | $4.0x10^{-11}$ | 2.1 |
| $^{85}Sr$ [3)] | 0.5 | $2.4x10^{-10}$ | 11 | $5.0x10^{-11}$ | 12 |
| | 1 | $7.0x10^{-11}$ | 5.0 | $2.0x10^{-11}$ | 6.0 |

[1)] Concentration of $NaClO_4$ in the external solution (mol $dm^{-3}$).
[2)] Slight variations from Fickian diffusion in a single porous medium were observed in some cases, which will need a more detailed evaluation in the future.
[3)] Tentative estimates from ongoing experiments.

It can be concluded that these fluxes were driven by changes in the external tracer concentration gradient built up of sorbed cations which are assumed to be mobile in the interlayer pore space (GLAUS et al., 2007).

The observed increase of effective diffusion coefficients of $^{36}Cl^-$ with increasing external salt concentrations can be attributed to the presence of fixed anionic surface charges on the clay leading to a decreased anion-accessible porosity (VAN LOON et al., 2007). Both the anion-accessible porosity, and the concentration gradients of cations in the interlayer pore space, depend on the external salt concentration. It can therefore be concluded that the pore water chemistry in montmorillonite (and also in bentonite, which consists mainly of montmorillonite) may have an impact on the flux of charged species at repository-relevant degrees of compaction.

Heterogeneities in the degree of compaction of samples of swelling clay minerals have occasionally been observed in previous experiments. For example, the water porosity (measured as the weight loss on heating) increased typically from 0.32 to ~0.45 within the outer 1mm of a 10 mm thick sample of montmorillonite compacted to 1900 kg $m^{-3}$.

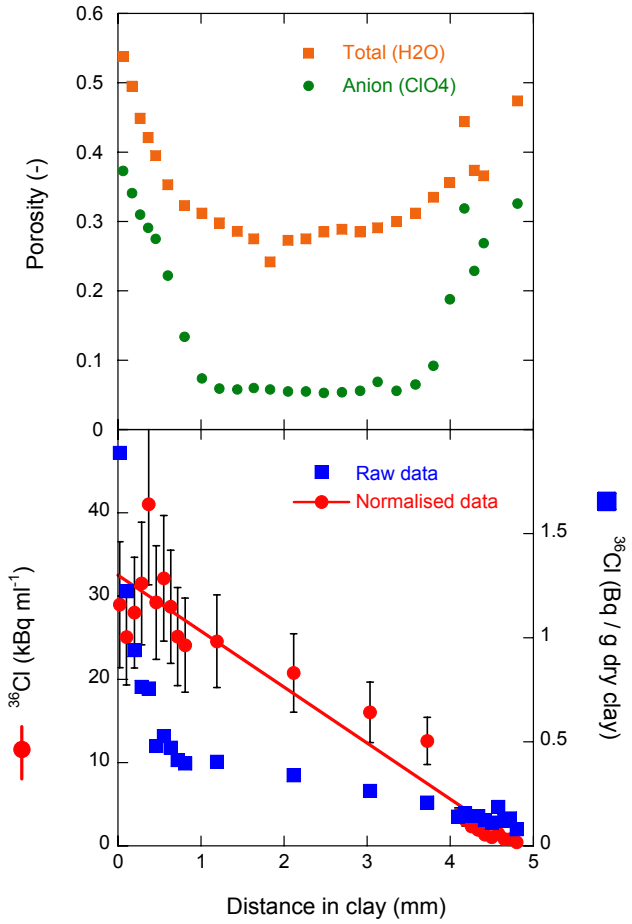


***Fig. 7.4:*** *Profile analysis of a sample of Na-montmorillonite after through-diffusion of $^{36}Cl$: Porosities were determined from water content and the content of the major anion $ClO_4^-$ (upper) and tracer profile (lower).*

This corresponded to a decrease in the degree of compaction from 1900 kg m$^{-3}$ to 1500 kg m$^{-3}$ in the boundary regions. In the experiments carried out over the past year these heterogeneities have not only been characterised in terms of the water content in sliced clay samples but also in terms of the content of the main salt ($NaClO_4$). The anion-accessible porosity was calculated from the amounts of $NaClO_4$ extracted from the slices, assuming that the concentration of $NaClO_4$ in the anion-accessible volume was equal to that in the contacting electrolyte solution. It could be observed that the anion-accessible porosity paralleled the water content (Fig. 7.4, upper figure) in the boundary regions of the clay sample. It was possible to reinterpret the observed tracer profiles for $^{36}Cl^-$ through a simple normalisation procedure (Fig. 7.4, lower figure). For the latter purpose it was assumed that the anion-accessible porosity was the same for $ClO_4^-$ and $^{36}Cl^-$. The activities of $^{36}Cl^-$ in the slices were normalised to the actual individual anion-accessible volumes of each slice.

The diffusion profiles typically measured in samples at these compactions exhibit two different slopes, which were interpreted as a fast and slow diffuson process in the literature (MOLERA et al., 2003). After normalisation of the profile data for anion-accessible porosity, a profile with a single slope is obtained, giving one effective diffusion coefficient which is in good agreement with values previously obtained in the through-diffusion experiments. This shows that there is no reason to assume more than one type of porosity for the description of anion diffusion in highly compacted swelling clays. No such anomalies were observed in samples of highly compacted kaolinite. This is an indication that the "edge effects" are a consequence of the swelling properties of the clay.

A "gradient-free" diffusion cell is being developed for diffusion experiments in which the diffusive resistance of the confining filters is larger than that of the clay sample. In this equipment the filters are flushed advectively with the contacting tracer solution in order to maintain constant concentrations within the filters. Two prototypes were tested in terms of the hydraulic properties of the flushed filters and the membrane filters used to prevent the ingress of clay particles into the porous steel filters. The experiments were accompanied by numerical modelling studies (cf. section 3.2.3). The hydraulic properties of the filters turned out to be satisfactory even at relatively low hydrostatic pressures (ca. 10-30 cm of water). First diffusion experiments are currently underway

## 7.4 Dynamics of water in compacted clay systems

The work performed in the framework of a PhD Thesis (GONZÁLEZ, 2007) was published in several peer reviewed journals (GONZÁLEZ et al., 2007; GONZÁLEZ SÁNCHEZ et al., 2008a; GONZÁLEZ SÁNCHEZ et al., 2008b; GONZÁLEZ SÁNCHEZ et al., 2008c; GONZÁLEZ SÁNCHEZ et al., 2008d).

A new proposal was written in co-operation with the Laboratory for Neutron Scattering (JURANYI et al., 2008). The proposal has been accepted by the Swiss National Science Foundation (SNF). The work will start as soon as a suitable candidate has been found. This PhD project is a continuation of some previous work (GONZÁLEZ, 2007) and will focus on the understanding of the observed difference in activation energy of water diffusion in different clay minerals (montmorillonite, illite, kaolinite) and on the characterisation of water dynamics in 2D confinement by neutron scattering techniques.

## 7.5 DINAPOR

The aim of the DINAPOR project was to develop an alternative method for determining the pore size distribution in compacted argillaceous materials. The basic idea was to extract this information from the diffusive behaviour of (macro-)molecules of different sizes. PAMAM (polyamidoamine) dendrimers were chosen for this work because of their well-defined structure, narrow polydispersity, well-defined nanoscale size and the ease of modifying the end groups (Fig. 7.5).

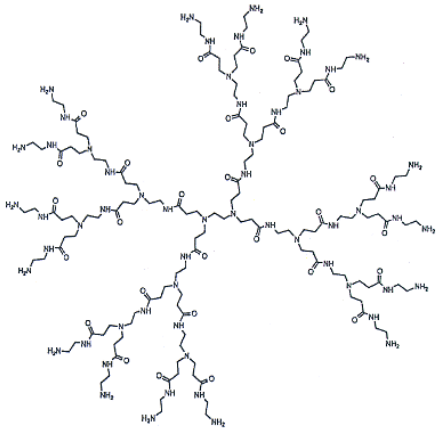

***Fig. 7.5:*** *Structure of a PAMAM (G2) dendrimer.*

The diffusion of 3 types of nano-particles through Opalinus Clay was studied (G3=3.6 nm, G5=5.4 nm, and G7=8.1 nm). It could be shown that only the G3 particles with a diameter of 3.6 nm were able to diffuse through the Opalinus Clay. Although having a diameter smaller than the average diameter of Opalinus Clay (~15 nm), the G5 and G7 did not migrate. One possible explanation might be found in a slot-like shape of the pores in OPA (Fig. 7.6). Such pores are known to be formed in highly consolidated rocks (ROBERTS AND SCHWARTZ, 1985).

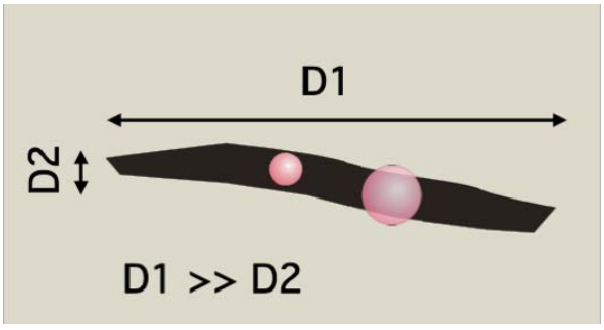


***Fig. 7.6 :*** *Cross-section view of a slot-like pore (D1>D2) in Opalinus Clay. Nanoparticles with a diameter larger than D2 cannot migrate through the clay.*

## 7.6 Micro-heterogeneous systems

Micro-heterogeneity represents an inherent and highly relevant characteristic of most natural and engineered (geo-)materials. Typical examples of such micro-heterogeneous materials include rocks and sediments, ceramics and composites, and engineered barrier materials such as bentonite and cement. Macroscopic physical properties as well as the chemical reactivity of these materials are often determined by the nature of their micro-domain configurations. Accordingly, in order to improve our knowledge of the behaviour of specific materials, and particularly their reactivity with contaminants, an adequate understanding of the impact of the assembly structure is required.

A PhD proposal devoted to this topic was written in co-operation with Prof. D. Günther (ETHZ). The proposal was submitted to, and accepted by the Swiss National Science Foundation (GROLIMUND et al., 2007). As soon as a suitable candidate has been recruited, the work will start.

## 7.7 References

APPELO C.A.J., VAN LOON L.R. (2008)
Modelling of Cs-data from diffusion experiments in the laboratory and in-situ in DI-A experiments (phase 12) in Opalinus Clay. Part 1: Modelling laboratory data. Mont Terri Technical Note 2007-44.

BRADBURY M.H., BAEYENS B. (2003)
Far field sorption databases for performance assessment of a HLW repository in an undisturbed Opalinus Clay host rock. PSI Bericht Nr. 03-08 and Nagra NTB 02-19.

GLAUS M., BAEYENS B., BRADBURY M.H., JAKOB A., VAN LOON L.R., YAROSHCHUK A. (2007)
Diffusion of $^{22}Na$ and $^{85}Sr$ in montmorillonite: Evidence of interlayer diffusion being the dominant pathway at high compaction. Environ. Sci. Technol. 41, 478-485.

GONZÁLEZ F. (2007)
Water diffusion through compacted clays analyzed by neutron scattering and tracer experiments. PhD. Thesis, University of Bern, Bern, Switzerland.

GONZÁLEZ F., JURÁNYI F., VAN LOON L., GIMMI T. (2007)
Translational diffusion of water in compacted clay systems. Eur. Phys. J. Special Topics 141, 65-68.

GONZÁLEZ SÁNCHEZ F., JURÁNYI F., GIMMI T. VAN LOON L.R., SEYDEL T., UNRUH T. (2008a)
Dynamics of supercooled water in highly compacted clays studied by neutron scattering. J. Phys.: Condens. Matter 20, 415102, 9pp.

GONZÁLEZ SÁNCHEZ F., VAN LOON L.R., GIMMI T., JAKOB A., GLAUS M.A., DIAMOND L.W. (2008b)
Self-diffusion of water and its dependence on temperature and ionic strength in highly compacted montmorillonite, illite and kaolinite. Appl. Geochem. 23, 3840-3851.

GONZÁLEZ SÁNCHEZ F., JURÁNYI F., GIMMI T., VAN LOON L., UNRUH T., DIAMOND L. (2008c)
Translational diffusion of water and its dependence on temperature in charged and uncharged clays: a neutron scattering study. J. Chem. Phys. 129, 174706, 11pp.

GONZÁLEZ SÁNCHEZ F., GIMMI T., JURÁNYI F., VAN LOON L., DIAMOND L.W. (2008d)
Comparison of the diffusion of water in compacted clays at two different time scales by macroscopic tracer through-diffusion and microscopic quasielastic neutron scattering. Submitted to Environ. Sci. Technol.

GROLIMUND D., VAN LOON L.R., GÜNTHER D. (2007)
Quantitative analysis of micro-heterogeneous systems: joined forces of complementary micro-beam techniques. PhD. proposal, Swiss National Science Foundation.

JURANYI F., VAN LOON L.R., GIMMI T., KOSAKOWSKI G. (2008)
Water dynamics in water-clay systems. PhD. proposal, Swiss National Science Foundation.

LAUBER M., BAEYENS B., BRADBURY M.H. (2000)
Physico-chemical characterisation and sorption measurements of Cs, Sr, Ni, Eu, Th, Sn and Se on Opalinus Clay from Mont Terri. PSI Bericht 00-10, Paul Scherrer Institut, Villigen, Switzerland.

MOLERA M., ERIKSEN T., JANSSON M. (2003)
Anion diffusion pathways in bentonite clay compacted to different dry densities. Appl. Clay. Sci. 23, 69-76.

ROBERTS J.N., SCHWARTZ L.M. (1985)
Grain consolidation and electrical conductivity in porous media. Phys. Rev. B 31, 5990-5997.

VAN LOON L.R., SOLER J.M., MÜLLER W., BRADBURY M.H. (2004)
Anisotropic Diffusion in Layered Argillaceous Rocks: A Case Study with Opalinus Clay. Environ. Sci. Technol. 38, 5721-5728.

VAN LOON L.R., EIKENBERG J. (2005)
A high-resolution abrasive method for determining diffusion profiles of sorbing radionuclides in dense argillaceous rocks. Appl. Radiat. Isot. 63, 11-21.

VAN LOON L.R., GLAUS M.A., MÜLLER W. (2007)
Anion exclusion effects in compacted bentonites: Towards a better understanding of anion diffusion. Appl. Geochem. 22, 2536-2552.

# 8 THE MICRO-XAS BEAMLINE PROJECT

*D. Grolimund, C.N. Borca, B. Meyer (SYN), M. Willimann (SYN)*

## 8.1 General

Within the Laboratory for Waste Management (LES), the micro-XAS beamline is operated as a dedicated high resolution hard X-ray microprobe station at the Swiss Light Source. This analytical facility allows materials and matter to be investigated by means of high intensity X-ray beams with a spatial resolution of approximately 1μm$^2$ (GROLIMUND et al., 2002). A combination of fluorescence, spectroscopy and diffraction techniques is available in an energy range of ~4 to ~23 keV.

During the first two years of user operation, several areas of core compentence evolved. The most prominent are: i) (spectro)microscopy (PODGÓRCZYK et al., 2008; JEFIMOVS et al., 2007; JOHNSON et al., 2008a; BORCA et al, 2008; FROIDEVAL et al., 2008a; RODENBURG et al., 2007), ii) ultrafast X-ray science involving diffraction and spectroscopy (BEAUD et al., 2007; JOHNSON et al., 2008b;, GAWELDA et al., 2007a,b; PHAM et al., 2007), iii) in-situ micro-diffraction (MAASS et al., 2007a,b; MAASS et al., 2008a,b), as well as iv) radioactive microprobe analysis (CAMMELLI et al., 2008; DEGUELDRE et al., 2008; FROIDEVAL et al., 2008a,b). As shown by the results and corresponding publications given above, a high level scientific tool is provided to a broad user community.

Every reasonable endeavour is being made to further strengthen the existing core areas and to establish new fields. Over the past year these efforts have been focused on two priority topics: two-dimensional micro-X-ray-diffraction and micro-X-ray-absorption-spectroscopy (as compared to spectromicroscopy). It should be noted that micro-XAS, in particular micro-EXAFS (extended X-ray absorption fine structure) spectroscopy, represents simultaneously both the ultimate analytical capability and also the 'piece de resistance' for any hard-X-ray microprobe with true micron resolution.

Within the present annual report we will document the progress made in the fields of micro-XRD and micro-XAS, based on selected scientific studies.

## 8.2 Two-dimensional micro-X-ray-diffraction

In the original concept of the micro-XAS beamline, micro-diffraction was not assigned a particularly high priority. However, due to the very high level of interest and commitment of the user community, micro-XRD rapidly developed into a core technique used at the micro-XAS beamline. The availability of micro-focused 'white light' allowed the devolpment of advanced, *in-situ* micro-Laue techniques (MAASS et al., 2007a,b). In addition to the original static, 'point' measurements, a two-dimensional raster scanning scheme was implemented recently by R. Maass, S. van Petegem et al. (NUM-PSI) in close collaboration with the beamline staff (MAASS et al., 2008a,b). This experimental technique allows two-dimensional images of crystallographic information to be recorded. Simultaneously, microscopic information can be retrieved, e.g. based on fluorescence radiation analysis (micro-XRF). Most recently, this technique was even used in radioactive measurement campaigns.

As an illustrative example, we will present preliminary results originating from a research project studying corrosion phenomena occuring on primary circuit components of nuclear power plants. Such corrosion phenomena are important for safety reasons (material brittleness, etc.) as well as radiation exposure within the plant. We intend to elucidate the complex chemical system at the 'steel/alloys – high-temperature water' interface by the combined use of X-ray microprobe techniques. Initially, we focused on the determination of the chemical identities of the corrosion products ('scratch samples') formed during full plant operation. So far, spectromicrosopy, micro-EXAFS and micro-XRD provided structural information on the different oxide phases formed. This feasibility study revealed considerable electronic and structural differences between the different individual oxide particles.

Fig. 8.1 shows one of the first two-dimensional micro-XRD images from a radioactive sample obtained at the micro-XAS beamline. The raster-scanning scheme allows crystallographic data as well as chemical information to be collected at each image pixel. In the present case, a two-dimensional Laue pattern was recorded at each pixel (Fig. 8.1a).

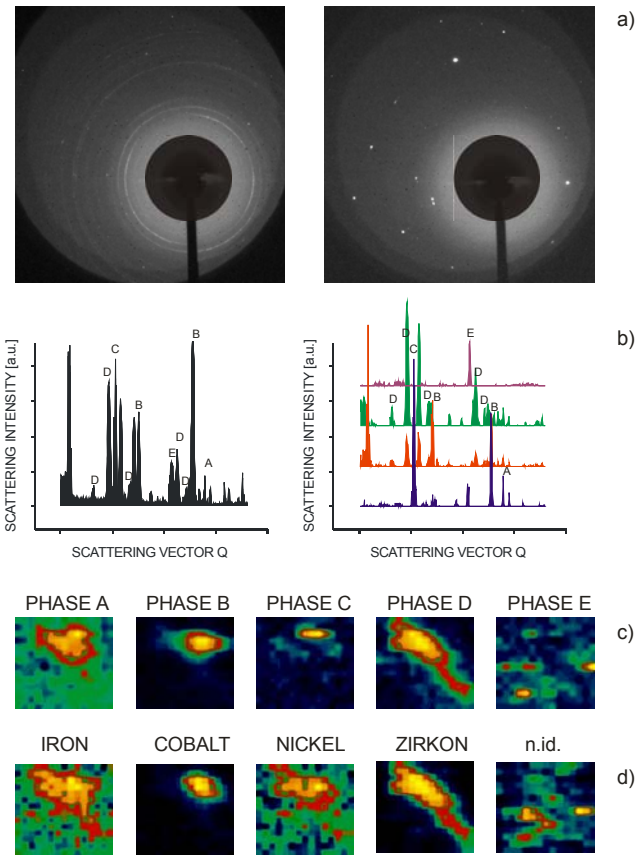


***Fig. 8.1:*** *Two-dimensional micro-diffraction. a) single spot Laue diffraction pattern indicative of a polycrystalline sample volume (left), and a single crystal (right). b) one-dimensional diffractogram of the entire sample volume (left), and of selected single pixels, c) two-dimensional distribution of different crystallographic phases d) simultaneously recorded elemental distribution maps (micro-XRF images).*

Based on such diffraction patterns, crystallographic phases, grain orientations, and even information as detailed as distortions, dislocations, or disorder can be determined. The two examples shown in Fig. 8.1a are representative of a large single micro-crystal (right) or a large number of nano-grains (left) present in the few $\mu m^3$ large sample volume. Based on the information provided from each individual pixel, the full image can be reconstructed. First, the two-dimensonal Laue pattern is reduced to one dimensional data by Q integration. Fig. 8.1b depicts the resulting diffractogram for the entire image (left) as well as selected single pixel Q integrations (right). Readily apparent is that different mineral entities are found at different locations (labels correspond to different mineral phases). Quantitative analysis of the different mineral constituents identified in each pixel can be compiled into images of mineral distribution pattern. As an exmple, Fig. 8.1.c depicts the distribution of five different crystallographic species. Such structural information can be compared to complementary chemical information such as elemental distributions (Fig. 8.1d) or oxidation state maps (not shown). Observed correlations between crystallographic species and chemical elements (as observed in the present case) yield valuable information concerning mineral phase identification and refinement.

## 8.3 Micro-X-ray-absorption-spectroscopy

In the case where both the object and the X-ray beam diameter are approaching about 1μm (or below) microspectroscopy becomes a real challenge. Inherent in spectroscopy is the necessity to vary the wavelength of the probing beam. In the case of an X-ray spectrometer this requires movable optical parts within a large-scale spectrometer (beamline). Considering that the opticals arrangement have to be changed using lever arms several meters in length, it may be immediately realized that meeting the requirement of 'zero' beam motion for the sample spot is technically extremely demanding. For example, high quality micro-EXAFS on a micron sized object with a $1\mu m^2$ beam would require that the magnitude of beam-to-sample fluctuations and drifts be as small as a few nanometers. Accordingly, most crucial aspect in the context of microspectroscopy is to adjust the measurement strategy to the specific characteristics of the investigated sample. Proper adaptation of the experimental setup allows the adverse effects of beam motion or vibrations (floor, sample, etc.) to be minimized (PODGÓRCZYK et al., 2008).

The following two examples illustrate the current microspectroscopic capabilities available at microXAS beamline.

### Micro-EXAFS I: Nickel microstructures

An 80 nm thick Ni patterned film fabricated by electron beam lithography using the lift-off technique (JEFIMOV et al., 2008, VILA-COMAMALA et al., 2008) was investigated using hard-X-ray microprobe techniques. First, the spatial extension of the nano-tracks of Ni was imaged using element-specific X-ray fluorescence micro-analysis. Second, the molecular structure of the deposited Ni within these nano-films was investigated using micro-EXAFS. Selected results are shown in Fig. 8.2. The top panels display a SEM image and the element specific spatial distribution of Ni. This latter image was constructed based on fluorescence intensity measurements using the fast 'on-the-fly' 2D scanning tool available at micro-XAS. The size of the grid lines was 1 μm in both horizontal and vertical directions, with a period of 10 μm. The

(sub)micro resolution achieved within this elemental distribution analysis is readily apparent. Note, the difference in resolution between the horizontal versus the vertical direction is directly related to the assymetric beam size used, 1.3 µm (H) x 0.5 µm (V).

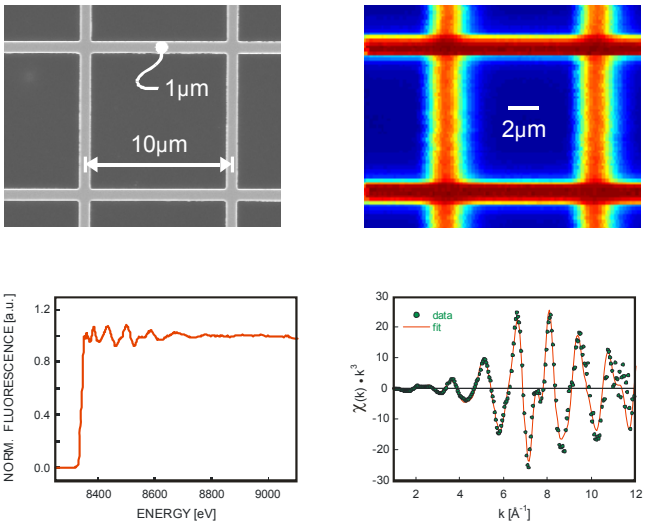


***Fig. 8.2:*** *SEM image(top left), micro-XRF map (top right), and micro-EXAFS collected at the Ni K-edge (bottom). The size of the Ni grid lines is 1 µm with a period of 10 µm. The bottom left panel shows an average of 5 unsmoothed micro-EXAFS scans acquired at the intersection of two Ni lines. The bottom right panel shows the corresponding EXAFS oscillations and the corresponding fit in k-space.*

The micro-EXAFS at the Ni K-edge was performed at the intersection of two grid lines, again using a beam size of 1.3 µm (H) x 0.5 µm (V). The average of 5 unsmoothed scans is shown in the bottom left panel of Fig. 8.2, while the corresponding EXAFS oscillations in k-space are shown in the bottom right panel. The spectrum is of excellent quality and is free of distortions and artefacts. This statement is further substanciated by the detailed EXAFS data analysis. As an illustration, a selected fitting result is shown by a continuous line. This fit was performed using the IFEFFIT package and indicates the presence of 6 Ni nearest neighbors at a distance of 2.45(8) Å, as expected for bulk metallic $Ni^0$.

The shown spectrum is based on a count rate of 20k fluorescence counts per second and a total count sum of 100kcts. A rough estimate based on the noise level at higher k values indicates a noise level as low as only three times the shot-noise limit. This result illustrates the potential and capabilities of performing micro-EXAFS analysis at the micro-XAS beamline using a (sub)micron hard X-ray beam and fluorescence detection.

**Micro-EXAFS II: Corrosion of irradiated cladding**

A zirconium alloy irradiated in a pressurized water reactor was analyzed using a combination of X-ray absorption spectroscopy and X-ray scanning microscopy. A tube segment, with an ~10 µm thick oxide layer, was cut from the irradiated Zr/Nb cladding.

A sophisticated sample preparation strategy has been developed and employed in order to obtain samples optimized for X-ray microbeam investigations. Using the Focused Ion Beam (FIB) technique, a window with a diagonal size of ~40 µm was 'blasted' out of the cladding material (Fig. 8.3a). The window thickness of 10 µm was chosen such that an optimized pathlength for transmission measurements was achieved.

First, *microscopic* investigations revealed an absorption contrast image (Fig. 8.3b) based on local transmission measurements. Following this, *spectromicroscopy* was performed. Basic results from spectromicroscopic investigations are elemental distribution maps (not shown, but see for example Fig. 8.1d). More sophisticated measurements provide oxidation state maps or images of different chemical species. For the later two cases, several images are recorded at different X-ray beam energies from which the distribution of chemical information can be reconstructed (GROLIMUND et al., 2004). For the present example, the oxidized form of Zr is imaged based on such chemical contrast techniques (Fig. 8.3c).

The oxidized form of Zr is constrained to the corroded 8µm thick top layer. Finally, element-specific microspectroscopy was conducted at the Zr and Nb K-edges either in transmission (Zr) or in fluorescence (Nb) mode. Due to the high spatial resolution, such molecular speciations could be performed in the pristine metal part, the 10µm thick oxide layer as well as directly at the metal/oxide interface. Several micro-EXAFS spectra were collected through the corrosion interface in one micron steps. Three selected single scans – each representative of a different zone in the material – are displayed in Fig. 8.3d. Again, the different spectra are of excellent quality. Up to k of 12Å$^{-1}$ the spectra are free of distortions or artefacts. Note that, the accessible k range was not limited to 12Å$^{-1}$ due to noise issues, but rather to a considerable glitch which severly distorted the spectra.

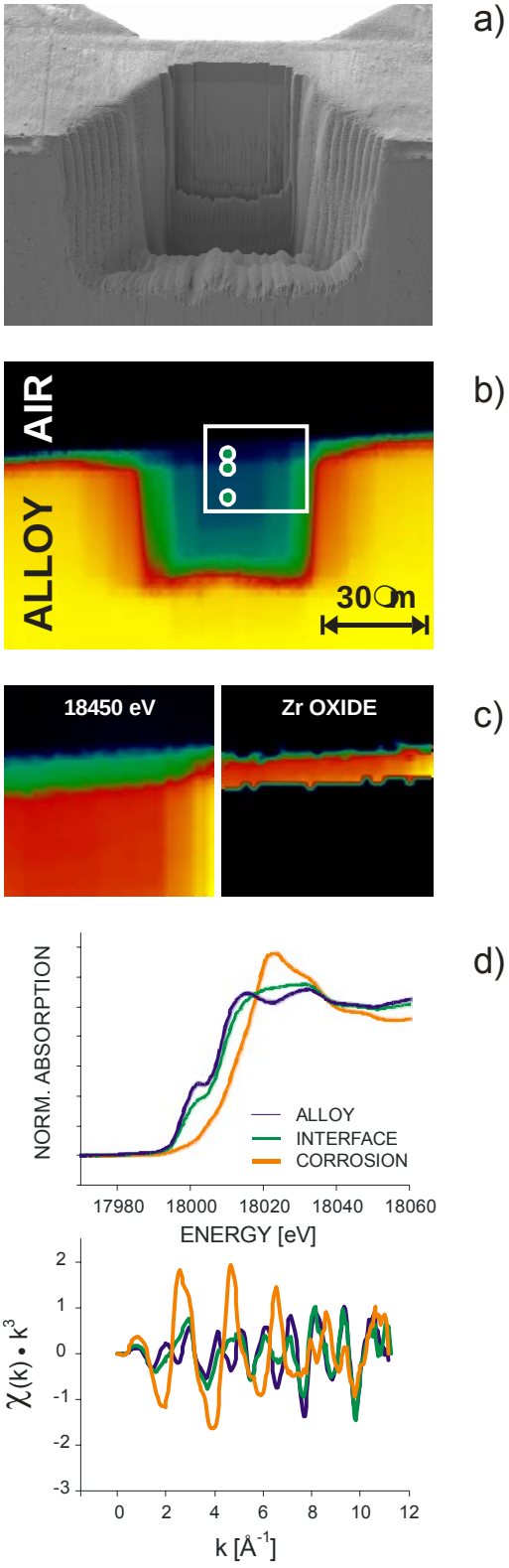


***Fig. 8.3:*** *Corrosion of irradiated cladding. a) SEM image of the sample, b) microscopy: transmission absorption contrast image, c) spectromicroscopy: absorption contrast image compared to oxidation state mapping. The square in b) corresponds to the image section shown, d) microspectroscopy: micro-XANES and micro-EXAFS. The circles in b) indicate the measurement locations. Single scans are shown.*

## 8.4 Outlook

In the near future, considerable improvements are planned for both two-dimensional micro-X-ray-diffraction and micro-X-ray-absorption-spectroscopy. Micro-XRD will be complemented with simultaneous full range XRF spectra recording. Further, several data analysis tools will facilitate the use of micro-XRD. In the context of microspectroscopy, an improved signal normalization scheme (constant I0, advanced I0 measurement, etc.) as well as the full implementation of the multi-element solid state detector are of the highest priority.

## 8.5 References

BEAUD P. JOHNSON S.L. STREUN A., ABELA R., ABRAMSOHN D., GROLIMUND D., KRASNIQI F., SCHMIDT T., SCHLOTT V., INGOLD G. (2007)
Temporal Stability of Femtosecond Hard X-ray Undulator Radiation Studied by Control of Coherent Optical Phonons. Phys. Rev. Lett. 99, 174801(1-4).

BORCA C.N., GROLIMUND D., WILLIMANN M., MEYER B., JEFIMOVS K., VILA-COMAMALA J., DAVID C. (2008)
The micro-XAS beamline at the Swiss Light source: towards nano-scale imaging. J. Phys. Conf. Series, submitted.

BORCA C.N., CANULESCU S., LOVIAT F., LIPPERT T., GROLIMUND D., DÖBELI M., WAMBACH J., WOKAUN A. (2007)
Analysis of the electronic configuration of the pulsed laser deposited $La_{0.7}Ca_{0.3}MnO_3$ thin films.
Appl. Surf. Sci. 254(4), 1352-1355.

CAMMELLI S., DEGUELDRE C., KURI G., BERTSCH J. (2008)
Study of a neutron irradiated reactor pressure vessel steel by X-ray absorption spectroscopy. Nucl. Instrum. Methods in Phys. - B, 22, 4775.

DEGUELDRE C., KURI G., BORCA C.N. GROLIMUND D. (2008)
X-ray micro- fluorescence, diffraction and absorption spectroscopy for local structure investigation of a radioactive zinc ferrite film, submitted.

FROIDEVAL A., ABOLHASSANI S., GAVILLET D., GROLIMUND D., BORCA C.N., KRBANJEVIC J., DEGUELDRE C. (2008a)
Microprobe analysis of neutron irradiated and autoclaved zirconium niobiumcladdings using synchrotron-based hard X-ray imaging and spectroscopy. J. Nucl. Mater., in press.

FROIDEVAL A., DEGUELDRE C., SEGRE C.U., POUCHON M.A., GROLIMUND D. (2008)
Niobium speciation at the metal/oxide interface of corroded niobium-doped Zircaloys: A X-ray absorption near-edge structure study. Corr. Sci. 50(5), 1313-1320.

GAWELDA W., PHAM V.-T., BENFATTO M., ZAUSHITSYN Y., KAISER M., GROLIMUND D, JOHNSON S.L., ABELA R., HAUSER A., CHERGUI M., BRESSLER CH. (2007a)
Structural Determination of a Short-lived Iron(II) Complex by Picosecond X-ray Absorption Spectroscopy. Phys. Rev. Lett. 98, 057401(1-4).

GAWELDA W., PHAM V.-T., EL NAHHAS A., KAISER M., ZAUSHITSYN Y., JOHNSON S.L., GROLIMUND D., ABELA R., HAUSER A., BRESSLER CH., CHERGUI M. (2007)
Capturing Transient Electronic and Molecular Structures in Liquids by Picosecond X-ray Absorption Spectroscopy. American Institute of Physics CP882 - X-ray Absorption Fine Structure—XAFS 13, 31-36.

GROLIMUND D., SCHEIDEGGER A.M., VAN DER VEEN J.F., ABELA R. (2002)
Layout of the micro-XAS beamline at SLS. PSI Scientific Report 4, 139-148.

GROLIMUND D., SENN M., TROTTMANN M., JANOUSCH M., BONHOURE I., SCHEIDEGGER A.M., MARCUS M. (2004)
Shedding new Light on Historical Metal Samples using Micro-focused Synchrotron X-ray Fluorescence and Spectroscopy. At. Spectrosc. 59, 1627-1635.

JEFIMOVS K., BUNK O., PFEIFFER F., GROLIMUND D., VAN DER VEEN J.F., DAVID C. (2007)
Fabrication of Fresnel zone plates for hard X-rays. Microelectron. Eng. 84, 1467–1470.

JOHNSON I., JEFIMOVS K., BUNK O., DAVID C., DIEROLF M., GRAY J., RENKER D., PFEIFFER F. (2008a)
Coherent Diffractive Imaging Using Phase Front Modifications. Phys. Rev. Lett. 100, Art. No. 155503 (1-4).

JOHNSON S.L., BEAUD P., KRASNIQI F., MILNE C., KAISER M., GROLIMUND D., ABELA R., INGOLD G. (2008)
Nanoscale depth-resolved coherent femtosecond motion in laser excited bismuth. Phys. Rev. Lett. 100(15): Art. No. 155501.

KRASNIQI F., JOHNSON S.L., BEAUD P., KAISER M., GROLIMUND D., INGOLD G. (2008)
Influence of Lattice Heating Time on the Laser-Induced Strain Waves in InSb. Phys. Rev. B 78, 174302.

MAAß R., VAN PETEGEM S., GROLIMUND D., VAN SWYGENHOVEN H., KIENER D., DEHM G. (2008a)
Crystal rotation in Cu single crystal micro pillars: insitu Laue and electron backscatter diffraction. App. Phys. Lett. 92(7), 071905.

MAAß R., VAN PETEGEM S., ZIMMERMANN J., BORCA C.N., VAN SWYGENHOVEN H. (2008b)
On the initial microstructure of metallic micropillars. Scr. Mater. 59, 471–474.

MAAß R., VAN PETEGEM S., VAN SWYGENHOVEN H., DERLET P.M., VOLKERT C.A., GROLIMUND D. (2007a)
Time resolved Laue diffraction of deforming micropillars, Phys. Rev. Lett. 99 (14): Art. No. 145505.

FROIDEVAL A., IGLESIAS R., SAMARAS M., SCHUPPLER S., NAGEL P., GROLIMUND D., VICTORIA M., HOFFELNER W. (2007)
Magnetic and structural properties of Fe-Cr alloys. Phys. Rev. Lett. 99, 237201(1-4).

MAAß R., VAN PETEGEM S., GROLIMUND D., VAN SWYGENHOVEN H., UCHIC M.D. (2007b)
A strong micropillar containing a low angle grain boundary. Appl. Phys. Lett. 91, 131909(1-3).

PHAM V.-T., GAWELDA W., ZAUSHITSYN Y., KAISER M., GROLIMUND D., JOHNSON S.L., ABELA R., BRESSLER CH., CHERGUI M. (2007)
Observation of the Solvent Shell Reorganization around Photoexcited Atomic Solutes by Picosecond X-ray Absorption Spectroscopy. J. Am. Chem. Soc. 129(6), 1530-1531 (Communication).

PODGÓRCZYK M., KWIATEK W.M., GROLIMUND D., BORCA C.N. (2008)
Technical aspects of Zn microanalysis of human prostate cancer tissues and cells. Radiat. Phys. Chem., submitted.

RODENBURG J.M., HURST A.C., CULLIS A.G., DOBSON B.R., PFEIFFER F., BUNK O., DAVID C., JEFIMOVS K,, JOHNSON I. (2007)
Hard-X-ray Lensless Imaging of Extended Objects. Phys. Rev. Lett. 98, 034801(1-4).

VILA-COMAMALA J., JEFIMOVS K., PILVI T., RITALA M., SARKAR S.S., SOLAK H.H., GUZENKO V.A., STAMPANONI M., MARONE F., RAABE J., TZVETKOV G., FINK R.H., GROLIMUND D., BORCA C.N., KAULICH B., DAVID C. (2008)
Advanced X-ray Diffractive Optics. J. Phys. Conf. Series, submitted.

# 9 PUBLICATIONS

## 9.1 Peer reviewed journals and reports

BEAUD P., JOHNSON S.L., STREUN A., ABELA R., ABRAMSOHN D., GROLIMUND D., KRASNIQI F., SCHMIDT T., SCHLOTT V., INGOLD G.
Spatiotemporal stability of femtosecond hard X-ray undulator radiation studied by control of coherent optical phonons. Phys. Rev. Lett. 99, 174801(1-4) (2007)

BUKOWIECKI N.[1], LIENEMANN P.[1], ZWICKY C.N.[1], FURGER M., RICHARD A., FALKENBERG G.[2], RICKERS K.[2], GROLIMUND D., BORCA C.N., HILL M.[1], GEHRIG R.[1], BALTENSPERGER U.
X-ray fluorescence spectrometry for high throughput analysis of atmospheric aerosol samples: The benefits of synchrotron X-rays. Spectrochim. Acta, Part B 63, 929–938 (2008)
[1] Empa, Dübendorf, Switzerland
[2] DESY, Hamburg, Germany

CHURAKOV S.V.
Hydrogen bond connectivity in jennite from ab initio simulations. Cem. Concr. Res. 38, 1359-1364 (2008)

CHURAKOV S.V., MANDALIEV P.
Structure of the hydrogen bonds and silica defects in the tetrahedral double chain of xonotlite. Cem. Concr. Res. 38, 300-311 (2008)

FROIDEVAL A., DEGUELDRE C., SEGRE C.U.[1], POUCHON M.A., GROLIMUND D.
Niobium speciation at the metal/oxide interface of corroded niobium-doped Zircaloys: A X-ray absorption near-edge structure study. Corros. Sci. 50, 1313-1320 (2008)
[1] Institute of Technology, Chicago, USA

FROIDEVAL A., IGLESIAS R., SAMARAS M., SCHUPPLER S., NAGEL P., GROLIMUND D., VICTORIA M., HOFFELNER W.
Magnetic and structural properties of Fe-Cr alloys. Phys. Rev. Lett. 99, 237201(1-4) (2007)

GIMMI T.
Modelling field diffusion experiments in clay rock: Influence of numerical representation of borehole and rock interface. J. Environ. Sci. Sustain. Soc. 2, 61-68 (2008)

GLAUS M.A., VAN LOON L.R.
Degradation of cellulose under alkaline conditions: new insights from a 12-years degradation study. Environ. Sci. Technol. 42, 2906–2911 (2008)

GLAUS M.A., VAN LOON L.R.
Chemical reactivity of α-isosaccharinic acid in heterogeneous alkaline systems, PSI Bericht 08-01, Nagra NTB 08-10 (2008)

GLAUS M.A., MÜLLER W., VAN LOON L.R.
Diffusion of iodide and iodate through Opalinus Clay: Monitoring of the redox state using an anion chromatographic technique. Appl. Geochem. 23, 3612-3619 (2008)

GLAUS M.A., VAN LOON L.R., SCHWYN B.[1], VINES S.[2], WILLIAMS S.J.[2], LARSSON P.[3], PUIGDOMÈNECH I.[3]
Long-term predictions of the concentration of α-isosaccharinic acid in cement pore water. Mater. Res. Soc. Proc. 1107, 605-612 (2008)
[1] NAGRA, Wettingen, Switzerland
[2] NDA, Oxon, United Kingdom
[3] SKB, Stockholm, Sweden

GONZÁLEZ SÁNCHEZ F., JURÁNYI F., GIMMI T., VAN LOON L.R., SEYDEL T.[1], UNRUH T.[2]
Dynamics of supercooled water in highly compacted clays studied by neutron scattering. J. Phys. Condens. Matter 20, 415102 (9) (2008)
[1] Institut Laue-Langevin, Grenoble, France
[2] Forschungsneutronenquelle Heinz Maier-Leibniz, Garching, Germany

GONZÁLEZ SÁNCHEZ F., VAN LOON L.R., GIMMI T., JAKOB A., GLAUS M.A., DIAMOND L.W.[1]
Self-diffusion of water and its dependence on temperature and ionic strength in highly compacted montmorillonite, illite and kaolinite. Appl. Geochem. 23, 3840-3851 (2008)
[1] Universität Bern, Switzerland

GONZÁLEZ SÁNCHEZ F., JURÁNYI F., GIMMI T., VAN LOON L., UNRUH T.[1], DIAMOND L.[2]
Translational diffusion of water and its dependence on temperature in charged and uncharged clays: a neutron scattering study. J. Chem. Phys. 129, 174706 (11) (2008)
[1] Forschungsneutronenquelle Heinz Maier-Leibniz, Garching, Germany
[2] Universität Bern, Switzerland

HARTMANN E.[1], BAEYENS B., BRADBURY M.H., GECKEIS H.[1], STUMPF T.[1,2]
A spectroscopic characterization and quantification of M(III)/clay mineral outer-sphere complexes. Environ. Sci. Technol. 42, 7601-7606 (2008)
[1] Karlsruhe Institute of Technology, Germany
[2] Ruprecht-Karls-Universität Heidelberg, Germany

HUMMEL W.
Radioactive contaminants in the subsurface: The influence of complexing ligands on trace metal speciation (Invited Review). Monatshefte für Chemie/ Chemical Monthly 139, 459-480 (2008)

JOHNSON S.L., BEAUD P., KRASNIQI F., MILNE CH.J.[1], KAISER M.[1], GROLIMUND D., ABELA R., INGOLD G.,
Nanoscale depth-resolved coherent femtosecond motion in laser excited bismuth. Phys. Rev. Lett. 100, 155501 (2008)
[1] EPFL, Lausanne, Switzerland

KOSAKOWSKI G., CHURAKOV S.V., THOENEN T.
Diffusion of Na and Cs in montmorillonite. Clays Clay Miner. 56, 190-206 (2008)

KOSAKOWSKI G., MCDERMOTT C. [1]
Modelling matrix diffusion - Results of a benchmark study. J. Environ. Sci. Sustain. Soc. 2, 57-62 (2008)
[1] School of Geosciences, University of Edinburgh, Scotland

KÜPPER F.C.[1,2,3], CARPENTER L.J.[4], MCFIGGANS G.B.[5], PALMER C.J.[5,6], WAITE T.J.[7], BONEBERG E.-M.[2,8], WOITSCH S.[2], WEILLER M.[2], ABELA R., GROLIMUND D., POTIN PH.[9], BUTLER A.[3], LUTHER III G.W.[7], KRONECK P.M.H.[2], MEYER-KLAUCKE W.[10], FEITERS M.C.[11]
Iodide in kelp: an inorganic antioxidant in life impacting atmospheric chemistry. PNAS 105(19), 6954-6958 (2008)
[1] Dunstaffnage Marine Laboratory, Oban, Scotland
[2] Universität Konstanz, Germany
[3] University of California, Santa Barbara, USA
[4] University of York, UK
[5] University of Manchester, UK
[6] University of Cape Town, South Africa.
[7] University of Delaware, Lewes, USA
[8] Biotechnologie Institut Thurgau, Kreuzlingen, Switzerland
[9] Centre National de la Recherche Scientifique and Université Pierre et Marie Curie Paris–VI, Roscoff, France
[10] European Molecular Biology Laboratory, Hamburg, Germany
[11] University Nijmegen, Nijmegen, The Netherlands

LENZ M.[1,2], VAN HULLEBUSCH E.D.[1,3], FARGES F.[4,5], NIKITENKO S.[6], BORCA C.N., GROLIMUND D., LENS P.N.L.[1,7]
Selenium speciation in anaerobic biofilms assessed by X-ray absorption spectroscopy and sequential extraction procedures. Environ. Sci. Technol. 42, 7587-7593 (2008)
[1] Wageningen University, Wageningen, The Netherlands
[2] Universite Paris-Est, La Marne, France
[3] University of Applied Sciences Northwestern Switzerland (FHNW), Muttenz, Switzerland
[4] Museum National d'Histoire Naturelle de Paris, Paris, France
[5] Stanford University, California, USA
[6] Netherlands Organization for Scientific Research (NWO), DUBBLE at European Synchrotron Radiation Facility(ESRF), Grenoble, France
[7] UNESCO-IHE Institute for Water Education, The Netherlands

MAASS R., VAN PETEGEM S., ZIMMERMANN J., BORCA C.N., VAN SWYGENHOVEN H.
On the initial microstructure of metallic micropillars. Scr. Mater. 59, 471–474 (2008)

MAASS R., VAN PETEGEM S., GROLIMUND D., VAN SWYGENHOVEN H., KIENER D.[1], DEHM G.[1]
Crystal rotation in Cu single crystal micropillars: in situ Laue and electron backscatter diffraction. Appl. Phys. Lett. 92, 071905 (2008)
[1] Department of Materials Physics, Montanuniversität Leoben, Austrian Academy of Sciences, Leoben, Austria

MAASS R., VAN PETEGEM S., VAN SWYGENHOVEN H., DERLET P.M., VOLKERT C.A., GROLIMUND D.
Time resolved Laue diffraction of deforming micropillars. Phys. Rev. Lett. 99, 145505 (2007)

MARQUES FERNANDES M., BAEYENS B., BRADBURY M.H.
The influence of carbonate complexation on lanthanide/actinide sorption on montmorillonite. Radiochim. Acta 96, 691-697 (2008)

NILSSON A.CH.[1], HEDQVIST I.[2], DEGUELDRE C.
Granitic groundwater colloids sampling and characterisation: a strategy for artefact elimination. Anal. Bioanal. Chem. 391, 1327-1333 (2008)
[1] Geosigma, Dandery, Sweden
[2] SKB, Figeholm, Sweden

VAN ENGEN SPIVEY A.G.[1], BORCA C.N., CUNDIFF S.T.[2]
Correlation coefficient for dephasing of light-hole excitons and heavy-hole excitons in GaAs quantum wells. Solid State Commun. 145, 303–307 (2008)
[1] Department of Physics, University of Puget Sound, Tacoma, Washington, USA 98416-1031
[2] JILA, University of Colorado and National Institute of Standards and Technology, Boulder, Colorado, USA 80309-0440

VAN DER VEEN R.M.[1], MILNE CH.J.[1], PHAM V.-T.[1], EL NAHHAS A.[1], WEINSTEIN J.A.[2], BEST J.[2], BORCA C.N., BRESSLER CH.[1], CHERGUI M.[1]
EXAFS structural determination of the $Pt_2(P_2O_5H_2)_4^{4-}$ anion in solution. Chimia 62, 287–290 (2008)
[1] EPFL, Lausanne, Switzerland
[2] The University of Sheffield, Department of Chemistry, S3 7HF Sheffield, UK

VAN LOON L.R., GLAUS M.A.
Mechanical compaction of smectite clays increases selectivity for cesium. Environ. Sci. Technol. 42, 1600-1604 (2008)

WENK H.-R[1], VOLTOLINI M.[1], MAZUREK M.[2], VAN LOON L.R., VINSOT A.[3].
Preferred orientations and anisotropy in shales: Callovo-Oxfordian shale (France) and Opalinus Clay (Switzerland). Clays Clay Miner. 56, 285-306 (2008)
[1] University of Calfornia, Berkeley, USA
[2] Universität Bern, Switzerland
[3] ANDRA, Bure, France

WERSIN P.[1], SOLER J.M.[2], VAN LOON L.R., EIKENBERG J., BAEYENS B., GROLIMUND D., GIMMI T., DEWONCK S.[3]
Diffusion of HTO, $Br^-$, $I^-$, $Cs^+$ and $^{60}Co^{2+}$ in a clay formation: Results and modelling from an in-situ experiment in Opalinus Clay. Appl. Geochem. 23, 678-691 (2008)
[1] Gruner AG, Basel, Switzerland
[2] CSIC-IJA, Barcelona, Spain
[3] ANDRA, Bure, France

WIELAND E., TITS J., D. KUNZ D., DÄHN R.
Strontium uptake by cementitious materials: A combined wet chemistry and EXAFS study. Environ. Sci. Technol. 42, 403-409 (2008)

WILTZIUS J.J.W, SIEVERS S.A., SAWAYA M.R., CASCIO D., POPOV D., RIEKEL C., EISENBERG D.
Atomic structure of the cross-beta spine of islet amyloid polypeptide (amylin). Protein Sci. 17, 1467-1474 (2008)

YAROSCHCHUK A.E.[1], GLAUS M.A., VAN LOON L.R.
Diffusion through confined media at variable concentrations in reservoirs. J. Membr. Sci. 319, 133-140 (2008)
[1] ICREA and Polytechnic University of Catalonia, Barcelona, Spain

YAROSCHCHUK A.E.[1], VAN LOON L.R.
Improved interpretation of in-diffusion measurements with confined swelling clays. J. Contam. Hydrol. 97, 67-74 (2008)
[1] ICREA and Polytechnic University of Catalonia, Barcelona, Spain

## 9.2 Conference Proceedings

MAZUREK M.[1], ALT-EPPING P.[1], GIMMI T., WABER H.N.[1], BATH A.[2], BUSCHAERT S.[3], GAUTSCHI A.[4]
Tracer profiles across argillaceous formations: A tool to constrain transport processes. In: Bullen, T.D. & Wang, Y. (eds.), Proceedings of the 12th International Symposium on Water-Rock Interaction, WRI-12, Kunming, China, 31 July - 5 August 2007, Taylor & Francis, 767-771 (2007)
[1] Universität, Bern, Switzerland
[2] IntelliSci, Loughborough, UK
[3] Andra, Châtenay-Malabry, France
[4] Nagra, Wettingen, Switzerland

PFINGSTEN W.
The influence of the experimental set-up and the model approach on the determination of diffusion coefficients for radionuclides in laboratory column experiments. In: J.C. Refsgaard, K. Kovar, E. Haarder and E. Nygaard (eds.), Calibration and Reliability in Groundwater Modelling: Credibility of Modelling. IAHS Publication 320, IAHS, Wallingford, UK, 278-283 (2008)

TITS J., FUJITA T., TSUKAMOTO M., WIELAND E.
Uranium(VI) uptake by synthetic calcium silicate hydrates. In: W.E. Lee, J.W Roberts, N.C. Hyatt, R.W. Grimes (eds.), Scientific Basis for Nuclear Waste Management XXXI. MRS proceedings Vol. 1107, 467-474 (2008)

## 9.3 Conferences/Workshops/Presentations

BORCA C.N., GROLIMUND D., WILLIMANN M., MEYER B., MAASS R., VAN PETEGEM S., VAN SWYGENHOVEN H., FARGES F.[1,2], VAN HULLEBUSCH E.[3,4], LENZ M.[3,5], LENS P.[3,6], FARQUHARSON M.J.[7], FROIDEVAL A.
The μXAS beamline: a multitechnique hard X-ray microprobe station at the Swiss Light Source. X-ray Microscopy Conference, Zurich, Switzerland, 21-25 July 2008
[1] Museum National d'Histoire Naturelle de Paris, Paris, France
[2] Stanford University, California, USA
[3] Wageningen University, Wageningen, The Netherlands
[4] University of Applied Sciences (FHNW), Muttenz, Switzerland
[5] Universite Paris-Est, La Marne
[6] UNESCO-IHE Institute for Water Education, The Netherlands
[7] City University, London, GB

BRESSLER CH., GROLIMUND D.
The Bermuda triangle of XAS Analysis. Workshop on X-ray Spectroscopies: Theory and Experiment, EPFL Lausanne, Switzerland, 30 January - 1 February 2008

CHURAKOV S.V.
Structure of cement phases from ab initio modelling. 2nd International Workshop on Mechanisms and Modelling of Waste/Cement Interactions, Le Croisic, France, 12-16 October 2008

DÄHN R., VESPA M., SHUH D.K.[1], TYLISZCZAK T.[1], WIELAND E.
Spectromicroscopic Investigation of Metal Precipitate Formation in Nuclear Waste Repository Materials. 7th International Conference on Nuclear and Radiochemistry, Budapest, Hungary, 24-29 August 2008
[1] Lawrence Berkeley National Laboratory, Berkeley, USA

DILNESA B.Z.[1], LOTHENBACH B.[1], WIELAND E., ULRICH A.[1]
Solubility of Fe-containing hydrates, 2nd International Workshop on Mechanisms and Modelling of Waste/Cement Interactions, Le Croisic, France, 12-16 October 2008
[1] Empa, Dübendorf, Switzerland

GROLIMUND D., BORCA C.N., NACHTEGAAL M., BUKOWIECKI N.[1], FERRI D.[1], ROBERT R.[1]
Workshop on X-ray absorption spectroscopy and advanced XAS techniques, Paul Scherrer Institut, 6-10 October 2008 (http://xas08.web.psi.ch/)
[1] Empa, Dübendorf, Switzerland

LEUPIN O.X.[1], DEWONCK S.[2], SAVOYE S.[3], WERSIN P.[4], VAN LOON L.R., GIMMI T., SAMPER J.[5], SOLER J.M.[6], EIKENBERG J., BAEYENS B.
Diffusion and retention experiment in clay formation: an international field, lab and modelling exercise. Goldschmidt Conference, Vancouver, Canada, 13-18 July 2008
[1] NAGRA, Wettingen, Switzerland
[2] ANDRA, Bure, France
[3] IRSN, Fontenay aux Roses, France
[4] Gruner AG, Basel, Switzerland
[5] University of La Coruña, La Coruña, Spain
[6] CSIC-IJA, Barcelona, Spain

LOTHENBACH B.[1], WIELAND E., FIGI R.[1], RENTSCH D.[1], SCHWYN B.[2]
Solubility of Fe-containing hydrates, 2nd International Workshop on Mechanisms and Modelling of Waste/Cement Interactions, Le Croisic, France, 12-16 October 2008
[1] Empa, Dübendorf, Switzerland
[2] NAGRA, Wettingen, Switzerland

MACÉ N., HARFOUCHE M., DÄHN R., TITS J., SCHEINOST A.[1], WIELAND E.
EXAFS investigation of U(VI) speciation in cementitious materials, 5th Workshop on Speciation, Techniques and Facilities for Radioactive Materials at Synchrotron Light Sources. Actinide XAS 2008, Saint-Aubin, France, 15–17 July 2008
[2] ESRF, Grenoble, France

MACÉ N., WIELAND E., TITS J., DÄHN R., KUNZ D., GEIPEL G. [1], SCHEINOST A. [1,2]
Spectroscopic investigations of U(VI) speciation in cementitious materials. 2nd International Workshop on Mechanisms and Modelling of Waste/Cement Interactions, Le Croisic, France, 12-16 October 2008
[1] Forschungszentrum Dresden-Rossendorf, Dresden, Germany
[2] ESRF, Grenoble, France

MARQUES FERNANDES M., RABUNG TH.[1], DÄHN R., BAEYENS B., BRADBURY M.H.
Macroscopic and microscopic study of actinide sorption on clay minerals: Influence of carbonate complexation. 1st ACTINET Research Fellow Exchange Meeting, Avignon, France, 17–19 March 2008
[1] Karlsruhe Institute of Technology, Karlsruhe, Germany

MARQUES FERNANDES M., DÄHN R., BAEYENS B., SCHEINOST A.[1], BRADBURY M.H.
Influence of carbonate complexation on the sorption of U(VI) on montmorillonite. 5th Workshop on Speciation, Techniques and Facilities for Radioactive Materials at Synchrotron Light Sources. Actinide XAS 2008, Saint-Aubin, France, 15–17 July 2008
[1] ESRF. Grenoble, France

MECA S.[1,2], COLÀS E. [1,3], ROJO I.[1,2], GAONA X., GRIVÉ M.[3], DURO L.[3], ROVIRA M.[1,2], MARTÍ V.[1,2], DE PABLO J.[1,2]
Uranium(VI) interaction with cement-based materials. 2nd International Workshop on Mechanisms and Modelling of Waste/Cement Interactions, Le Croisic, France, 12-16 October 2008
[1] CTM, Manresa, Spain
[2] UPC, Barcelona, Spain
[3] AMPHOS, Valldoreix, Spain

MERINO J.[1], GUIMERÀ J.[1], GAONA X., LUNA M.[1], DELOS A.[1], BRUNO J.[1]
Risk assessment of a landfill for wastes containing naturally occurring radionuclides through infiltration to groundwater. International Conference 'Uranium Mining and Hydrogeology V', Freiberg/Saxony, Germany, 14–18 September 2008
[1] AMPHOS, Valldoreix, Spain

PFINGSTEN W., SHAO H.
Benchmark calculations using alternative geochemical modules implemented within reactive transport codes. Int. Workshop on Modelling Reactive Transport in Porous Media, Strasburg, France, 21-24 January 2008

PFINGSTEN W.
Reactive Transport Modelling. Swiss Bentonite Workshop, Haus der Universität, Bern, Switzerland, 9 June 2008

ROZOV K., BERNER U., TAVIOT-GUÉHO C.
Synthesis, characterization and thermodynamics of hydrotalcite-like solid solutions. 2nd International Workshop on Mechanisms and Modelling of Waste/Cement Interactions, Le Croisic, France, 12-16 October 2008

TITS J., MACÉ N., GEIPEL G.[1], EILZER M.[1], WIELAND E.
U(VI) uptake by calcium silicate hydrates. Goldschmidt Conference 2008, Vancouver, Canada, 13–18 July, 2008
[1] Forschungszentrum Dresden, Dresden, Germany

TITS J., MACÉ N., GEIPELG.[1], EILZER M.[1], WIELAND E.
Uranium(VI) uptake by calcium silicate hydrates. 2nd International Workshop on Mechanisms and Modelling of Waste/Cement Interactions, Le Croisic, France, 12-16 October 2008.
[1] Forschungszentrum Dresden, Germany

WIELAND E., MANDALIEV P., DÄHN R., TITS J., STUMPF T.[1]
Mechanisms of lanthanide binding by cementitious materials. Proceedings of the 7th International Conference on Nuclear and Radiochemistry (NRC-7), Budapest, Hungary, 24–29 August, 2008
[1] Karlsruhe Institute of Technology, Karlsruhe, Germany

WIELAND E., DÄHN R., LOTHENBACH B.[1], VESPA M.[2]
Micro-spectroscopic investigations of the Al and S speciation in hardened cement paste. 2nd International Workshop on Mechanisms and Modelling of Waste/Cement Interactions, Le Croisic, France, 12-16 October 2008

[1] Empa, Dübendorf, Switzerland
[2] ESRF, Grenoble, France

## 9.4 Invited talks

CHURAKOV S.
Ab initio modelling of crystalline cement phases. EPFL Lausanne, Switzerland, 15 May 2008

GROLIMUND D., BORCA C.N., GAVILLET D., WIELAND E., FROIDEVAL A., MEYER B., WILLIMANN M.
Beaming in on radioactive materials: The micro-XAS beamline project at the Swiss Light Source. 5th Workshop on Speciation, Techniques and Facilities for Radioactive Materials at Synchrotron Light Sources. Actinide XAS 2008, Saint-Aubin, France, 15–17 July 2008

GROLIMUND D., BORCA C.N., MEYER B., WILLIMANN M.
Micro-XAS Beamline Project: Beauty or Beast? Int. Workshop on Hard X-ray Micro/Nano probe at PETRA III, HASYLAB/DESY, Hamburg, Germany, 22-23 January 2008

DÄHN R.
Determination of the speciation of radionuclides in cementitious materials by STXM and EXAFS. 5th Workshop on Speciation, Techniques and Facilities for Radioactive Materials at Synchrotron Light Sources. Actinide XAS 2008, Saint-Aubin, France, 15–17 July 2008

GIMMI T.
Investigating transport through Opalinus Clay: Laboratory and field activities. International Symposium on Computational and Experimental Methods for Processes in Deep Geological Environment, Okayama University, Okayama, Japan, 18 January 2008

HUMMEL W.
Recent and prospective developments of the Nagra/PSI database. Séminaire Spéciation, Journées d'information CETAMA, Montpellier, France, 22-23 January 2008

KOSAKOWSKI G., JAKOB A.
Modelling water and radionuclide transport in clays – results of a benchmark study. International Symposium on Computational and Experimental Methods for Processes in Deep Geological Environment, Okayama University, Okayama, Japan, 18 January 2008

KULIK D., BERNER U., CURTI E., HUMMEL W., THOENEN T.
Advanced solubility concepts and tools in geochemical modelling related to nuclear waste disposal. 13th International Symposium on Solubility Phenomena & Related Equilibrium Processes (ISSP), Dublin, Ireland, 27-31 July 2008

KULIK D.
Improvement of the C-S-H solid solution model using recent spectroscopic and structural information. 2nd International Workshop on Mechanisms and Modelling of Waste/Cement Interactions, Le Croisic, France, 12-16 October 2008

VAN LOON L.R.
Effect of exchangeable cations and pore water chemistry on the diffusion of radionuclides in compacted bentonite. International Workshop on Iron-Bentonite Interaction, Kanazawa, Japan, 18-19 November 2008

VAN LOON L.R.
Understanding diffusion of radionuclides in argillaceous materials: beyond applying Fick's Law. Hokkaido Universtiy, Sapporo, Japan, 21 November 2008

## 9.5 Other presentations

DEGUELDRE C.
Colloid analysis in a single particle mode: status of results at PSI and outlook for phase II. 5th CFM project meeting, Briegens, 13-14 November 2008

DEGUELDRE C., BESSHO K.
Contribution to the study of colloid generation & sedimentation from FEBEX bentonite samples. CFM meeting, at CRIEPI, Tokyo, 13-14 November 2008

DEGUELDRE C., RAABE J., WOLD S.
Scanning transmission X-ray microscopy investigations of bentonite colloid aggregates in water. CFM meeting, at CRIEPI, Tokyo, 13-14 November 2008

GIMMI T.
Overview FUNMIG WP3.3 – In Situ Diffusion and Retention at Intermediate to Large Scales. FUNMIG Meeting, Paris, France, 28-29 May 2008

GIMMI T.
Solute diffusion and retention in Opalinus Clay: Field experiments at the Mont Terri Rock Laboratory. University of Bern, Forum Current Research on Internal Earth, Isotopic and Geodynamic Processes, Bern, Switzerland, 12 November 2008

GIMMI T.
DR Experiment Mont Terri: Compilation of Data and DR Experiment Mont Terri: Modelling borehole data. Presentation at DR project meeting, La Coruña, Spain, 12-13 June 2008

GIMMI T.
DR Experiment Mont Terri: Solute diffusion and retention in Opalinus Clay at the field scale. Presentation at LES-FZR coordination meeting, Rossendorf, Germany, 3-4 November 2008

KOSAKOWSKI G.
Chemistry and Transport at LES: recent developments and applications related to reactive transport models. Zentrum für Angewandte Geowissenschaften der Universität Tübingen, Deutschland, 7 November 2008

KULIK D.
Modelling aqueous-solid solution systems in GEMS. Presentation at the Helmholtz Society Virtual Institute 13 on Advanced Radiogeochemistry (HG VI 13) kick-off meeting (KIT INE, 27-28.02.2008) and at the HG VI 13 work meeting at KIT (Karlsruhe), 13-14 November 2008

MACÉ N., WIELAND E., TITS J., DÄHN R.
Microscale investigations of the speciation and mobility of uranium in cementitious materials (MISUC). 1st ACTINET Research Fellow Exchange Meeting, Avignon, France, 17–19 March 2008

PFINGSTEN W.
Reactive Transport Calculations to Investigate Competitive Sorption Effects. Institut für Nukleare Entsorgung, Karlsruhe Institute of Technology, Germany, 11 April 2008

PFINGSTEN W.
Porosity permeability relationships, cement leaching modelling, LCS activity. LCS meeting - video conference with Japan JAEA, Nagra, Wettingen, CH, 19 May 2008

TITS J.
Wet chemistry and luminescence spectroscopy investigations of the uranyl retention by cementitious materials. Institut für Nukleare Entsorgung, Karlsruhe Institute of Technology, Germany, 30 May 2008

MARQUES FERNANDES M., RABUNG TH.[1], R. DÄHN R.[1], BAEYENS B., BRADBURY M.H.
Macroscopic and microscopic study of actinide sorption on clay minerals: Influence of carbonate complexation1st ACTINET Research Fellow Exchange Meeting, Avignon, France, 17–19 March 2008
[1] Karlsruhe Institute of Technology, Karlsruhe, Germany

## 9.6 Internal reports

ALT-EPPING P.[1], GIMMI T., WABER H.N.[1]
Porewater chemistry (PC) experiment: Reactive transport simulations. Mont Terri Technical Note TN 2006-66 (2007)
[1] Universität, Bern, Switzerland

BRADBURY M.H., BAEYENS B., THOENEN T.
Sorption Data Bases for Generic Swiss Argillaceous, Crystalline and Calcareous Rock Systems. Nagra Arbeitsbericht NAB 08-50. Nagra, Wettingen (2008)

GIMMI T., VONTOBEL P., SALADIN L., LEHMANN E
Neutron imaging of cores of Opalinus Clay: First estimates of neutron transmission and of drying behaviour. PSI Experimental Report (2008)

PFINGSTEN W.
The influence of competitive sorption processes on radionuclide migration. In: S. Capper (ed.) PSI Scientific Report 2007. Paul Scherrer Institut, Villigen, Switzerland, 68-69, (2008)

## 9.7 Internal presentations

BAEYENS B.
Sorption on clays, towards a thermodynamic sorption database

CHURAKOV S.
Ab initio modelling of crystaline cement phases

CURTI E.
An overview on more than 12 years of glass corrosion at PSI

GIMMI T.
Solute diffusion and retention in Opalinus Clay at the field scale

KOSAKOWSKI G.
Latest developments in reactive transport modelling at LES

MARQUES M.
Influence of carbonate on the sorption of Eu and trivalent actinides on montmorillonite: A combined macroscopic and microscopic (TRLFS, EXAFS) approach

K. ROZOV
Synthesis, analysis and thermodynamics of hydrotalcite-like solid solutions

TITS J.
A fluorescence spectroscopy study of the U(VI) interaction with C-S-H phases.

### 9.8 Others/Teachings

BORCA C.N., GROLIMUND D., WILLIMANN M., MEYER B., FARQUHARSON M.J., AL EBRAHEEM A., FROIDEVAL A., ABOLHASSANI-DADRAS S.
Recent micro-spectroscopy studies at the micro-XAS beamline. SLS Symposium Series, Paul Scherrer Institut, Villigen, Switzerland, October 2008

GIMMI T., MAZUREK M.[1], MERCOLLI I.[1], PETTKE T.[1]
Fluids in the Crust. Lecture (2.25 ECTS, 2h/week), fall semester 2008, Master Course in Environmental and Resource Geochemistry, University of Bern (2008)
[1] Universität Bern, Switzerland

GIMMI T.
Determination of Transport Parameters at the Laboratory Scale; Determination of Transport Parameters at the Field Scale; Natural Tracers: Transport at Very Large Scales. Okayama University, Japan, 14-18 January 2008

GIMMI T.
Wasserbewegung im gesättigten und ungesättigten Untergrund – Implikationen für den Transport von Schadstoffen. Lecture as part of a two-day advanced training course for experts for contaminated sites, University of Bern, 11-12 September 2008

JOHNSON A., HUMMEL W., PLÖTZE L.M.
Landfilling, nuclear repositories and contaminated sites. Course for Major in Biogeochemistry and Pollutant Dynamics (Master of Environmental Sciences) and for Major in Ecological Systems Design and Waste Management (Master of Environmental Engineering), ETH Zurich, Autumn Semester 2008

KOSAKOWSKI G.
Geostatistics I. Lecture series for the course "Masters in Applied Environmental Geoscience", University of Tübingen, Germany, 2008

KOSAKOWSKI G.
Geostatistics II. Lecture series for the course "Masters in Applied Environmental Geoscience", University of Tübingen, Germany, WS 2008/2009

KOSAKOWSKI G., GIMMI T., KOLDITZ O.[1], KALLBACHER TH. [2]
Computational and Experimental Methods for Processes in the Deep Geological Environment. Block course, University of Okayama, Okayama, Japan, January 2008
[1)] TU Dresden, Germany
[2] Uni Okayama, Japan

NACHTEGAAL M., FROMMER J.[1], BORCA C.N., GROLIMUND D., HARFOUCHE M.
Cook and Look: Synchrotron Techniques. Master-level hands-on training, SLS and ETHZ/UNIZ, Paul Scherrer Institut, Villigen, Switzerland, July 2008
[1] ETH Zurich, Switzerland

PRASSER H.-M., GÜNTHER-LEOPOLD I., HIRSCHBERG S., HUMMEL W., WILLIAMS T., ZUIDEMA P.K.
Nuclear Energy Systems. Lecture course with exercises, ETH Zurich, Spring Semester 2008

### 9.9 PhD and Diploma Theses

MANDALIEV P.
"Mechanisms of Nd(III) and Eu(III) uptake by cementitious materials". PhD Thesis, Swiss Federal Institute of Technology Zürich (ETH), Diss. ETH Nr. 18095, Zürich, 2008


Paul Scherrer Institut, 5232 Villigen PSI, Switzerland
Tel. +41 (0)56 310 21 11, Fax +41 (0)56 310 21 99
www.psi.ch